

NASA TECHNICAL NOTE



NASA TN D-4804

e.l

NASA TN D-4804

LOAN COPY: 1  
AFWL (V  
KIRTLAND AI



TECH LIBRARY KAFB, NM

EFFECTS OF REDUCED AIRSPEED FOR  
LANDING APPROACH ON FLYING QUALITIES  
OF A LARGE JET TRANSPORT  
EQUIPPED WITH POWERED LIFT

*by Harold L. Crane, Robert W. Sommer,  
and Frederick M. Healy*

*Langley Research Center  
Langley Station, Hampton, Va.*



NATIONAL AERONAUTICS AND SPACE ADMINISTRATION • WASHINGTON, D. C. • OCTOBER 1968



EFFECTS OF REDUCED AIRSPEED FOR LANDING APPROACH ON  
FLYING QUALITIES OF A LARGE JET TRANSPORT

EQUIPPED WITH POWERED LIFT

By Harold L. Crane, Robert W. Sommer,  
and Frederick M. Healy

Langley Research Center  
Langley Station, Hampton, Va.

~~NATIONAL AERONAUTICS AND SPACE ADMINISTRATION~~

---

For sale by the Clearinghouse for Federal Scientific and Technical Information  
Springfield, Virginia 22151 - CFSTI price \$3.00



**EFFECTS OF REDUCED AIRSPEED FOR LANDING APPROACH ON  
FLYING QUALITIES OF A LARGE JET TRANSPORT  
EQUIPPED WITH POWERED LIFT**

By Harold L. Crane, Robert W. Sommer,  
and Frederick M. Healy  
Langley Research Center

**SUMMARY**

A flight research program was conducted to determine the effects of reduced landing-approach speeds on the flying qualities of a typical large jet transport for simulated instrument approaches. The reduced approach speeds were made possible by a powered-lift system which blew air over the upper surface of the wing flaps. This paper discusses the effects of reduced approach speeds on flying qualities and flying-qualities requirements. It was found that a 25-percent reduction in landing-approach speed would not necessarily result in new requirements for satisfactory flying qualities. However, such items as pitch response and trim characteristics, Dutch roll damping, and lateral-directional coupling are likely to be more difficult to maintain at satisfactory levels.

**INTRODUCTION**

Take-off and landing speeds of transport airplanes have increased considerably over the years so that it has been necessary to make successive increases in runway lengths to accommodate the speed increases. To counteract this trend, continuing efforts have been made to equip transport airplanes with improved high-lift devices. Recently, the Boeing Company equipped their jet-transport prototype with an experimental powered-lift or blown-flap boundary-layer-control system to improve the high-lift or short-field capability of the jet transport. Langley Research Center contracted to use the boundary-layer-control equipped Boeing airplane to investigate the flying qualities and performance margins of this configuration for the landing approach and touchdown at reduced speeds. With the boundary-layer-control system operating, the power available for take-off with the existing engines (JT3D-1) at reduced speeds was marginal. Therefore, only the landing-approach configuration was investigated.

Objectives of this Langley low-speed flight program included the establishment of rational criteria for performance margins for the approach and investigation of the effects of reduced approach speeds on the flying qualities of and flying-qualities requirements for

a typical jet transport. Most of the data were obtained and evaluated by use of simulated instrument flight in the landing-approach configuration as the primary pilot task. This paper deals with the flying-qualities aspects of the instrument-landing-approach tests. The stability and control characteristics of the test airplane are documented in the appendix. The appendix also describes the test airplane, the boundary-layer-control system, and the test instrumentation. Performance margins are discussed in reference 1. The development of this boundary-layer-control system and flight data on system performance and stability and control characteristics are discussed in reference 2.

## SYMBOLS

$a_x$	longitudinal acceleration, g units
$a_y$	lateral acceleration, g units
$a_z$	normal acceleration, g units
$b$	wing span, feet
$C_{1/2}$	cycles to half-amplitude
$C_n$	yawing-moment coefficient
$C_{np}$	variation of yawing-moment coefficient with roll helix angle, $\frac{\partial C_n}{\partial \frac{pb}{2V}}$
$C_{n\dot{\beta}}$	variation of yawing-moment coefficient with sideslip rate, $\frac{\partial C_n}{\partial \dot{\beta}}$
$C_{n\delta_a}$	variation of yawing-moment coefficient with aileron deflection, $\frac{\partial C_n}{\partial \delta_a}$
$C_{n\delta_r}$	variation of yawing-moment coefficient with rudder deflection, $\frac{\partial C_n}{\partial \delta_r}$
$C_\mu$	mass-flow coefficient, $\frac{\text{Blowing momentum}}{qS}$
$C_{n\dot{\phi}}$	variation of yawing-moment coefficient with roll rate, $\frac{\partial C_n}{\partial \dot{\phi}}$

$\bar{c}$	mean aerodynamic chord, feet (meters)
$E_g$	glide-slope error, millivolts (positive when below glide slope)
$E_L$	localizer error, millivolts (positive when to left of center line)
$F_c$	column force, pounds (newtons) (pull is positive)
$\Delta F_{max}$	maximum force increment, pounds (newtons)
$F_p$	rudder pedal force, pounds (newtons) (positive to right)
$F_w$	control wheel force, pounds (newtons) (positive to right)
$g$	acceleration due to gravity, feet/second <sup>2</sup> (meters/second <sup>2</sup> )
$h$	altitude (true), feet (meters)
$h_p$	pressure altitude, feet (meters)
$I_x, I_y, I_z$	moments of inertia about X, Y, and Z body axes, respectively, slug-feet <sup>2</sup> (kg-m <sup>2</sup> )
$\alpha$	incidence angle, degrees
$\alpha_s$	stabilizer incidence, degrees
$T$	period, seconds
$\dot{\phi}$	roll rate, degrees/second
$\dot{\alpha}$	dynamic pressure, pounds/square foot (newtons/meter <sup>2</sup> ) or pitch rate, degree/second
$r$	yaw rate, degrees/second
$S$	wing area, square feet (meters <sup>2</sup> )
$s$	Laplace operator

$T_2$	time to double amplitude, seconds
$t$	time, seconds
$V$	true airspeed, knots
$\Delta V$	airspeed increment, knots (positive = increase)
$V_e$	equivalent airspeed, knots
$V_s$	stalling speed at 1g, powered lift on, knots
$v_e$	equivalent side velocity, feet/second (meters/second)
$W$	airplane gross weight, pounds (newtons)
$\alpha$	angle of attack from fuselage reference line, degrees
$\beta$	sideslip angle, degrees
$\beta_{vane}$	uncorrected sideslip angle, degrees
$\gamma$	flight-path angle, degrees
$\delta$	deflection, degrees
$\zeta$	damping ratio
$\theta$	pitch angle, degrees
$\tau$	time constant, seconds
$\phi$	roll angle, degrees or radian
$\phi/v_e$	amplitude of roll angle to equivalent side velocity, degree/foot/second (degree/meter/second)
$\psi$	change in heading, degrees

Subscripts and sign conventions:

For  $\delta$ :

$a$  aileron, positive for left roll (right aileron down)

c control column, positive aft

e elevator, positive for trailing edge down

f wing trailing-edge flap, positive for trailing edge down

p rudder pedal, forward is positive for right pedal

R thrust reverser or modulator door position

r rudder, positive for left rudder deflection

s stabilizer, positive for trailing edge down

sp spoiler, deflects upward only

T throttle

w aileron control wheel, positive to right

For flare analysis:

i initial

t touchdown

Dots over symbols indicate derivatives with respect to time.

#### TEST AIRPLANE

The airplane used for this investigation was the Boeing 707 four-engine jet-transport prototype with modified leading- and trailing-edge flaps and a powered-lift system. This system bled off compressed air from the engines and blew it over the upper surface of the trailing-edge flaps. With boundary-layer control, it was possible to use flap deflections of  $70^\circ$  or more compared with about  $40^\circ$  for plain flaps without boundary-layer control. The maximum lift coefficient was thereby increased enough to reduce the minimum landing-approach speed by more than 25 knots (1 knot = 0.514 meter/second). This equipment is described more fully in the appendix.

In order to operate the engines at the high powers required for the powered-lift system and still obtain the reduced thrust settings required for the landing-approach condition, the thrust-modulation system described in the appendix was used. The normal

clamshell-type thrust reversers located in each of the four engine primary tailpipes were modified to be continuously variable through their entire operation range from maximum thrust to essentially zero thrust by a set of four levers located on the pilot's console. This thrust-modulation system offered a very fast-acting speed control during the landing approach when compared with the response of the normal throttle control. The system was used in place of the normal throttle control during all powered-lift conditions.

The Dutch roll damping of the test airplane at normal approach speeds with no augmentation was below satisfactory levels. Therefore, it was necessary to install a system of lateral and directional stability-augmenting devices to counteract the further deterioration of flying qualities due to powered lift and reduced approach speeds. This stability-augmentation equipment was used to make the Dutch roll mode convergent and to eliminate adverse sideslip at speeds as much as 30 knots below the previous minimum approach speed for the test airplane. The characteristics of the stability-augmentation devices are presented in the appendix.

## PROCEDURES FOR TESTS AND EVALUATIONS

### Configurations

The configurations tested are outlined in table I.

TABLE I.- TEST CONFIGURATIONS

Configuration	Flap deflection, deg	Mass-flow coefficient, $C_{\mu}$	Approach airspeed, knots	Weight		Center of gravity, percent c	Augmentation
				lb	N		
I	30	0	115 to 125	$140 \times 10^3$ to $170 \times 10^3$	$630 \times 10^3$ to $760 \times 10^3$	30	Lateral, on and off
II	50	0.035 to 0.04	95 to 105	$140 \times 10^3$ to $170 \times 10^3$	$630 \times 10^3$ to $760 \times 10^3$	30	Lateral, on; autospeed, on and off
III	60	0.09 to 0.10	85 to 95	$140 \times 10^3$ to $165 \times 10^3$	$630 \times 10^3$ to $740 \times 10^3$	30	Lateral, on and off

### Preliminary Evaluation

Preliminary evaluation tests were made under conditions of visual flight rules (VFR) at a safe altitude to define the desired flight conditions for the final landing-approach evaluation tests. The preliminary evaluation at altitude consisted of four basic tests of landing-approach characteristics which were as follows:

- (1) Indications of performance capability: Minimum altitude loss go-arounds from a 500 foot/minute (150 meter/second) rate of descent
- (2) Indications of maneuver capability: Simulated flares at various pitch rates from an initial rate of descent of 1000 feet/minute (300 meters/second)

(3) Indications of static longitudinal stability characteristics: Increasing and decreasing speed by 5 knots from reference speed by using elevator only and observing the ability to maintain specified speed changes and

(4) Indications of lateral directional characteristics: Attain heading changes of  $\pm 5^{\circ}$  and bank angles of  $\pm 20^{\circ}$

The approach speeds used both for preliminary evaluation and the instrument-flight-rule (IFR) approaches were based on the stalling speeds with powered lift on and the power-required characteristics of the three test configurations. Tentative values of approach speeds were selected and then evaluated at a safe altitude (5000 feet (1500 meters)). The approach speeds were selected largely on the basis of normal-acceleration capability and pitch attitude for the approach. The engineers felt that the normal-acceleration capability should be about 1.4g to match the capability of a conventional configuration. The pilots also felt that the body attitude during the approach should be within about  $2^{\circ}$  of the normal touchdown attitude. The selection and evaluation of approach speeds for the three test configurations is discussed further in reference 1.

The evaluation at an altitude of 5000 feet (1500 meters) was made at three speeds including the speed which provided a maneuver capability of 1.4g as well as approximately 15 knots above and 10 knots below this speed. The prescribed series of test runs was made during the altitude evaluation for each speed and configuration. Each of the three evaluation pilots went through this procedure to become familiar with the test configurations and to determine what each considered to be the minimum acceptable approach speeds for the three test configurations.

#### Simulated Instrument Landing Approaches

The final pilot evaluation was obtained under conditions of simulated (hooded) instrument flight rules (IFR) during approaches to landing. Hooded approaches were used in order to provide a precision pilot task that was representative of actual flight operations. All flight tests were conducted during good ceiling and visibility conditions with light-to-moderate winds of 15 knots or less and gusts below 5 knots. The approaches were made manually by using ILS-type information from a AN/GSN-5 radar system. The sensitivity of the flight path and localizer signals differed moderately from a standard instrument landing system. A brief description of the radar system and a comparison of the guidance sensitivity pattern as used for these tests with a typical ILS pattern are presented in the appendix.

Intercept of the localizer was made with landing gear down approximately 8 miles (12.8 kilometers) from the runway at an altitude of 1500 feet (460 meters). The flaps and airspeed were then adjusted for the landing approach as required by the test plan. At the intercept of the glide slope, approximately 5 miles (8 kilometers) from the runway,

a descent was initiated and the pilot attempted to fly the prescribed flight path as closely as possible down to approximately 200 feet (60 meters) and, if conditions were favorable, continue visually to touchdown at or near a bullseye on the runway 1500 feet (460 meters) from the threshold. Some tests were made with the localizer offset 200 feet (60 meters) from the runway center line during the approach to evaluate the lateral maneuverability. After the simulated IFR breakout at an altitude of 200 feet (60 meters) with the lateral offsets, the pilot performed a visual sidestep maneuver in order to line up with the runway.

### Pilot Qualifications and Ratings

Three pilots with varying backgrounds were selected for this research program. One pilot was highly experienced in flying the test airplane on various research programs. Another pilot was an experienced research pilot with no previous experience in a large jet airplane. The third pilot was new to flight research but had military experience on a multiengine jet airplane. The two pilots who were new to the test airplane were given 2 to 3 hours of instruction in this airplane including five or six landings before the start of this test program. At the end of the test program, six pilots from three airlines, FAA, and other NASA centers each made one flight to evaluate the effects of boundary-layer control on the airplane flying qualities.

In addition to describing their impressions of each configuration, the pilots rated each configuration numerically by using the Cooper pilot rating system shown in table II. Both the longitudinal and lateral control-force gradients were high for the experimental configurations tested. Furthermore, the trim switches were on the center console rather than on the control wheel. Therefore, it was decided that the pilots should try to disregard the control forces in making numerical ratings.

### Evaluation of Task Performance and Pilot Effort

To assess the relative amounts of pilot effort used or required to obtain a level of tracking accuracy for the various test configurations without referring to the high force gradient of the test airplane, an average rate of control application parameter was used. To minimize the effects on the analysis of lost motion in the control system and of inadvertent control inputs, incremental control motions of less than approximately 2 percent of total travel were not considered (2.5 percent of wheel travel). With this qualification, the absolute values of total control travel during a run were summed and divided by the duration of the run to obtain the average rate of control application. This procedure was applied to the control deflections of the column, wheel, rudder pedals, and either a throttle or thrust-modulating lever, depending on which mode of power control was used, for a given test configuration. The portion of each approach used for this analysis was from the first intercept of the glide-slope center line to the simulated

TABLE II. - COOPER PILOT RATING SYSTEM

Mode of operation	Adjective rating	Numerical rating	Description of rating	Primary mission accomplished	Can be landed
Normal	Satisfactory	1	Excellent, includes optimum	Yes	Yes
		2	Good, pleasant to fly	Yes	Yes
		3	Satisfactory, but with some mildly unpleasant characteristics	Yes	Yes
Emergency	Unsatisfactory	4	Acceptable, but with unpleasant characteristics	Yes	Yes
		5	Unacceptable for normal operation	Doubtful	Yes
		6	Acceptable for emergency condition only: failure of stability augments	Doubtful	Yes
Inoperable	Unacceptable	7	Unacceptable even for emergency condition: failure of stability augments	No	Doubtful
		8	Unacceptable - dangerous	No	No
		9	Unacceptable - uncontrollable	No	No
Inoperable	Catastrophic	10	Motions possibly violent enough to prevent pilot escape	No	No

breakout which included a time interval of 2 or 3 minutes depending on the approach speed. No restriction was put on trimming with stabilizer or trim tabs.

Accuracy of task performance was determined for the same intervals from the root-mean-square errors with respect to the glide slope and localizer center lines and from the preselected approach speed for each simulated ILS approach. The root-mean-square tracking errors were determined and are presented in feet (meters). The root-mean-square errors were also determined in millivolts which are proportional to glide-slope deviation in degrees from the desired approach path. Either index of tracking accuracy led to similar conclusions. It should be noted, however, that large errors early in the approach will bias the root-mean-square error in feet (or meters).

Landing-approach data from a series of runs are frequently analyzed in terms of the size of "windows" through which a reference point on the airplane passed at various ranges from the intended touchdown location. One set of data of this type was also determined for a range of 5000 feet (1527 meters) which corresponds to the airplane position just before transition from instrument to visual flight.

## RESULTS AND DISCUSSION

### Examples of Typical Instrument Landing Approach Data

Figures 1 to 3, each of which include four parts, present typical time histories of one hooded ILS landing approach for each of the three test configurations with stability augmentation on. All three runs were made by the same pilot. Figure 1 is for a run with  $30^\circ$  flap deflection with blowing off (configuration I). Figure 2 shows an approach with the flaps at  $50^\circ$  and a mass-flow coefficient  $C_\mu = 0.035$  to  $0.04$  (configuration II). Figure 3 shows a run for the third test configuration with  $60^\circ$  flap deflection and  $C_\mu = 0.09$  to  $0.10$ . Parts (a) and (b) of each figure show the landing approaches from about the time the localizer signal is acquired to touchdown. Parts (c) and (d) show the last minute including touchdown to an expanded time scale.

A comparison of glide slope and localizer errors for typical hooded approaches with and without powered lift is shown in figure 4. In this example the pilot tracked the localizer more closely in configuration III than he did for the configuration I approach. The glide-slope tracking was also as good for configuration III as for configuration I except that at the start of the run the pilot permitted the airplane to gain altitude during the transition to powered lift.

### Flying-Qualities Problem Areas

Although there were no large detrimental effects on flight characteristics resulting from flight at reduced speeds which was made possible by the use of powered lift, there were some areas where the handling qualities did noticeably deteriorate. These areas were related to Dutch roll, lateral directional cross coupling, and longitudinal trim changes in ground effect. It is felt that the deterioration of the handling qualities in these three areas was not a function of the particular test airplane but rather of inherent problem areas which must be considered during the STOL-type operation of jet transports made possible by the increased lift capability available with powered-lift systems of the type used.

Dutch roll. - It was apparent before the start of the test program that stability augmentation would be required to make the lateral and directional characteristics acceptable for landing approaches at the reduced approach speed of the powered-lift configuration. In fact, such augmentation would have been desirable at the higher approach speed used without powered lift. The Dutch roll damping which was very low for configuration I ( $\zeta \approx 0.03$ ) became negative ( $\zeta \approx -0.05$ ) at approximately the same speed for the powered-lift configurations II and III. As a result, it was difficult to make an approach at the reduced speeds of the powered-lift configurations without exciting the Dutch roll oscillation. However, by means of a sideslip rate damper which deflected the rudder, the

damping ratio with powered lift operating was increased for configuration III to about 0.15 which is low but is acceptable. Figure 5 shows these effects of powered lift and the  $\dot{\beta}$  damper on the Dutch roll damping ratio. A gradual reduction of damping was also indicated as the airspeed was reduced. Figure 6 presents time histories of roll rate which illustrate the lightly damped Dutch roll oscillations for the unaugmented basic airplane, the gradually divergent oscillations for the powered-lift configuration, and the improved damping of the oscillation for the powered-lift configuration with a sideslip rate damper. The period of the Dutch roll was 8 to 9 seconds as indicated in figure 5. A desirable feature of the sideslip rate damper was that it decreased the period slightly. In contrast, a yaw rate damper which produced the same damping ratio increased the period to 10 to 12 seconds. Additional Dutch roll data are presented in the appendix.

Cross coupling.- Preliminary evaluation also showed that for the powered-lift configurations, there was an appreciable amount of adverse sideslip during maneuvers. To relieve the pilot of the need for coordinating wheel and pedal inputs during turn entries or roll corrections, both a turn-coordination mode and a roll-decoupler mode of stability augmentation were provided. The turn coordinator supplied rudder deflection which was a lagged function of control wheel deflection. The roll decoupler supplied a favorable yawing moment proportional to rolling velocity. Figure 7 illustrates the response to step roll inputs with and without the stability augmentation. It is evident from the figure that adverse sideslip and a hunting roll response occurred with no augmentation. With stability augmentation, there was no adverse sideslip to oppose the roll response. Most of the low-speed landing-approach test program was flown with stability augmentation. In the following discussion, the lateral-stability augmentation should be considered to be in operation unless it is specified otherwise.

A comparison of approaches for configuration III with and without lateral-stability augmentation is presented in figure 8. The figure shows glide slope and localizer information from coordinate plotters. These data show that although the pilot had a good start with respect to the localizer with no augmentation, excessive wandering ( $\pm 200$  feet (60 meters)) developed halfway through the approach. The pilot was distracted from the task of following the localizer by the tendency for either control inputs or gusts to excite the slightly divergent Dutch roll oscillation. The unaugmented approaches were made in relatively smooth air with a 5-mile-per-hour crosswind. However, an objectionable amount of wandering in azimuth still developed on two of the three runs made. The tracking with respect to the glide slope was good on this approach except that the pilot flew too high while making lateral corrections from an altitude of 500 feet (150 meters) to the threshold. It is evident from the figure that for the last mile before touchdown the tracking error with respect to the localizer was much smaller with stability augmentation on. As a result of the Dutch roll and cross-coupling characteristics, no landings were made with augmentation off.

## Flare and Touchdown Characteristics

The flare and touchdown data for the three basic test configurations were analyzed to determine the control column deflection and force used for flaring and the changes in altitude, pitch attitude, airspeed, and rate of descent during the flare. Touchdown distance from the intended spot and flare duration were also determined. These data are presented in table III.

TABLE III.- FLARE AND TOUCHDOWN DATA

Run	Configuration	Pilot	h <sub>i</sub>		ΔV, knots	V <sub>t</sub> , knots	Distance beyond spot		h <sub>i</sub>		h <sub>t</sub>		ΔF <sub>max</sub>		Δδ <sub>c</sub> , deg	θ <sub>i</sub> , deg	θ <sub>t</sub> , deg	Δθ, deg	Δt, sec
			ft	m			ft	m	ft/min	m/sec	ft/min	m/sec	lb, pull	N					
2	I	A	35	10.7	2	124	800	244	510	2.58	0	0	26	116	4.5	3.5	4.5	1.0	13
3	II	A	110	33.5	3	104	100	30.5	500	2.53	120	.61	36	160	6	1.5	3.0	1.5	15
4	II	A	100	30.5	11	109	1500	457	510	2.58	60	.31	26	116	3	1.0	1.5	.5	13
5	II	A	90	27.4	1	102	250	76	480	2.43	140	.71	28	125	6.5	0	1.0	1.0	12
6	III	A	70	21.4	0	93	1000	305	520	2.65	100	.51	46	205	7.5	-1.0	2.0	3.0	14
7	III	A	100	30.5	5	89	0	0	550	2.80	80	.41	21	93	6.0	-1.0	2.0	3.0	14
8	I	B	70	21.4	1	123	175	53.5	400	2.03	100	.51	29	129	3.0	3.5	5.0	1.5	10
9	I	B	70	21.4	-2	123	250	76	380	1.93	0	0	30	133	3.5	3.5	4.5	1.0	13
10	I	B	80	24.4	-7	121	600	183	620	3.15	80	.41	43	191	6	4.0	4.5	.5	12
42	II	B	80	24.4	1	103	-100	-30.5	460	2.33	180	.91	30	133	5.5	1.5	3.5	2.0	17
11	II	B	70	21.4	-2	104	75	22.8	360	1.83	200	1.02	50	222	6.5	2.0	3.0	1.0	11
12	II	B	80	24.4	-1	102	800	244	540	2.75	160	.81	25	111	5.5	0	1.5	1.5	16
13	II	B	60	18.3	0	94	60	18.3	580	2.95	170	.86	40	178	6	-5	1.5	2.0	11
16	III	B	---	---	-5	92	---	---	470	2.38	190	.97	40	178	10.5	-1.0	2.0	3.0	12
17	I	C	110	33.6	-6	112	400	122	410	2.08	150	.76	11	49	5	2.5	4.0	1.5	15
18	I	C	130	39.6	-5	114	-25	-7.6	650	3.30	120	.61	20	89	3.5	2.5	4.0	1.5	14
19	I	C	70	21.4	-3	112	100	30.5	540	2.75	260	1.32	22	98	4	2.0	4.0	2.0	11
20	II	C	90	27.4	1	107	1000	305	460	3.33	100	.51	25	111	5	-1.0	1.0	2.0	14
21	II	C	100	30.5	-5	102	-100	-30.5	500	2.53	340	1.73	45	200	7.5	0	2.5	2.5	13
22	II	C	60	18.3	2	103	700	213	480	2.43	70	.36	40	178	7.5	1.5	2.5	1.0	12
24	III	C	90	27.4	-1	86	250	76	460	2.33	130	.66	54	240	8.5	-1.0	1.0	2.0	11
Averages	I		80	24.4	-3	118	370	113	500	2.53	100	0.51	26	116	4.2	3.0	4.3	1.3	13
			85	25.9	1	103	470	143	490	2.48	160	.81	35	156	6.0	.6	2.1	1.5	13
			90	27.4	0	90	420	128	500	2.53	130	.66	39	174	8.0	-1.0	1.8	2.8	13

On the average the flares were started at an altitude of 80 to 90 feet (24 to 27 meters) and a rate of descent of approximately 500 feet (150 meters) per minute. The average time interval from the start of the flare to touchdown was 13 seconds for all three configurations. The average rate of descent at touchdown was about 130 feet (40 meters) per minute. It is interesting to note that the most experienced pilot made the hardest touchdowns at 260 and 340 feet per minute (1.32 and 1.73 meters/second) apparently in the process of making spot landings. The average touchdown dispersion was about 400 feet (120 meters) either at about 90 knots with powered lift or at 120 knots without powered lift. (It should be noted, however, that only three touchdowns were recorded for configuration III.)

The pilots reported that the nose-down pitching moment due to ground effect occurred about 30 to 50 feet (9 to 15 meters) above the ground and that the trim change was larger for the powered-lift configurations. The average control force required during the flare was about 25 pounds (110 newtons) at 120 knots and 40 pounds (180 newtons) at 90 knots with powered lift. The average control column input required to flare was about 4° at 120 knots or 8° at 90 knots with powered lift. Examples of the variation of elevator deflection with altitude during the flare which are presented in figure 9 also show that the elevator deflections used to flare were about twice as great with powered lift. However, it is not certain how much of the increased deflection is due to a nose-down trim change caused by ground effect, and how much is simply due to the reduced approach speed of the powered-lift configuration.

### Sidestep Maneuvers

One sidestep maneuver was made in each test configuration with stability augmentation on. Sidesteps of about 200 feet (60 meters) were started from a simulated breakout at an altitude of 150 to 200 feet (45 to 60 meters) above the runway. This type of maneuver is not permitted by some airlines, but it does provide a good measure of maneuverability near the ground. In this program a sidestep from breakout to touchdown was completed successfully for each test configuration on the first attempt. Several parameters measured for the two segments of the sidesteps are:

Configuration	V, knots	Weight		Initial offset		$\Delta t$ , sec	$\Delta \phi$ , deg (*)	$\Delta \psi$ , deg	$\Delta \delta_w$ , deg	$\Delta \delta_p$	
		lb	N	ft	m					in.	cm
I	111	$146 \times 10^3$	$655 \times 10^3$	210	65	26	-4	-8	10	-0.4	-1.0
							8	3	-15	.4	1.0
II	95	$142 \times 10^3$	$636 \times 10^3$	225	69	30	-7	-9	10	-.2	-.5
							7	0	-5	.15	.38
III	85	$135 \times 10^3$	$605 \times 10^3$	215	66	30	-3	-5	15	-.2	-.5
							5	5	-15	.4	1.0

\*  $\Delta$  values measured from approximate trim or initial value.

These data indicate that the sidestep was made with a smaller bank angle at the reduced speed of configuration III. However, the maneuver requires precise control application as indicated in part by the fact that touchdown occurred within about 3 seconds after completion of the sidestep. On all three sidestep runs, the airplane landed well beyond the intended touchdown point 1500 feet (460 meters) from the threshold. Touchdown occurred 2600 feet (800 meters) beyond the threshold for configuration I, 2300 feet (700 meters) for configuration II, and 2100 feet (640 meters) for configuration III.

## Asymmetric Power Effects

Several runs were made with the glide slope displaced upward about 1500 feet (460 meters) to investigate the transient effects of loss of an outboard engine in the powered-lift configurations. One outboard throttle was cut midway down the glide slope. No appreciable loss in lift or abrupt rolling tendency was encountered. The pilot was able to maintain the approach speed on the 3° glide slope, but on the experimental test configuration three engines did not supply enough power for level flight in configuration III. For configuration III, the approach speed was also below the minimum straight and level (three-engine) directional control speed. After the simulated loss of an engine in configuration III, the pilot maintained control with less than 5° sideslip by gradually moving the rudder to full deflection as he increased the thrust of the other three engines.

### Task Performance and Control Input Rates

To supplement pilot opinion about the various test configurations, an analysis was made of the amount of control activity and of the root-mean-square tracking errors with respect to the glide path, localizer, and preselected approach airspeed. Table IV shows the tracking accuracy and table V shows the average control input rates for 24 approaches for the three basic test configurations with stability augmentation on. Table VI presents average values of tracking performance and control activity parameters for each configuration by each pilot and for each configuration by all three pilots and vice versa. Tables VII and VIII are similar to tables IV and V, but show task performance and control activity data for landing-approach runs made to investigate the effects of using automatic speed control, and of operating without stability augmentation.

Several plots are presented to illustrate the tabulated data. Figure 10 shows plots of root-mean-square glide-slope error against column input rate and root-mean-square localizer error against wheel input rate for the three basic test configurations. Figure 11 shows similar data for configuration II with automatic speed control and for configurations I and III with the lateral-stability augmentation off.

Glide path. - The data of table IV and figure 10 indicate that the root-mean-square errors from the glide slope ranged from 15 to 90 feet (4.6 to 27.4 meters). The overall tracking-error averages of table VI for 24 approaches for three basic test configurations with stability augmentation on show that the average root-mean-square deviation from the glide path was 51 feet (15.5 meters). The average values of tracking errors for the three basic test configurations varied about ±20 percent, an amount which is likely to be insignificant. It is interesting to note that during a few runs (not shown) made with doubled glide-slope sensitivity, the glide-slope deviations were approximately inversely proportional to the sensitivity. However, the pilots noticed and objected to the more sensitive glide-slope error indication because any benefit from more accurate

TABLE IV. - TRACKING ACCURACY FOR ILS LANDING APPROACHES WITH AND WITHOUT POWERED LIFT

Test conditions								Tracking accuracy, root-mean-square deviation from -				Breakout window at 5000 ft (1527 m) range				
Run	Configuration	Pilot	Weight		Wind*		Selected airspeed, knots	Glide slope		Localizer		Airspeed, knots	Vertical error		Lateral error	
			lb	N	Speed, knots	Quarter, deg		ft	m	ft	m		ft	m	ft	m
1	I	A	172 × 10 <sup>3</sup>	765 × 10 <sup>3</sup>	2	270	120	76.6	23.4	59.1	18.0	4.4	8	2.4	58	17.7
2	I	A	168	747	0	270	119	76.0	23.2	194.2	59.3	4.8	34	10.4	-46	-14.0
3	II	A	159	707	5	270	101	31.5	9.6	54.6	16.7	3.2	10	3.0	58	17.7
4	II	A	154	685	5	270	99	27.3	8.3	90.0	27.4	3.3	-12	-3.7	-28	-8.5
5	II	A	151	672	0	240	98	35.6	10.9	68.8	21.0	3.1	30	9.1	62	18.9
6	III	A	145	645	0	240	87	88.9	27.1	157.1	48.0	6.2	54	16.5	16	4.9
7	III	A	141	627	4	225	86	51.0	15.5	90.2	27.3	2.1	3	.9	30	9.1
8	I	B	170	756	10	210	124	30.2	9.2	90.1	27.4	2.8	** -42	-12.8	-8	-2.4
9	I	B	167	743	10	195	123	37.2	11.4	99	30.2	3.2	-50	-15.2	12	3.7
10	I	B	164	729	9	190	122	46.6	14.2	148.1	45.2	2.9	-50	-15.2	-22	-6.7
11	II	B	157	698	10	180	103	85.8	26.1	164.8	50.2	2.8	-78	-23.8	40	12.2
12	II	B	154	685	10	240	102	27.9	8.5	48.9	14.9	1.7	-22	-6.7	16	4.9
13	II	B	141	627	4	90	96	23.5	7.2	256.6	78.2	1.8	18	5.5	-136	-41.5
14	III	B	163	725	0	60	95	57.3	17.5	134.8	41.0	2.6	-78	-23.8	-60	-18.3
15	III	B	159	707	0	345	93	55.8	17.0	105.9	32.2	3.1	-46	-14.0	-80	-24.4
16	III	B	154	685	0	30	93	83.0	25.3	149.6	45.6	9.1	-8	-2.4	-12	-3.7
17	I	C	149	663	5	90	116	44.5	13.6	134.4	41.0	2.5	13	4.0	78	23.8
18	I	C	145	645	5	90	115	64.9	19.8	48.0	14.6	1.8	6	1.8	12	3.7
19	I	C	143	636	5	90	114	28.9	8.8	74.9	22.8	1.9	19	5.8	16	4.9
20	II	C	168	747	6	160	105	27.9	8.5	113.0	35.4	2.7	-31	-9.4	20	6.1
21	II	C	164	729	5	135	104	37.6	11.5	140.7	42.9	3.0	4	-1.2	40	12.2
22	II	C	160	711	6	160	103	51.6	15.7	58.4	17.8	3.1	-12	-3.7	-2	-6
23	III	C	141	627	3	105	90	15.6	4.7	89.9	27.4	1.9	0	0	8	2.4
24	III	C	139	618	3	105	89	72.0	22.0	47.1	14.3	5.4	0	0	32	9.8

\*Runway heading is 280°.

\*\*Pilot B flew below the glide slope deliberately near the breakout altitude.

TABLE V.- CONTROL ACTIVITY FOR ILS LANDING APPROACHES  
WITH AND WITHOUT POWERED LIFT

Run	Configuration	Pilot	Control inputs, long-term average rate, deg/sec						
			Column	Wheel	Power*		Rudder		
					Throttle	Reverser	Pilot (**)	Augmenter (***)	Total
1	I	A	0.134	0.596	0.40		0.547	0.34	0.891
2	I	A	.074	1.384	.246		.166	.68	.844
3	II	A	.069	1.282		0.178	.123	.60	.726
4	II	A	.057	2.063		.095	.251	.91	1.162
5	II	A	.051	2.630		.147	.287	.61	.900
6	III	A	.075	2.380		.184	.309	.53	.843
7	III	A	.100	2.236		.170	.542	.60	1.138
8	I	B	.403	3.96	.210		.477	1.63	2.113
9	I	B	.616	2.25	.248		.387	1.65	2.035
10	I	B	.321	3.62	.150		.440	2.01	2.45
11	II	B	.632	4.01		.302	.476	2.63	3.103
12	II	B	.440	3.99		.247	.281	2.48	2.759
13	II	B	.559	4.28		.614	.377	1.32	1.699
14	III	B	.358	2.58		.885	.180	.91	1.092
15	III	B	.353	2.57		1.405	.326	1.01	1.335
16	III	B	.497	1.82		.790	.307	1.10	1.405
17	I	C	.147	1.865	.587		.066	.86	.921
18	I	C	.161	1.378	.283		.033	.62	.654
19	I	C	.104	2.385	.262		.233	.83	1.062
20	II	C	.311	2.39		.491	.147	1.79	1.943
21	II	C	.214	2.38		.408	.056	1.51	1.566
22	II	C	.305	2.14		.482	.037	1.62	1.658
23	III	C	.208	1.04		.277	0	.32	.322
24	III	C	.210	1.285		.884	0	.40	.422

\*For each throttle or reverser for I and II. Outboard reversers only for III.

\*\*Measured at pedal. Converted to equivalent rudder deflection.

\*\*\*Obtained by subtraction.

TABLE VI.- SUMMARY OF TRACKING ACCURACY AND CONTROL ACTIVITY DATA

Configuration	Average tracking error, root mean square								Average control input rate, deg/sec			
	Pilot						Configuration average	Pilot			Configuration average	
	A	B	C		A	B		C				
	Glide-slope deviation, root mean square								Control column, for increments greater than 1/2°			
ft	m	ft	m	ft	m	ft	m					
I	76	23.2	38	11.6	46	14.0	53	16.2	0.10	0.45	0.14	0.23
II	32	9.8	46	14.0	39	11.9	39	11.9	.06	.54	.28	.29
III	70	21.5	65	19.8	44	13.4	60	18.3	.09	.40	.21	.23
Average	59	18.0	50	15.2	43	13.1	51	15.5	.08	.46	.21	.25
	Localizer deviation, root mean square								Control wheel, for increments greater than 5°			
	ft	m	ft	m	ft	m	ft	m				
I	127	38.7	134	40.8	86	26.2	116	35.4	1.0	3.3	1.9	2.1
II	71	21.6	157	47.8	104	31.7	111	33.8	2.0	4.1	2.3	2.8
III	124	37.8	130	39.6	68	20.7	107	32.6	2.3	2.3	1.2	1.9
Average	107	32.6	140	42.7	86	26.8	111	33.8	1.8	3.2	1.8	2.3
Airspeed deviation root mean square, knots												
I	4.6		3.0		2.1		3.2					
II	3.2		2.1		2.9		2.7					
III	4.2		4.9		3.6		4.2					
Average	4.0		3.3		2.9		3.4					
Test conditions												
Configuration	Pilot								Pilot			
	A		B		C		Average		A	B	C	Average
	Airplane weight, average								Selected approach airspeed, average, knots			
	lb	N	lb	N	lb	N	lb	N				
I	170 × 10 <sup>3</sup>	760 × 10 <sup>3</sup>	167 × 10 <sup>3</sup>	743 × 10 <sup>3</sup>	146 × 10 <sup>3</sup>	649 × 10 <sup>3</sup>	160 × 10 <sup>3</sup>	712 × 10 <sup>3</sup>	120	123	115	119
II	155	695	151	672	164	729	157	698	99	101	104	101
III	143	640	159	707	140	623	147	654	87	94	90	90

TABLE VII.- TRACKING ACCURACY FOR ILS LANDING APPROACHES, SUPPLEMENTARY CONFIGURATIONS

Test conditions								Tracking accuracy, root-mean-square deviation from -					Breakout window at 5000 ft (1527 m) range			
Run	Configuration	Pilot	Weight		Wind		Selected airspeed, knots	Glide slope		Localizer		Airspeed, knots	Vertical error		Lateral error	
			lb	N	Speed, knots	Quarter,* deg		ft	m	ft	m		ft	m	ft	m
With autospeed and lateral augmentation																
25	II	A	157 × 10 <sup>3</sup>	698 × 10 <sup>3</sup>	10	165	100	42.6	13.0	100.4	30.6	1.3	38	11.6	-12	-3.7
26	II	A	154	685	11	140	99	50.9	15.5	53.5	16.3	1.3	12	3.7	12	3.7
27	II	B	158	703	4	90	103	34.4	10.5	175	53.3	1.0	-34**	-10.4	52	15.9
28	II	B	161	716	0	120	104	40.0	12.2	127.2	38.8	1.0	-14	-4.3	16	4.9
29	II	C	150	667	5	90	98	38.8	11.8	28.4	8.7	.75	26	7.9	16	4.9
Augmentation off																
30	I	A	169 × 10 <sup>3</sup>	752 × 10 <sup>3</sup>	5	160	119	58.8	17.9	90.4	27.6	4.1	10	3.0	-160	-48.8
31	I	A	167	743	6	160	118	67.0	20.4	199	60.6	2.6	-58	-17.7	-84	-25.6
32	I	A	164	729	5	135	117	62.5	19.1	118	36.0	4.3	-10	-3.0	-60	-18.3
33	III	A	160	711	4	135	92	34.6	10.6	192.9	58.9	4.2	26	7.9	72	21.9
34	III	A	153	681	5	160	90	88.9	27.1	191.6	58.4	6.8	6	1.8	40	12.2
35	III	A	150	667	6	160	89	36.7	11.2	155.7	46.5	3.1	53	16.2	-124	-37.8

\*Runway heading is 280°.

\*\*Pilot B deliberately flew below the glide path at breakout to reduce touchdown dispersion.

TABLE VIII.- CONTROL ACTIVITY FOR ILS LANDING APPROACHES, SUPPLEMENTARY CONFIGURATIONS

Run	Configuration	Pilot	Control inputs, average rate						
			Column	Wheel	Power*		Rudder		
					Throttle	Reverser	Pilot	Augmenter (**)	Total (***)
With autospeed and lateral augmentation									
25	II	A	0.28	2.54		0.60	0.24	1.3	1.59
26	II	A	.40	4.04		.82	.53	1.3	1.87
27	II	B	.159	1.208		.317	.048	.43	.483
28	II	B	.386	2.553		.517	.038	.56	.600
29	II	C	.230	.469		.461	0	.24	.242
Augmentation off									
30	I	A	0.10	3.01	0.51		0.47	0	0.33
31	I	A	.09	3.37	.18		.69	0	.54
32	I	A	.08	2.26	.18		.45	0	.42
33	III	A	.12	4.01		0.15	.26	0	.19
34	III	A	.22	3.57		.15	.26	0	.26
35	III	A	.04	3.99		.07	.19	0	.17

\*For each throttle or reverser for I and II. Outboard reversers only for III.

\*\*Not measured directly.

\*\*\*Measurement of total rudder deflection is believed to be considerably more accurate than that of pilot input.

tracking of the glide slope was not considered great enough to justify the increased workload.

The pilot effort or control input rate parameter shown in table V and figure 10 was not greatly affected by configuration. The overall average column rate for 24 runs was 0.25 degree per second (neglecting motions smaller than 2 percent of total travel).

Localizer.- For the localizer, where one needle width on the cockpit indicator represents over three times as large an error as on the glide slope, the root-mean-square errors were much larger and ranged from about 50 to 250 feet (15.2 meters to 76 meters). The effects of configuration changes were not large enough to be obvious from these data. The average root-mean-square localizer deviation for 24 runs was 111 feet (33.8 meters) with no significant difference between the three configurations as shown in table V and figure 10. The average rate of wheel deflection was 2.3 degrees per second.

The pilot comments included little reference to the use of rudder during the landing approach. Insofar as possible, use of the rudder was minimized in normal (coordinated) banking and turning maneuvers. Rudder input data for individual runs are shown in table V and averaged in table VIII. With stability augmentation on, only 30 percent or less of the rudder inputs were pilot induced. In fact, one pilot supplied less than 5 percent of the rudder inputs.

Approach speed.- The overall average root-mean-square deviation from the target approach speed was 3.4 knots. Power settings were made with the throttles for configuration I and with the similar thrust modulator levers, which had about the same deflection range, for the powered-lift configurations II and III.

Comment on task performance (augmentation on).- From an examination of three basic pilot input parameters and three airplane response error parameters, it appears that with stability augmentation for the powered-lift configurations, all three test configurations could be flown on an IFR landing approach with the same level of physical effort with only minor variations in task performance.

It was found that of the three pilots, the one with the most experience in this airplane had the most consistent root-mean-square deviations in task performance. His control input rates were close to the three pilot average. Of the other two pilots, one moved the controls energetically in an attempt to minimize errors whereas the other adopted more of a wait-and-see attitude between control inputs. When individual runs for the same configuration are compared, there was a ratio of up to 10 to 1 for column inputs and 7 to 1 for wheel input activity between the three pilots.

Task performance, stability augmentation off.- Landing approaches with stability augmentation off in configurations I and III were made by one pilot. The requirement for

stability augmentation was greater for configuration III which permitted lower approach speeds. The data of tables V and VIII or figures 10 and 11 show that the pilot (pilot A) worked harder at lateral control by approximately a factor of two with no stability augmentation. In addition, for configuration III the average root-mean-square deviation from the localizer was increased more than 50 percent (to 180 feet (55 meters)) with augmentation off. The root-mean-square values of glide-slope deviation were actually slightly less with the lateral stability augmentation off, perhaps as a result of the additional experience the pilot had had in this airplane since making the runs with augmentation on. The pilot who flew the unaugmented configurations assigned them slightly poorer Cooper ratings. The smooth-air rating of 3.6 for the unaugmented configuration III seems to be somewhat more favorable than might be expected for a case where, in spite of a 100-percent increase in lateral-control activity, the root-mean-square localizer tracking error increased over 50 percent to 180 feet.

Task performance, breakout window.- The breakout window data of figure 12 and table IV show that except for one case, the reference point on the nose gear passed through a square which was about 150 feet (47 meters) on a side. No consistent effect of configuration was apparent. It should be noted again that one pilot intentionally flew below the glide path at the breakout point. The airplane was very accurately positioned with respect to the glide slope on three of the four runs in configuration III by the other two pilots.

Breakout window data for the supplementary test configurations are presented in figure 13 and table VII. With augmentation off, the lateral errors were larger (80 to 160 feet or 25 to 50 meters) on three of the six runs for both configurations I and III.

#### Evaluation of Automatic Speed Control

During the program, tests were conducted to determine whether it was possible to improve glide path and speed control during the powered-lift airplane approaches. One of the systems investigated which appeared to offer considerable promise was an automatic speed control. In operation, the actual speed is compared with a reference speed selected by the pilot and the thrust modulators are automatically adjusted to obtain the correct reference speed. To anticipate speed changes and provide damping of the system, longitudinal-accelerometer, vertical-gyro, and pitch-rate-gyro inputs are also used.

The data of table VII for runs made with use of automatic speed control with configuration II showed speed control within 1 knot root mean square compared with about 3 knots when manual thrust modulation is used. The pilots generally felt that their work load was reduced with automatic speed control. The average Cooper rating (from two pilots) was improved from 3.4 to 2.9. However, since the pilot no longer could anticipate trim changes due to thrust modulation for this particular installation, some unfavorable comments were received. The data of table VII and figure 11 did not show any significant

reduction either in errors with respect to the 3° glide-slope pattern or in control-column activity as a result of using automatic speed control.

### Pilot Ratings

In addition to describing their impressions of each configuration, the pilots rated each configuration numerically by using the Cooper pilot rating system which was shown in table II. Table IX summarizes the overall pilot ratings for simulated instrument flight on the landing approach.

TABLE IX.- SUMMARY OF COOPER RATINGS

Configuration	Pilot			Average
	A	B	C	
With stability augmentation				
I	3.0	3.5	3.4	3.3
II	3.0	3.7	3.5	3.4
III	3.2	4.0	3.6	3.6
Without stability augmentation				
I	3.2			
II	---			
III	3.6			
With automatic speed control and stability augmentation				
II	3.0	2.8	---	2.9

As shown by the average pilot ratings, the pilots considered the flying qualities of the augmented configurations I and II to be slightly better than the minimum level for satisfactory flying qualities. Configuration III was considered to be slightly below the minimum level for satisfactory handling qualities. The pilots felt that the reduced approach speeds of the powered-lift configurations would be desirable if other characteristics remained constant. However, the increased control deflections and larger control forces required with configurations II and III for both pitch and roll corrections were considered to be undesirable.

### Comments on Requirements for Satisfactory Flying Qualities

Based on the results of this research program, the requirements for satisfactory flying qualities of powered lift or STOL airplanes similar to the one tested are likely to

be largely the same as those for current large jet transports. At present, the most nearly adequate source of flying-qualities requirements is still reference 3 which is a military specification. Some proposed revisions to the requirements of reference 3 are discussed in reference 4.

Methods of defining boundaries for satisfactory Dutch roll damping and satisfactory pitch response for large transport airplanes are still not well established. However, the results of the present program indicate that it is likely to be more difficult to obtain satisfactory pitch response and pitch trim characteristics, adequate Dutch roll damping, and minimized adverse sideslip characteristics without stability augmentation as STOL capability is built into the large jet transport.

## CONCLUSIONS

The following conclusions were reached with respect to effects of reduced approach speed and of the type of powered lift used on the flying qualities of a jet transport for the instrument landing approach:

1. Use of either powered lift or reduced approach speeds had a destabilizing effect on the Dutch roll mode. A configuration intended for use with this type of boundary-layer control should be designed to compensate for the possible reduction in Dutch roll damping due to either reduced approach speed or boundary-layer control. This result may be most easily obtained by means of stability augmentation such as a sideslip rate damper.

2. At the reduced airspeeds made possible with powered lift, adverse sideslip became objectionable and required stability augmentation to compensate for adverse yawing moments due to lateral-control deflection and roll rate.

3. A reduction of approach speed from about 120 knots to about 90 knots was achieved with powered lift. At the reduced approach speed, the angular rate response about all three axes was somewhat more sluggish. With stability augmentation to improve Dutch roll damping and reduce adverse sideslip, the flying qualities for instrument landing approach were then slightly degraded from those of the conventional jet-transport configuration.

4. Average values of both the tracking errors with respect to the localizer and glide path and the pilot control input rates were approximately equal for the conventional jet-transport configuration and for the slower flying powered-lift configuration.

5. The pitching moment due to ground effect was larger for the powered-lift configuration so that, including the effects of reduced speed, the elevator deflection required to flare was approximately double the value for the conventional jet-transport configuration or about  $8^\circ$  compared with  $4^\circ$ .

6. Requirements for satisfactory flying qualities for the landing approach which apply to conventional jet transports are likely also to apply for the type of powered-lift configuration tested.

Langley Research Center,  
National Aeronautics and Space Administration,  
Langley Station, Hampton, Va., March 25, 1968,  
126-62-01-08-23.

## APPENDIX

### DESCRIPTION OF TEST AIRPLANE, STABILITY AND CONTROL CHARACTERISTICS, AND INSTRUMENTS

#### Basic Airplane

The airplane used in the investigation was a large four-engine jet transport, typical of subsonic types currently in commercial service, with several modifications to provide high-lift capability and to improve flying qualities at low speeds. The general arrangement of the airplane is shown in figure 14 and a photograph of the airplane is given in figure 15. Weight and moment-of-inertia characteristics are indicated in figure 16.

The airplane was powered by four wing-pod-mounted JT3D-1 turbofan engines of approximately 17 000 pounds (76 000 newtons) thrust each. Annular slotted intakes shown in the photograph of figure 17 were provided to avoid inlet separation at high flow angles possible at the low speeds.

#### Wing Modifications

The 35° swept wing was extensively modified for the high-lift program. Leading-edge devices installed included a fixed slat from the wing tip to the inboard engine pylon, and a fixed cambered Kreuger-type flap from the inboard pylon halfway to the fuselage. The trailing edges of the flaps were extended, and thus increased the wing root chord and provided an additional wing area of 17 percent.

Lateral control was provided by outboard ailerons and spoilers. The ailerons, which were tab operated, had a span equal to 28 percent of the wing semispan and a chord equal to 18 percent of the wing chord. Basic aileron deflection characteristics were modified to improve the lateral-control characteristics for small wheel inputs at low speeds and the results based on flight measurements are shown in figure 18. The four-panel spoilers were located immediately forward of the flaps. Spoiler deflection characteristics are presented in figure 19. Average control wheel force characteristics for the range of test airspeeds are shown in figure 20.

The trailing-edge flap was a simple hinged or plain flap rather than double slotted as on production 707 airplanes. It extended from the fuselage 68 percent of the wing semispan. The average flap chord to wing chord ratio was 22.2 percent. The maximum flap deflection was 85°.

## APPENDIX

### Horizontal Tail

To improve longitudinal stability and trim characteristics of the boundary-layer-control configuration, a horizontal tail having 25 percent more area than that originally provided was installed. A full-span inverted slat on the leading edge also helped to compensate for the large nose-down pitching moment encountered at high lift. Longitudinal trim was obtained by the normal stabilizer adjustment. The elevators were actuated indirectly by a control tab which was manually operated. Elevator forces and deflection characteristics are given in figure 21.

### Rudder

The rudder is hydraulically powered with emergency manual tab backup provision. The rudder-deflection characteristics are shown in figure 22 and the rudder pedal force characteristics are shown in figure 23. The stability-augmentation system deflected the rudder independently of the pilot as is discussed more fully in the stability-augmentation-equipment section.

### Powered-Lift System

The operation of the powered-lift system is illustrated in figure 24. The boundary-layer-control air was bled from each of the four engine compressors into two separate ducting systems. Each ducting system covered the full span of the flaps. The boundary-layer-control blowing nozzles alternated between these two distribution ducts to minimize the loss of lift in the event of failure of one of the systems. These nozzles blew air out through the ejector, entrained secondary air, and increased the blowing momentum by approximately 30 percent.

### Thrust-Modulation System

In order to operate the engines at the high power settings required for the boundary-layer-control system and still obtain the low thrust required for the landing-approach condition, the thrust-modulation system shown in figure 25 was used.

The clamshell-type thrust reversers (see fig. 26) located in each of the four primary engine tailpipes were used for modulation and were modified to be manually controllable through their entire operation range from maximum thrust to essentially idle thrust by the set of four levers located on the pilots' console shown in figure 27.

This thrust-modulation system was used in place of the throttle for all powered-lift tests and offered a very powerful and fast-acting thrust control during the landing approach. A comparison of the difference in the rate of response through normal throttle control and modulator control is shown in figure 28.

## APPENDIX

### Automatic Speed Control

The thrust-modulation system was also used in conjunction with an automatic speed control system in some of the flights to stabilize airspeed during landing approaches. Figure 29 shows a block diagram of the automatic speed control system. In operation, the actual airspeed was compared with the reference airspeed selected by the pilot, and the modulators were automatically adjusted as required. To anticipate speed changes and to provide damping for the system, longitudinal-accelerometer, vertical-gyro, and pitch-rate-gyro inputs were also used in the system.

### Stability-Augmentation Equipment

Stability-augmentation devices were incorporated into the rudder-control system to improve the low-speed handling qualities. These stability-augmentation devices were designed to operate independently from the pilot so that their operation would not be felt by the pilot in his rudder control. For safety of flight, the control authority of the augmentation devices was limited to a small portion of that available to the pilot. During the initial tests, the stability-augmentation rudder authority was initially  $\pm 4^\circ$ , but when it was found that the stability-augmentation equipment was saturating during some of the maneuvers, this authority was extended to  $\pm 9^\circ$ .

The following stability-augmentation devices were used during the flight-test program:

Sideslip rate damper.- The sideslip rate damper  $\Delta C_{n\dot{\beta}}$  deflected the rudder proportionally to the rate of change of sideslip angle. This system increases the damping of the Dutch roll oscillation without affecting the other lateral-directional dynamic characteristics of the airplane. The rate of change of sideslip angle was obtained with an electrical differentiator by using an input signal from a sideslip vane.

Roll decoupler.- The roll decoupler ( $\Delta C_{n\dot{p}}$  with lag network) deflected the rudder proportionally to roll rate as indicated by the roll-rate gyro to overcome the dynamic adverse yaw (yaw due to roll rate) which is particularly strong in low-speed high-lift flight.

Turn coordinator programmer.- The turn coordinator programmer ( $\Delta C_{n\delta_a}$  with lag network) deflected the rudder proportionally to the lateral-control deflection in order to quicken the airplane's entry into a turn and to reduce the buildup of adverse sideslip on turn entry. Since the buildup of sideslip begins only after the airplane has started to roll, a small time lag is incorporated for better rudder phasing.

During the initial flight tests at Langley, brief tests were conducted to obtain near optimum values and combinations of the stability-augmentation equipment for the flight

## APPENDIX

program. The resulting transfer functions determined for each of the stability-augmentation systems along with simple block diagrams of the systems are shown in figure 30.

### Instrumentation

Instrumentation was provided in the airplane for the recording of all in-flight information required for evaluation of the test results and for correlation with pilot opinions. Two data acquisition systems were employed to record the data on magnetic tape.

One system, a frequency modulation system, obtained continuous records of high frequency or transient functions. In the data reduction, values from these records could be obtained continuously. The other system, a pulse-duration modulation system, recorded quasi-static variables at a rate of 2.5 samples per second.

These functions and the accuracies recorded by the tape systems are indicated in table X. In addition, the following functions were recorded by oscillograph for preliminary evaluation and selection of the portions of the flight-test data to be specifically processed:

Lateral acceleration (at center of gravity)	Thrust-modulator position (engine 2)
Longitudinal acceleration (at center of gravity)	Roll attitude
Angle of attack	Pitch attitude
Roll rate	Control-column force
Yaw rate	Control-column position
Pitch rate	Rudder-pedal-arm position
ILS glide-path error	Control-wheel position
ILS localizer error	Control-wheel force
Throttle position (engine 1)	Rudder-pedal force
Throttle position (engine 2)	Sideslip differential pressure
Indicated airspeed	Normal acceleration (at center of gravity)
Pressure altitude	Flap handle position
Thrust-modulator position (engine 1)	

An airborne theodolite was installed on the airplane for acquisition of data by photographing the runway and runway markers during the final phase of the landing approach and the touchdown. The camera was installed on the lower forward fuselage of the airplane just aft of the nose wheels and is shown in figure 31. The following variables were obtained from the photographic records: (1) forward speed, (2) altitude, (3) sinking speed, and (4) pitch attitude. In order for the data obtained to be accurate, it was necessary for the airplane to follow the runway center line with wings level.

TABLE X.- INSTRUMENTATION FUNCTIONS RECORDED ON TAPE

Type of data	Function	Approximate accuracy
Pulse duration modulation	Control-column force	±3 lb (13.5 N)
Pulse duration modulation	Control-wheel force	±2 lb (9 N)
Pulse duration modulation	Rudder-pedal force	±8 lb (36 N)
Pulse duration modulation	Control-column deflection	±0.6°
Pulse duration modulation	Control-wheel deflection	±4.3°
Pulse duration modulation	Rudder-pedal-arm deflection	±0.16 in. (4 mm)
Pulse duration modulation	Throttle positions	±2°
Pulse duration modulation	Thrust-modulator positions	±1°
Pulse duration modulation	Flap setting	±3°
Frequency modulation	Aileron deflection	±1°
Frequency modulation	Elevator deflection	±1°
Frequency modulation	Rudder deflection	±1°
Pulse duration modulation	Stabilizer deflection	±0.5°
Pulse duration modulation	Spoiler deflection	±1°
Pulse duration modulation	Indicated airspeed	±1 knot
Pulse duration modulation	Pressure altitude	±150 ft (45.72 m)
Frequency modulation	Angle of attack ±0.25° repeatability	±1° absolute
Pulse duration modulation	Sideslip ±0.25° repeatability	±1° absolute
Pulse duration modulation	Pitch attitude	±1°
Pulse duration modulation	Roll attitude	±3°
Pulse duration modulation	Normal acceleration	±0.05g
Frequency modulation	Longitudinal acceleration	±0.02g
Frequency modulation	Lateral acceleration	±0.02g
Frequency modulation	Roll rate	±1.0°/sec
Frequency modulation	Pitch rate	±0.8°/sec
Frequency modulation	Yaw rate	±0.8°/sec
Frequency modulation	Glide-path error	±0.1°
Frequency modulation	Localizer error	±0.2°
Pulse duration modulation	Fuel consumed	±0.5 percent

## APPENDIX

### GSN-5 Instrument Landing System

In the flight program, the final pilot evaluation tasks for each configuration tested were simulated instrument-flight rules or hooded approaches to landing. These approaches were made by using guidance from a modified GSN-5 radar unit shown in figure 32. This unit consists of a precision tracking K-band radar, a flight-path computer, and a data link to normal ILS indicators in the aircraft cockpit.

In operation, the equipment provided satisfactory simulation of a normal ILS type of localizer and glide slope. Typical radar approach system coordinate boundaries or sensitivities as used in the flight program for a  $3^{\circ}$  glide slope are compared with normal ILS glide path and localizer profiles in figure 33. The GSN-5 system is equipped for variation of nominal glide paths, horizontal offsets from the runway center line, and vertical offsets from runway level.

During the test program for special runs, the glide slope was varied from  $3^{\circ}$  to  $9^{\circ}$ , the horizontal offset from 0 to 200 feet (0 to 60 meters) to the right, and the vertical offset from altitudes of 0 to 1500 feet (460 meters). This equipment was further equipped to supply ground-based data records of the position coordinates X,Y and X,Z for the airplane position during the landing approach.

The only airborne installation required on the airplane for use of the GSN-5 approach system was the installation of the corner reflector shown in figure 34. This reflector was mounted on the nose-wheel strut in the place normally used for the installation of the airplane's taxi lights.

### Stability and Control Characteristics

The following data document the stability and control characteristics of the test airplane. Most of these data were obtained before the test configurations were selected for the landing-approach program. As a result, this appendix often shows powered-lift data with flaps at  $50^{\circ}$  and  $70^{\circ}$  rather than the maximum flap deflection of  $60^{\circ}$  which was used in the landing-approach program.

Longitudinal stability and control.- The longitudinal characteristics of the airplane are presented in figures 35 through 41. The dynamic longitudinal motions were investigated at flap deflections of  $50^{\circ}$  and  $70^{\circ}$  with maximum powered lift. Elevator-step and pulse inputs were applied from an initial trim speed of  $1.2V_S$ . The characteristics were very similar for all powered-lift configurations. The period of the phugoid was approximately 31 seconds with a damping ratio of 2.9 percent, and the period of the short-period motion was approximately 4 seconds with heavy damping ( $\zeta > 0.7$ ). The period of the phugoid of the airplane without powered lift and  $30^{\circ}$  flap deflection was approximately

## APPENDIX

49 seconds with a damping ratio of 28.2 percent. The short-period motion had a period of approximately 6 seconds and a damping ratio of 70 percent.

The static longitudinal stability was determined for various flap and boundary-layer-control configurations. The airplane was trimmed with the stabilizer at approximately  $1.3V_S$  with powered lift on, and the speed was varied with the elevator through the  $1.1V_S$  to  $1.5V_S$  range. The static longitudinal stability was satisfactory for all configurations investigated. Stick-free and stick-fixed longitudinal results are given in figures 35 and 36 for the condition of  $30^\circ$  flap deflection with no powered lift, and for  $50^\circ$  and  $70^\circ$  flap deflections with maximum powered lift ( $C_{\mu} \approx 0.09$ ). Stick-fixed static longitudinal stability characteristics of the airplane for flight-test configurations I, II, and III are also presented in figure 37. The slopes of  $\delta_e/C_L$  corresponding to these results were  $14^\circ$  for configuration I,  $13.6^\circ$  for configuration II, and  $12.7^\circ$  for configuration III.

Stick-fixed and stick-free maneuvering stability was obtained for configurations I, II, and III. The approximate variation of  $\delta_e/g$  with airspeed for the three configurations is shown in figure 38. The approximate slopes of  $F_c/g$  were 83 for configuration I, 139 for configuration II, and 172 for configuration III. These results are plotted in figure 39.

During the flight program, the range of center-of-gravity travel was less than 2-percent  $\bar{c}$ ; therefore, in estimating the neutral point, wind-tunnel data were used to supplement flight-test results. The stick-fixed neutral point was at about 48-percent  $\bar{c}$ .

The effects of thrust-reverser modulation are shown in figure 40. The airplane was flown with maximum powered lift and flap deflections of  $50^\circ$  and  $70^\circ$  at maximum continuous thrust. The results in figure 40 indicate that several degrees variation of the flight-path angle was possible by using either all four reversers or only the outboard reversers. Larger reverser deflections were required when only the outboard reversers were used, but the associated trim changes were smaller. Figure 40 also shows the effect of various thrust conditions on the stabilizer incidence required for trim for flap deflections of  $50^\circ$  and  $70^\circ$  with maximum powered lift. Thrust variations were provided by modulation of the thrust reversers. For each flap deflection, the conditions of all engines producing equal thrust, the inboard engines producing greater thrust than the outboard engine, and the outboard engines producing greater thrust than the inboard engines were investigated.

The results indicate that for either flap deflection, the change in stabilizer trim setting due to variations in thrust-modulator setting was small.

The variation of stabilizer incidence required to trim the airplane for several configurations with and without powered lift is shown in figure 41. The configurations

## APPENDIX

include 50° and 70° flap deflections without boundary-layer-control operation and with maximum powered lift. The results indicate that the effects on stabilizer trim setting due to the configuration modifications including the effect of jet impingement on the flaps were not excessive.

Lateral-directional stability and control.- The lateral-directional characteristics of the airplane are presented in figures 42 to 45. (The only stability augmentation which applies for the data of these figures was the sideslip rate damper.)

The spiral stability characteristics of the airplane are given in figure 42. The value of the spiral divergence parameter  $1/T_2$  was close to zero when the flap deflection was 30°. At a flap deflection of 50°, the airplane was much less stable when the sideslip rate damper was used for stability augmentation than without augmentation. The characteristics at a flap deflection of 70° were generally more convergent with the damper operating than without augmentation. (Neutral spiral stability is usually preferred.)

The damping of the Dutch roll oscillation is indicated by the values of the damping parameter  $\frac{1}{C_{1/2}}$  plotted as a function of the rolling parameter  $\frac{\phi}{v_e}$  in figure 43. The damping parameter is the inverse ratio of cycles to damp to half-amplitude. The rolling parameter is the ratio of amplitudes of rolling and equivalent side velocity. The basic airplane configuration has low or neutral damping. In the powered-lift configuration without stability augmentation, the Dutch roll oscillation is unstable. The sideslip rate damper gives the powered-lift configuration stable damping characteristics with a damping ratio of about 0.2.

The static lateral-directional stability characteristics of the airplane (with sideslip rate damping) were obtained in cross-control sideslip maneuvers. Results for the 50° and 70° flap deflections with powered lift are presented in figure 44. The results for the 50° and 70° flap deflections were generally similar. The directional-control effectiveness enabled large sideslip angles to be obtained; and as the linearity of the lateral control was satisfactory, the airplane could be stabilized at sideslip angles up to 10° with augmentation. Beyond this angle the airplane tended to oscillate in yaw and roll.

The directional-control response was determined to be satisfactory. The rudder was powerful enough to provide large sideslip angles. Applying rudder step inputs indicated typical yaw acceleration of about 0.6 degree per second<sup>2</sup> and a yaw rate of approximately 2 degrees per second for 4° rudder deflection. The rudder provided satisfactory flight characteristics with one engine inoperative. Without powered lift, control could be maintained with wings level to approximately 130 knots with an outboard engine inoperative and the other three engines at maximum continuous power at sea level. With powered

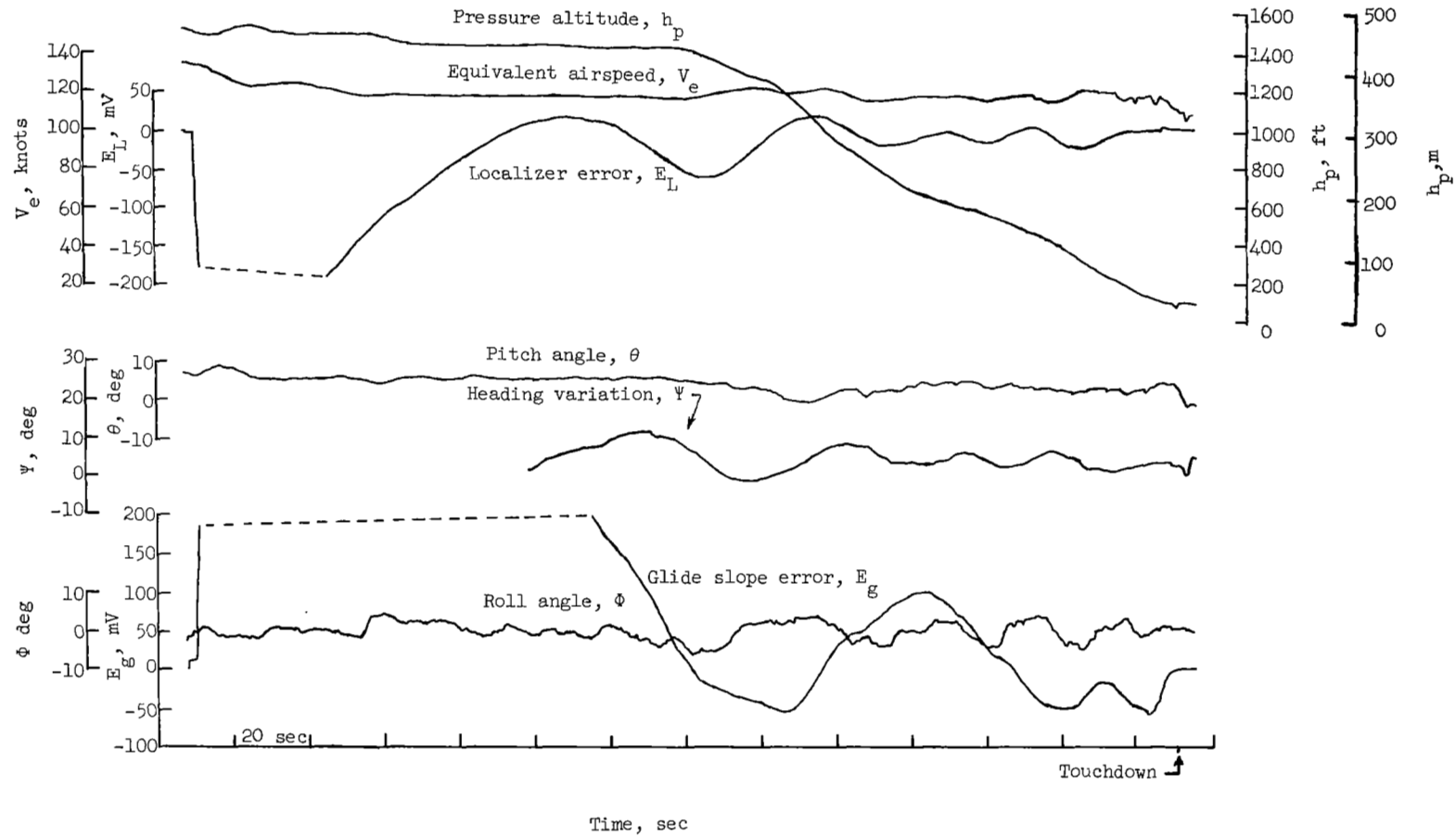
## APPENDIX

lift, the minimum control speed was approximately 100 knots for straight and level flight or 85 knots with less than  $5^{\circ}$  of bank.

The lateral-control response characteristics of the airplane at  $50^{\circ}$  and  $70^{\circ}$  flap deflections with powered lift are presented in figure 45. The variation of roll rate with lateral-control wheel deflection was approximately linear for each configuration. A roll rate of 10 degrees per second was obtained with about  $40^{\circ}$  of wheel deflection.

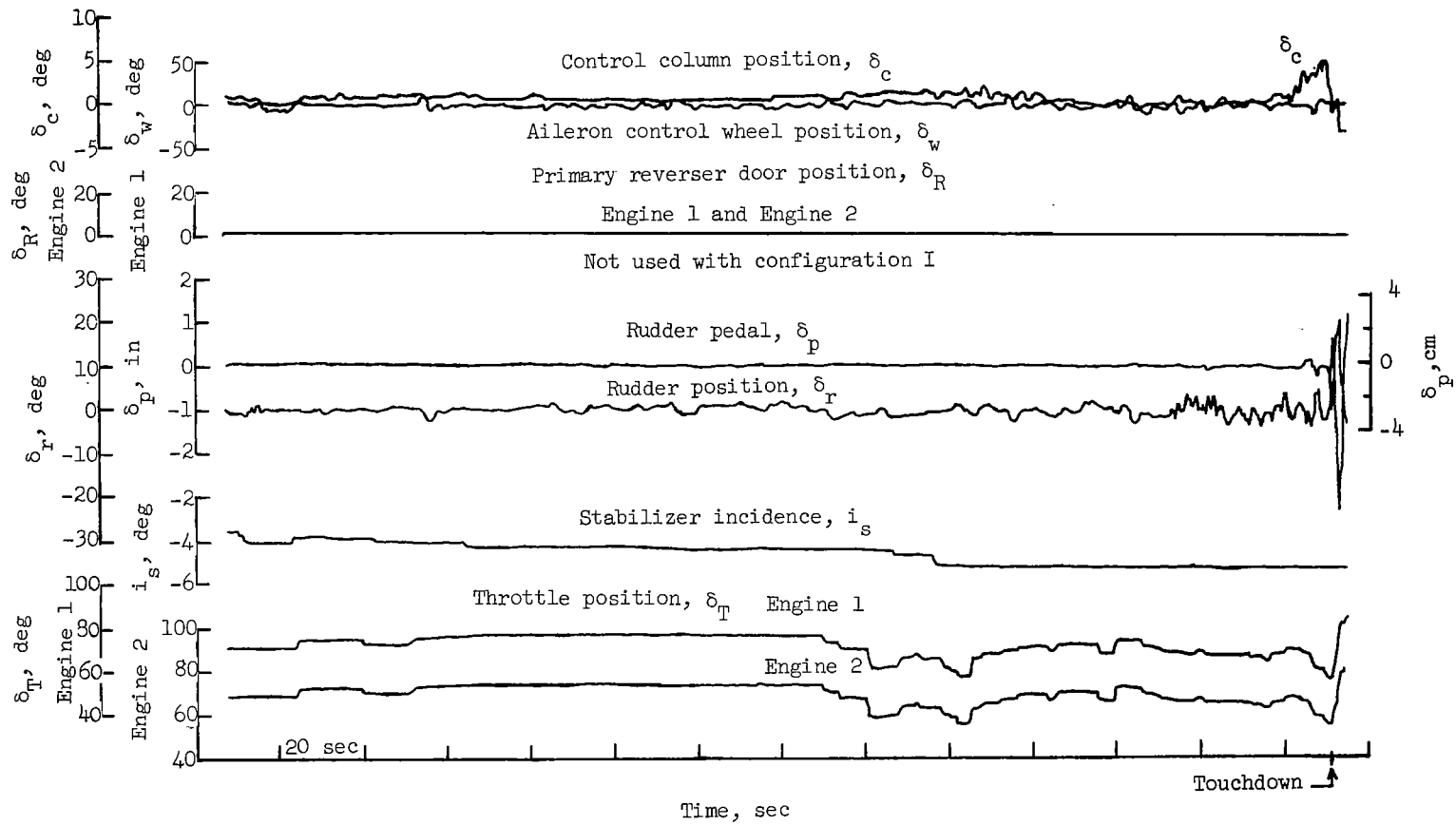
## REFERENCES

1. Hall, Albert W.; Grunwald, Kalman J.; and Deal, Perry L.: Flight Investigation of Performance Characteristics During Landing Approach of a Large Powered-Lift Jet Transport. NASA TN D-4261, 1967.
2. Gratzner, L. B.; and O'Donnell, T. J.: The Development of a BLC High-Lift System for High-Speed Airplanes. J. Aircraft, vol. 2, no. 6, Nov.-Dec. 1965, pp. 477-484.
3. Anon.: Flying Qualities of Piloted Airplanes. Military Specification MIL-F-8785(ASG), Sept. 1, 1954; Amendment -4, Apr. 17, 1959.
4. Carlson, John W.; and Wilson, Richard K.: Flying Qualities Criteria Problems and Some Proposed Solutions. Stability and Control, Pt. 1, AGARD CP No. 17, Sept. 1966, pp. 177-210.



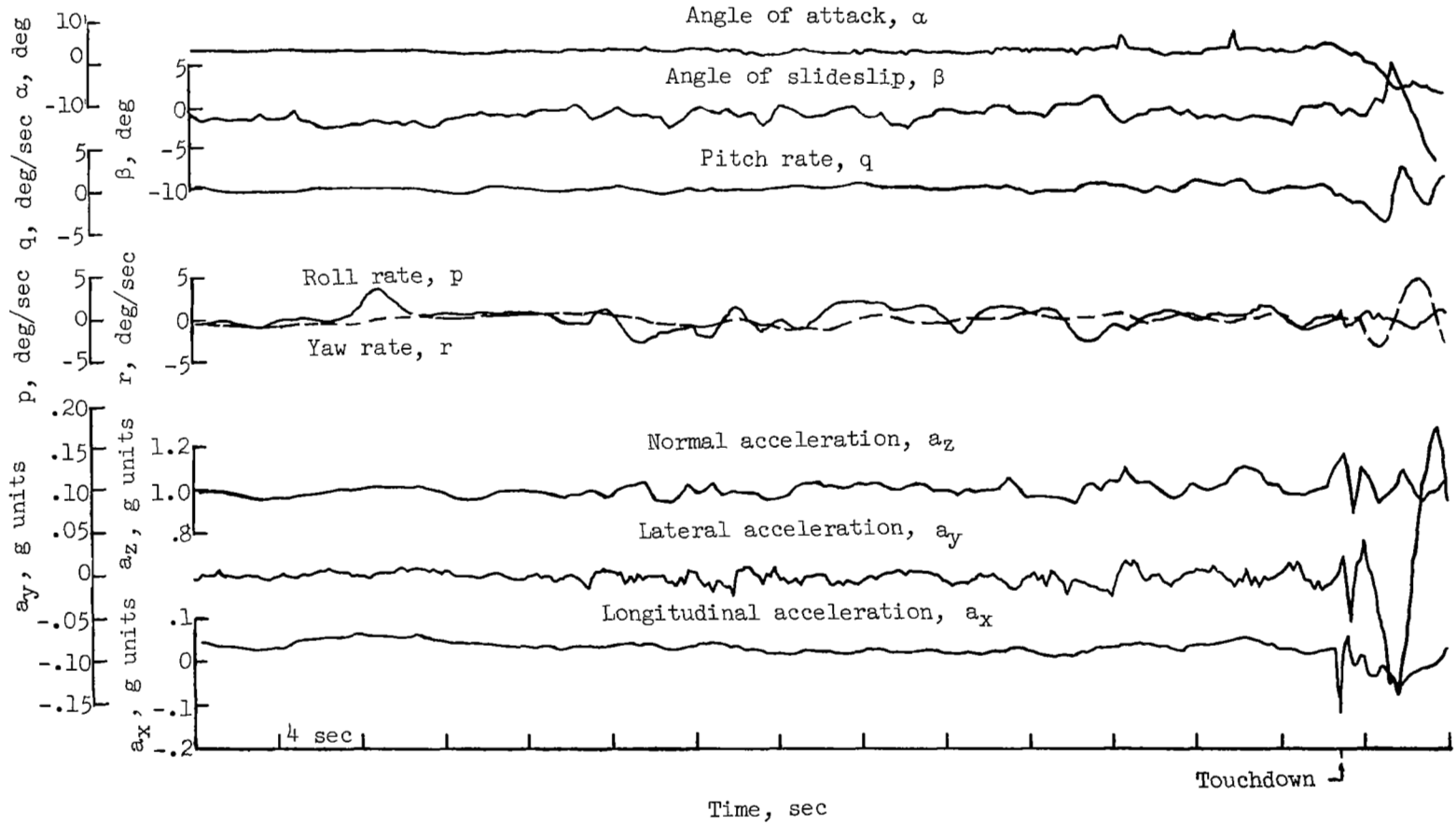
(a) Airplane response parameters.

Figure 1.- Time history of simulated instrument landing approach in configuration I.  $\delta_f = 30^\circ$ .



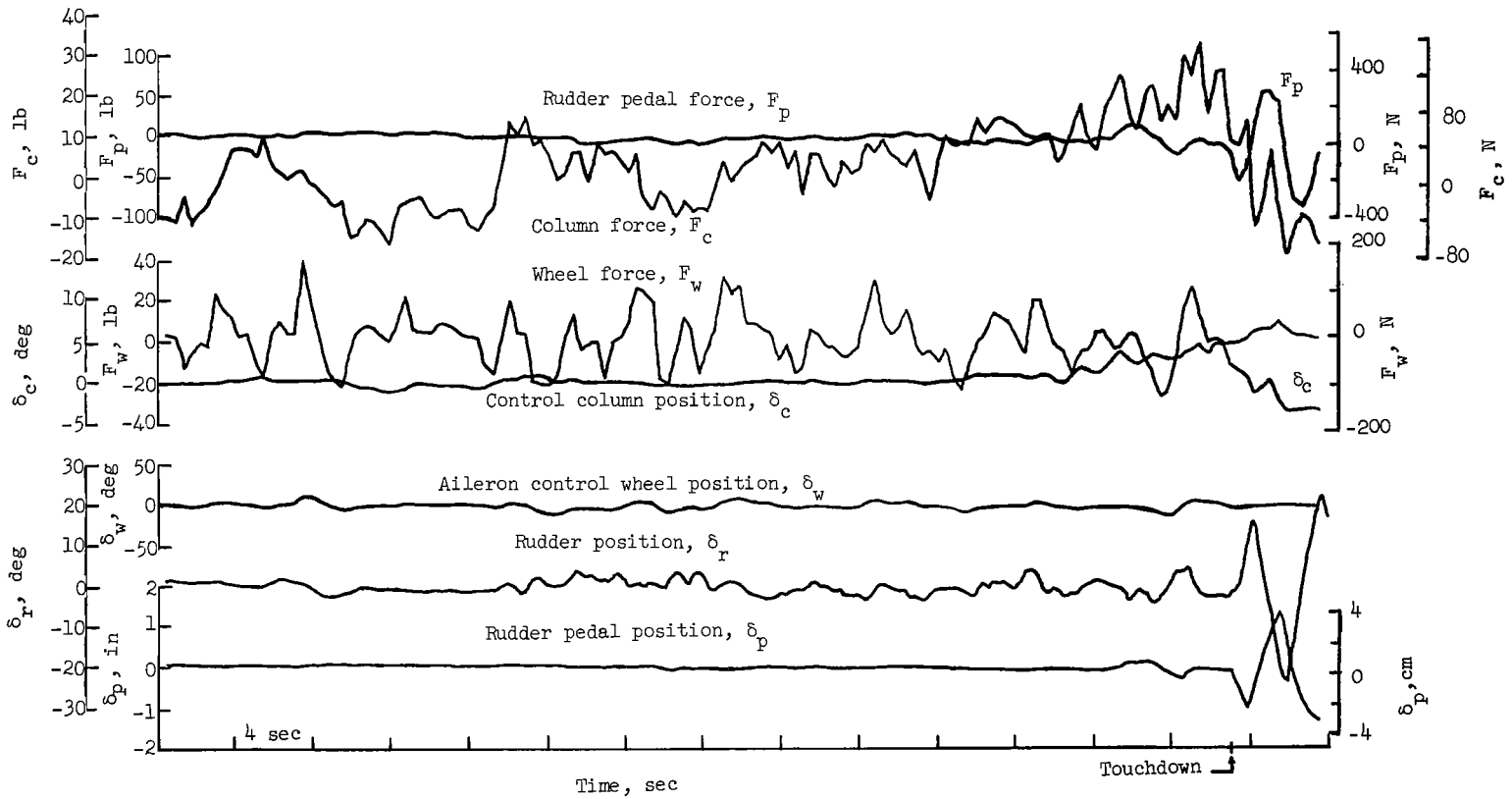
(b) Pilot inputs.

Figure 1.- Continued.



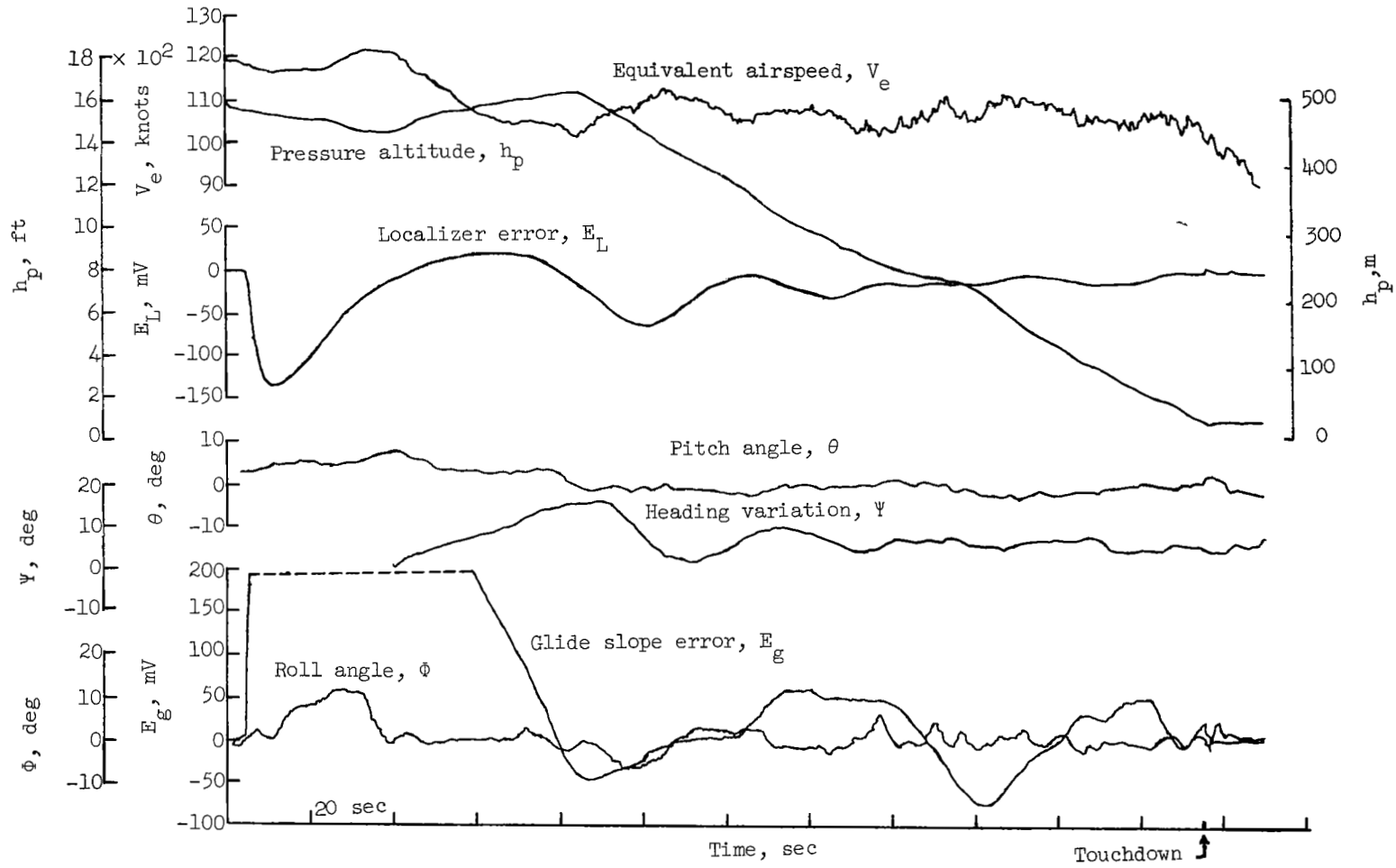
(c) Response quantities with expanded time scale.

Figure 1.- Continued.



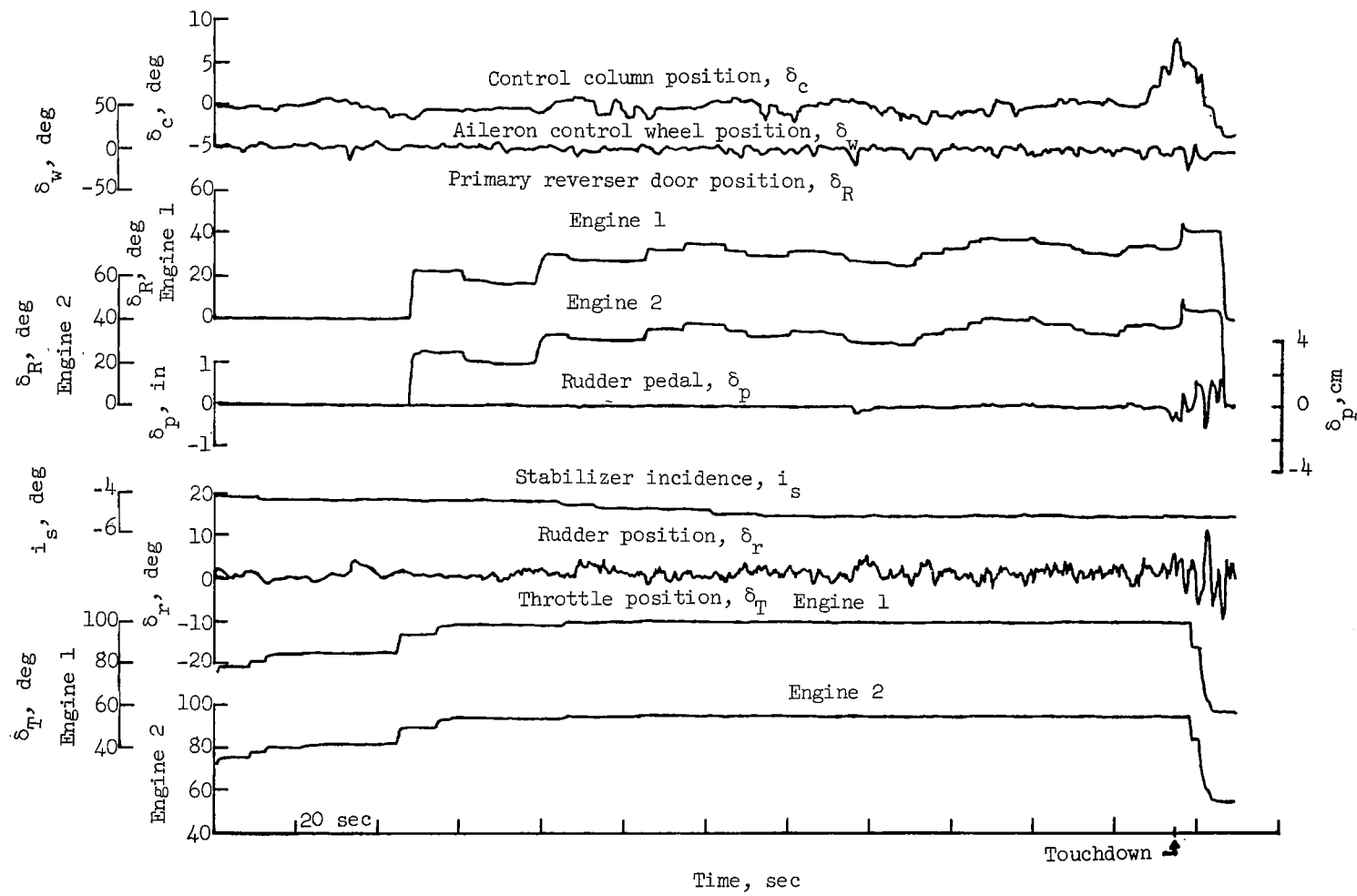
(d) Pilot inputs with expanded time scale.

Figure 1.- Concluded.



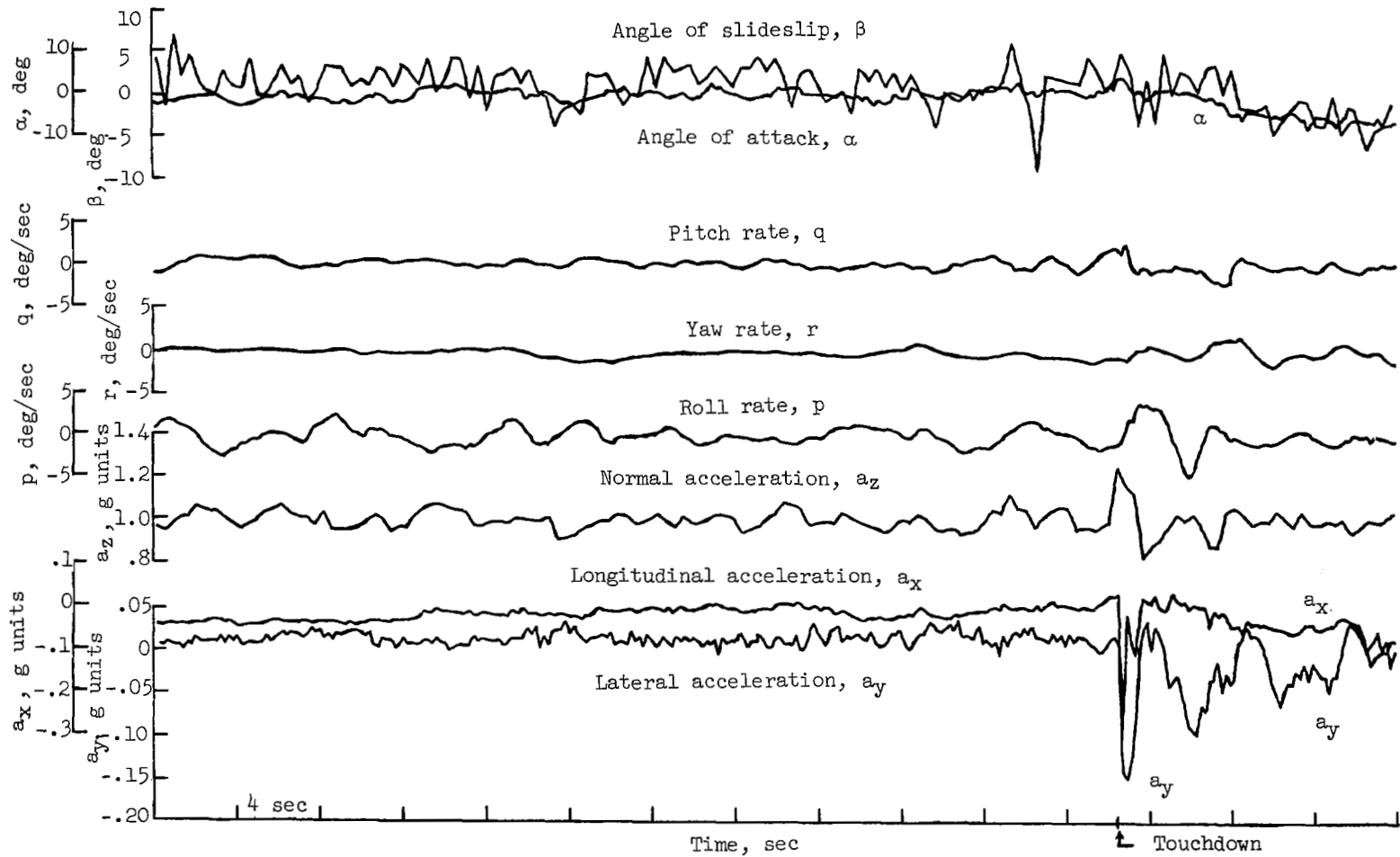
(a) Airplane response parameters.

Figure 2.- Time history of simulated instrument landing approach in configuration 11.  $\delta_i = 50^\circ$ ;  $C_{\mu} \approx 0.04$ .



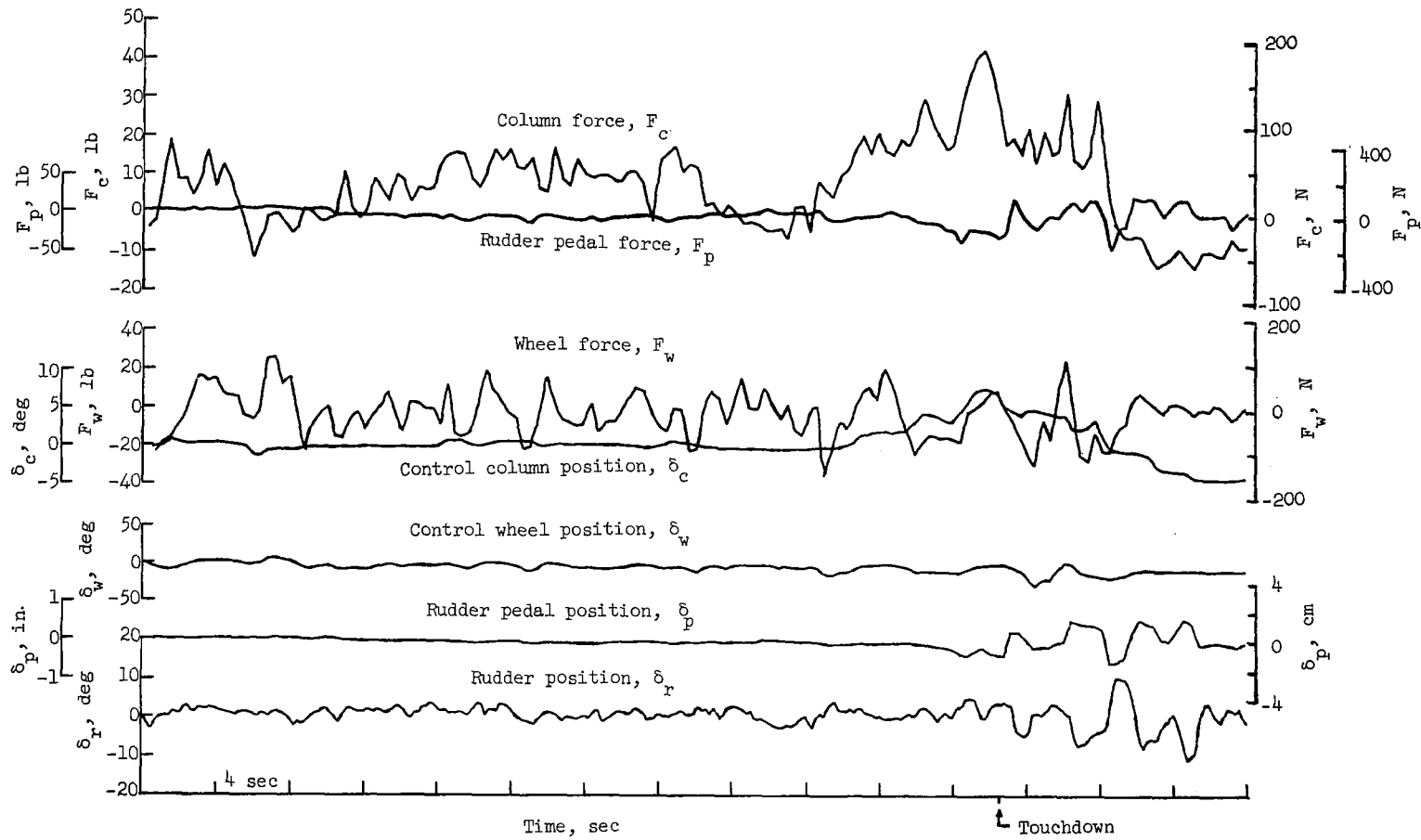
(b) Pilot inputs.

Figure 2.- Continued.



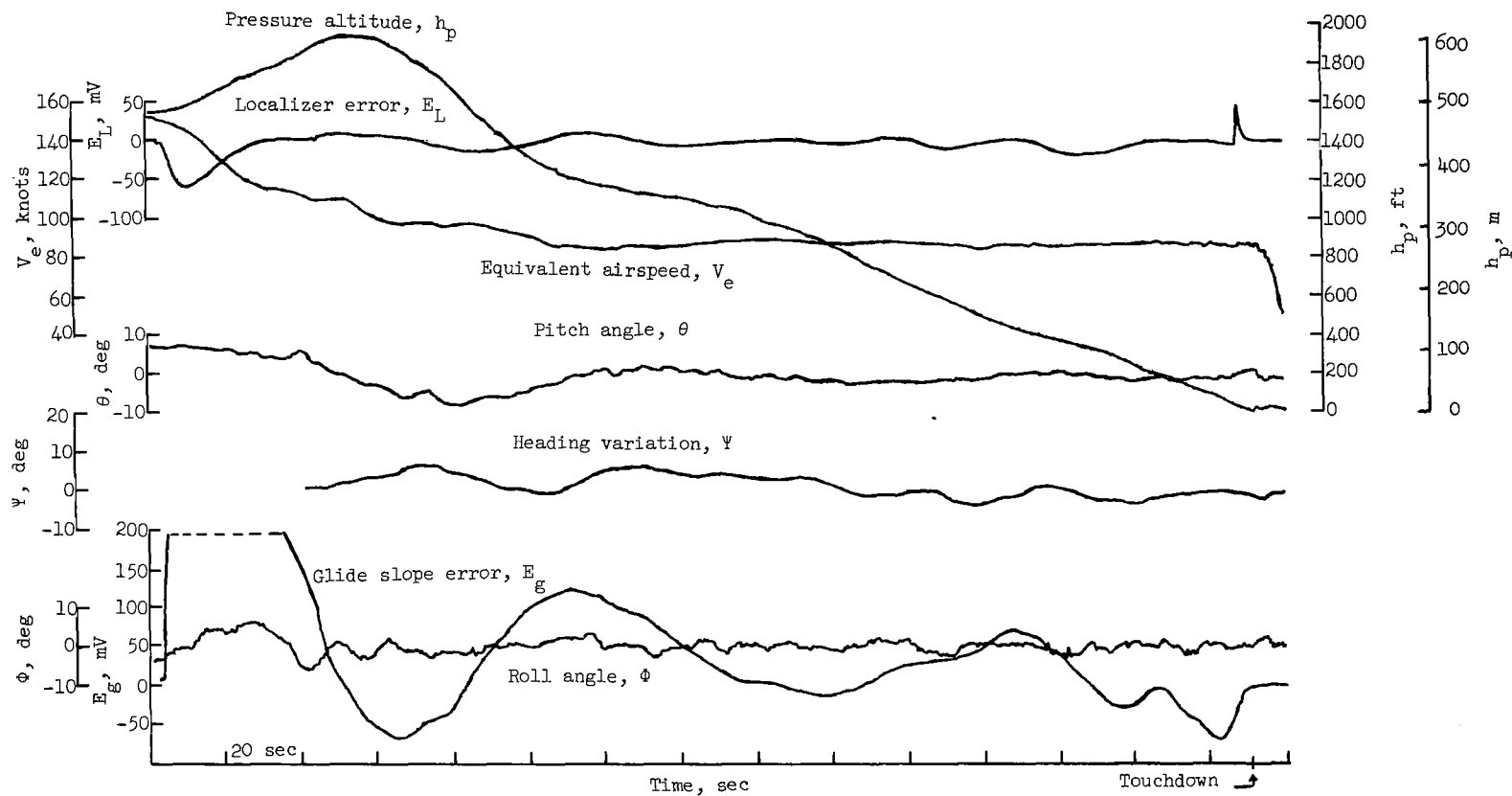
(c) Response quantities with expanded time scale.

Figure 2.- Continued.



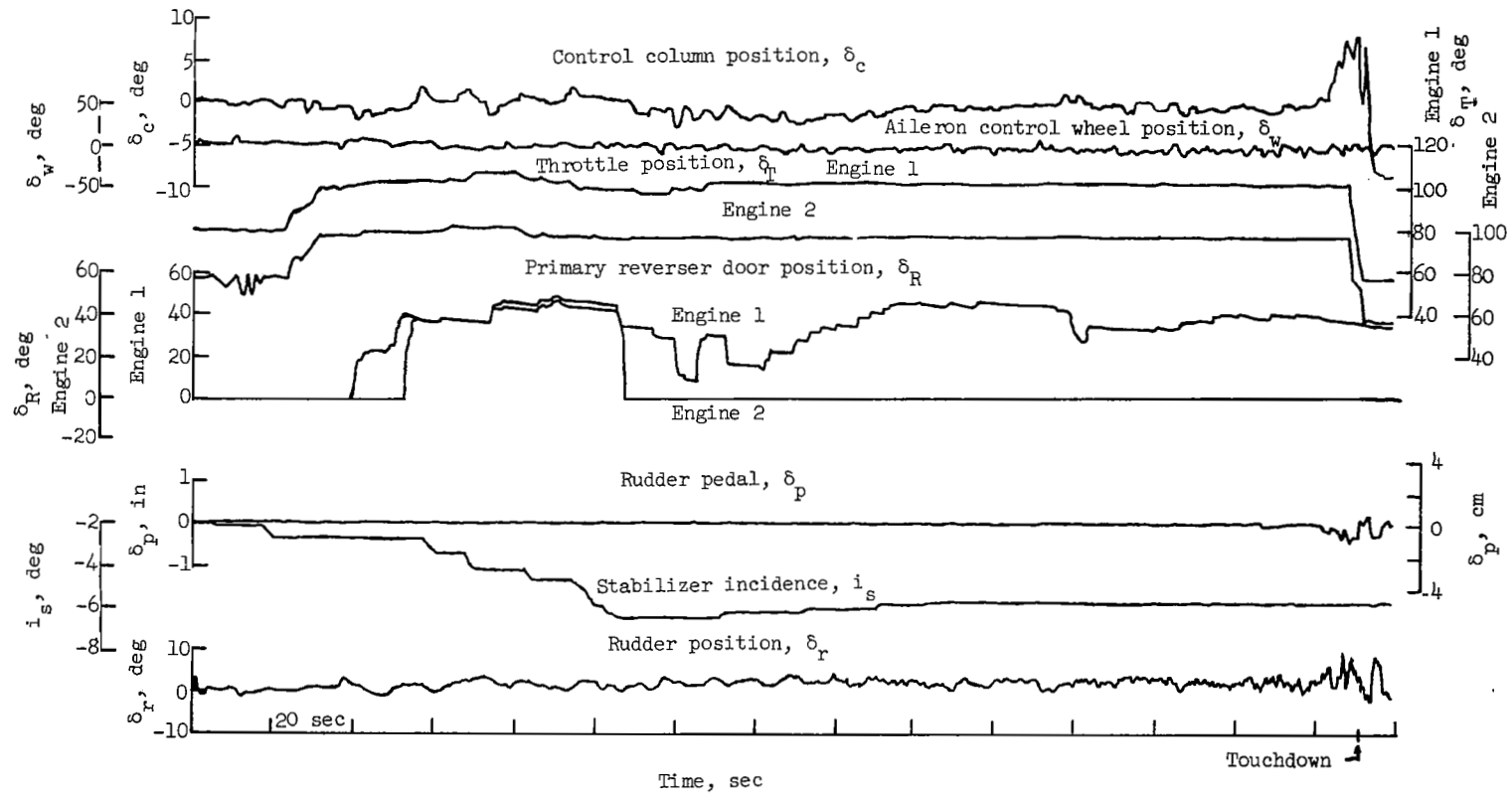
(d) Pilot inputs with expanded time scale.

Figure 2.- Concluded.



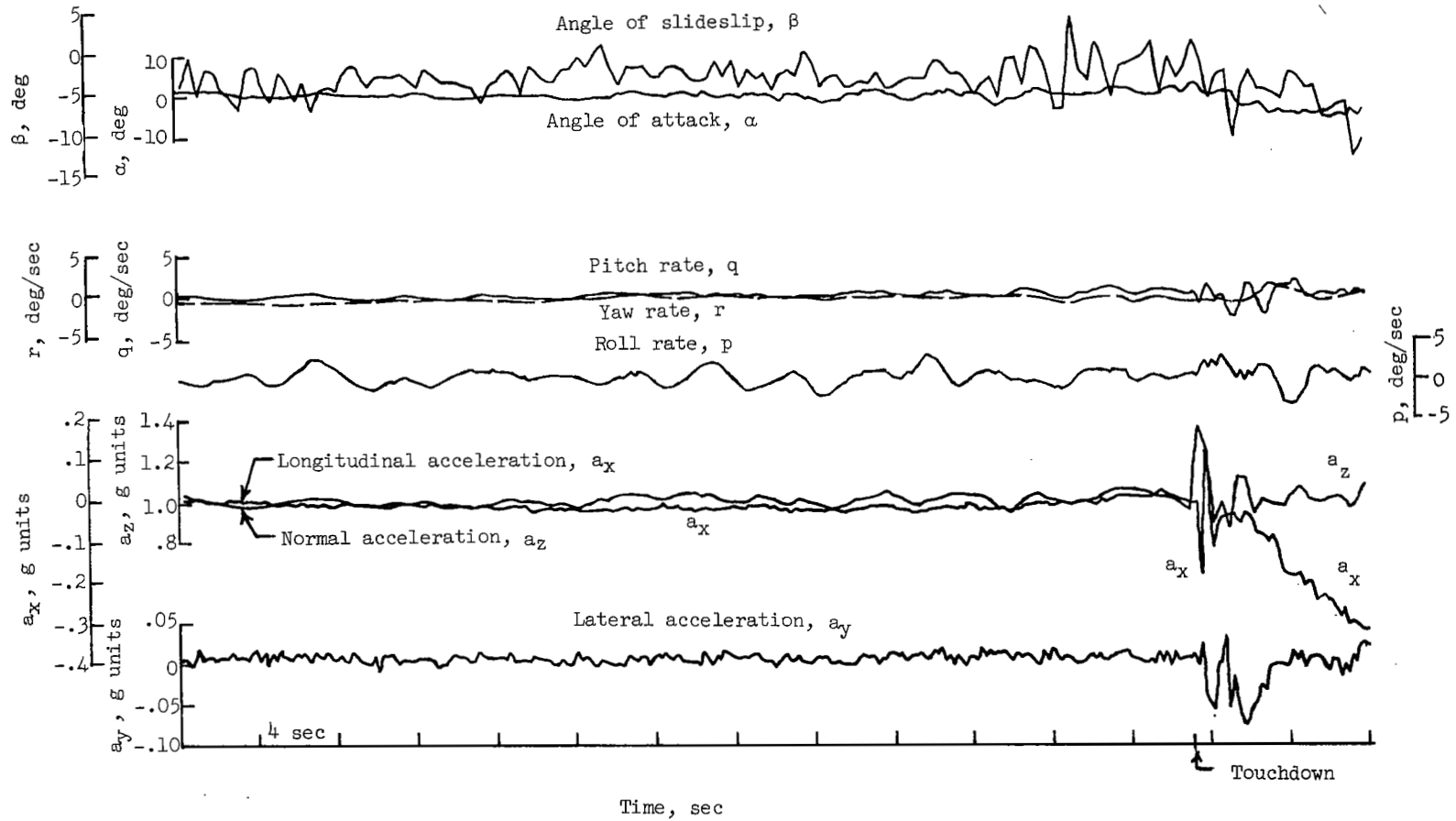
(a) Airplane response parameters.

Figure 3.- Time history of simulated instrument landing approach in configuration III.  $\delta_f = 60^\circ$ ;  $C_{\mu} \approx 0.09$ .



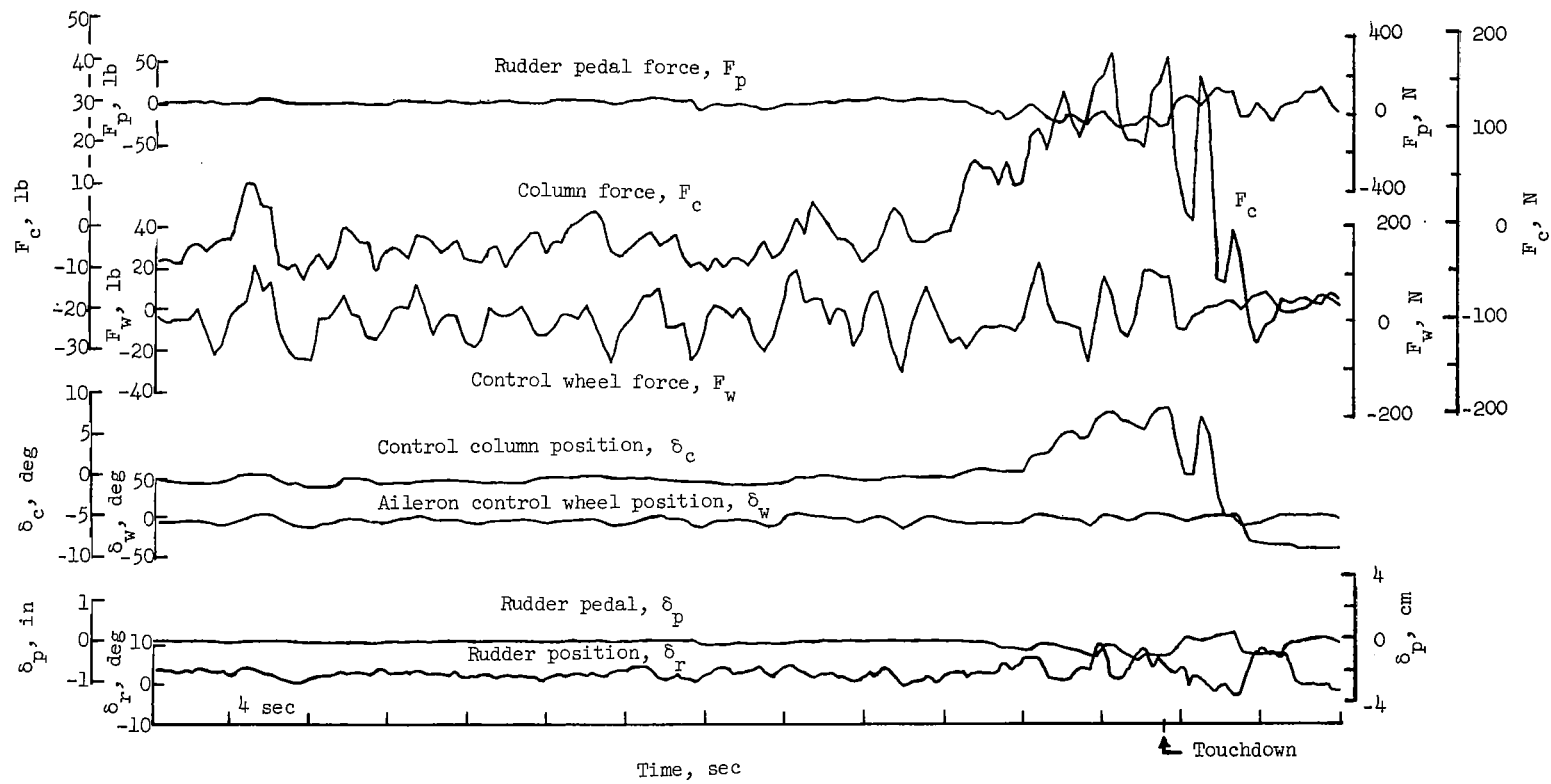
(b) Pilot inputs.

Figure 3.- Continued.



(c) Response quantities with expanded time scale.

Figure 3.- Continued.



(d) Pilot inputs with expanded time scale.

Figure 3.- Concluded.

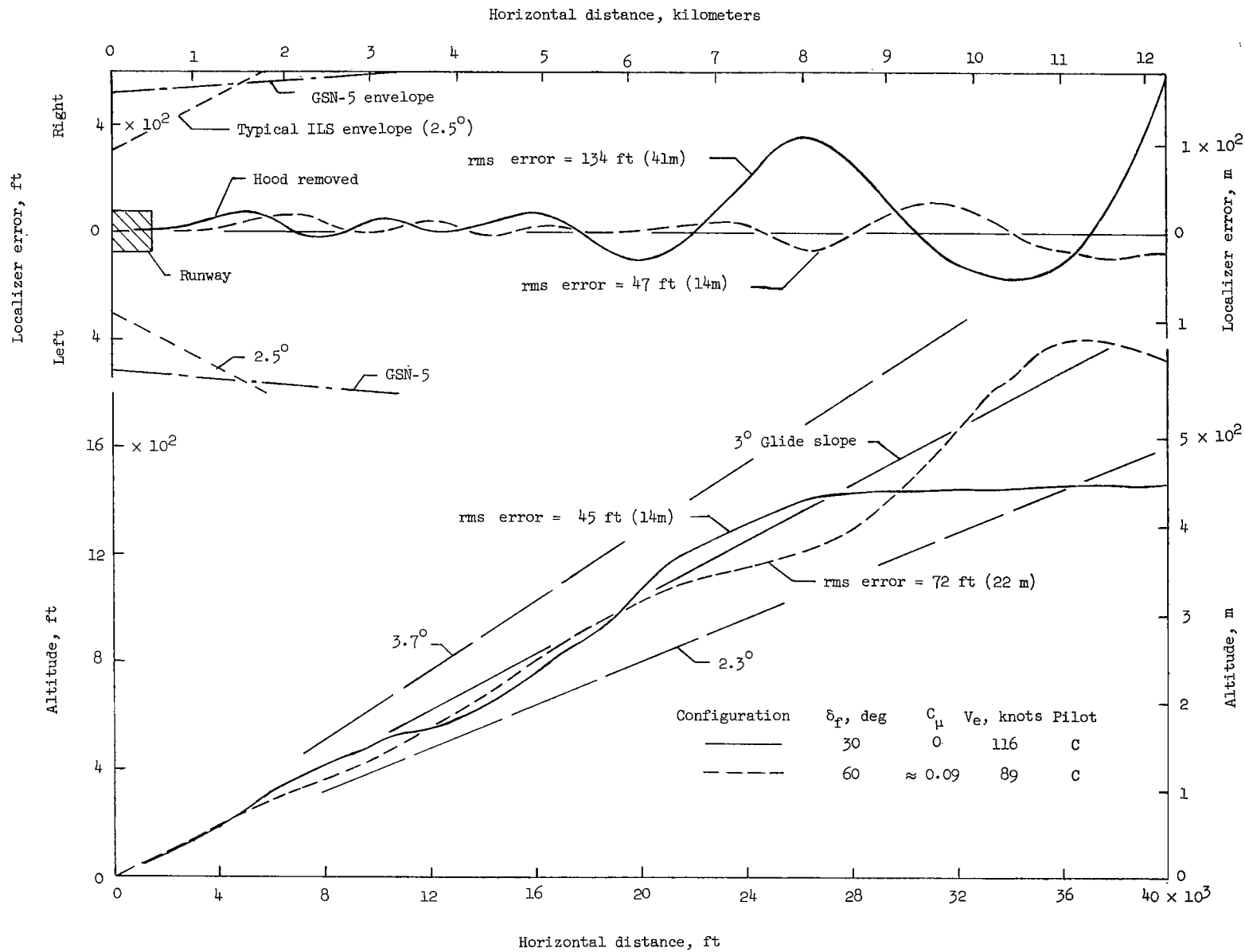


Figure 4.- Comparison of hooded approaches with and without powered lift.

Configuration (approximate)	Augmented	$\delta_f$ , deg	$C_\mu$	ft	$h_p$ , m	P, sec
⊙ ——— III	$\dot{\beta}$ damper	50	$\approx 0.09$	4000	1300	9
□ - - - III	No	50	$\approx 0.09$	4000	1300	9
◇ ———	No	50	0	4000	1300	8
△ — - - I	No	20	0	11,400	3730	8

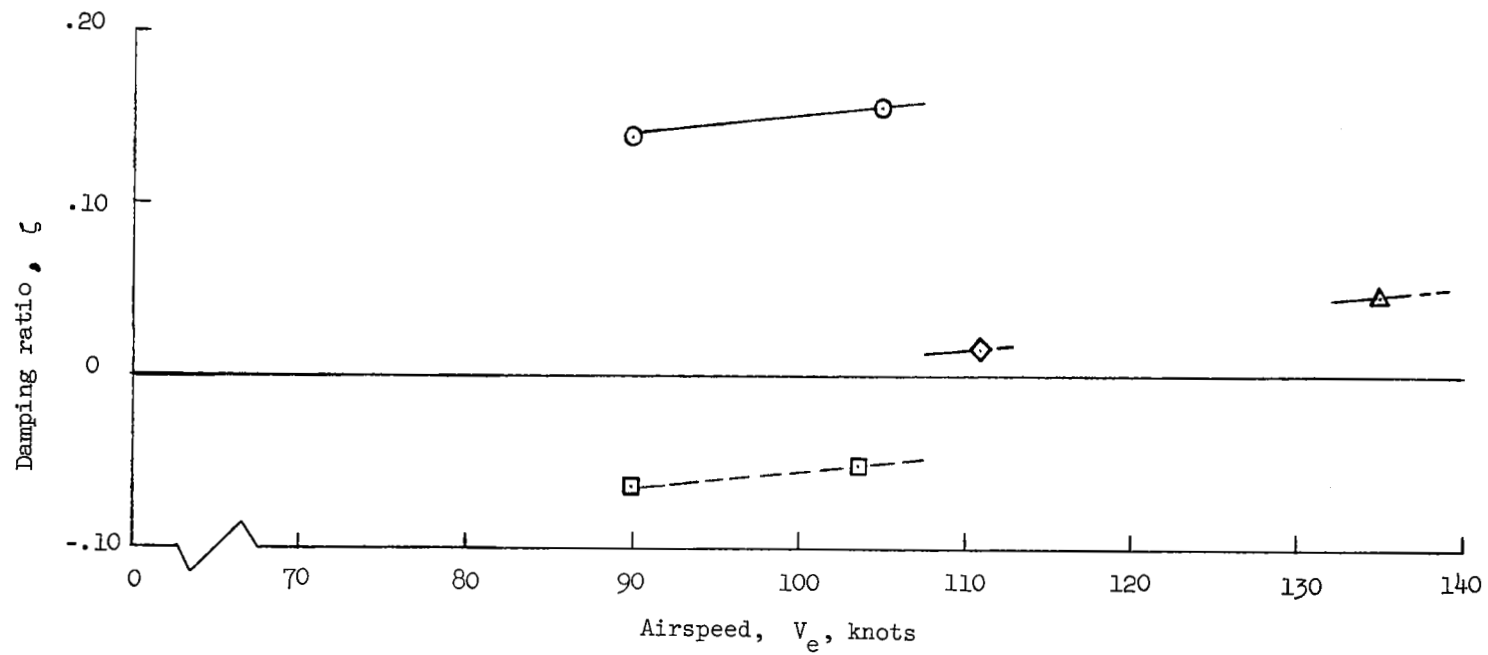


Figure 5.- Effects of powered lift and stability augmentation on the Dutch roll damping ratio of landing-approach configurations.

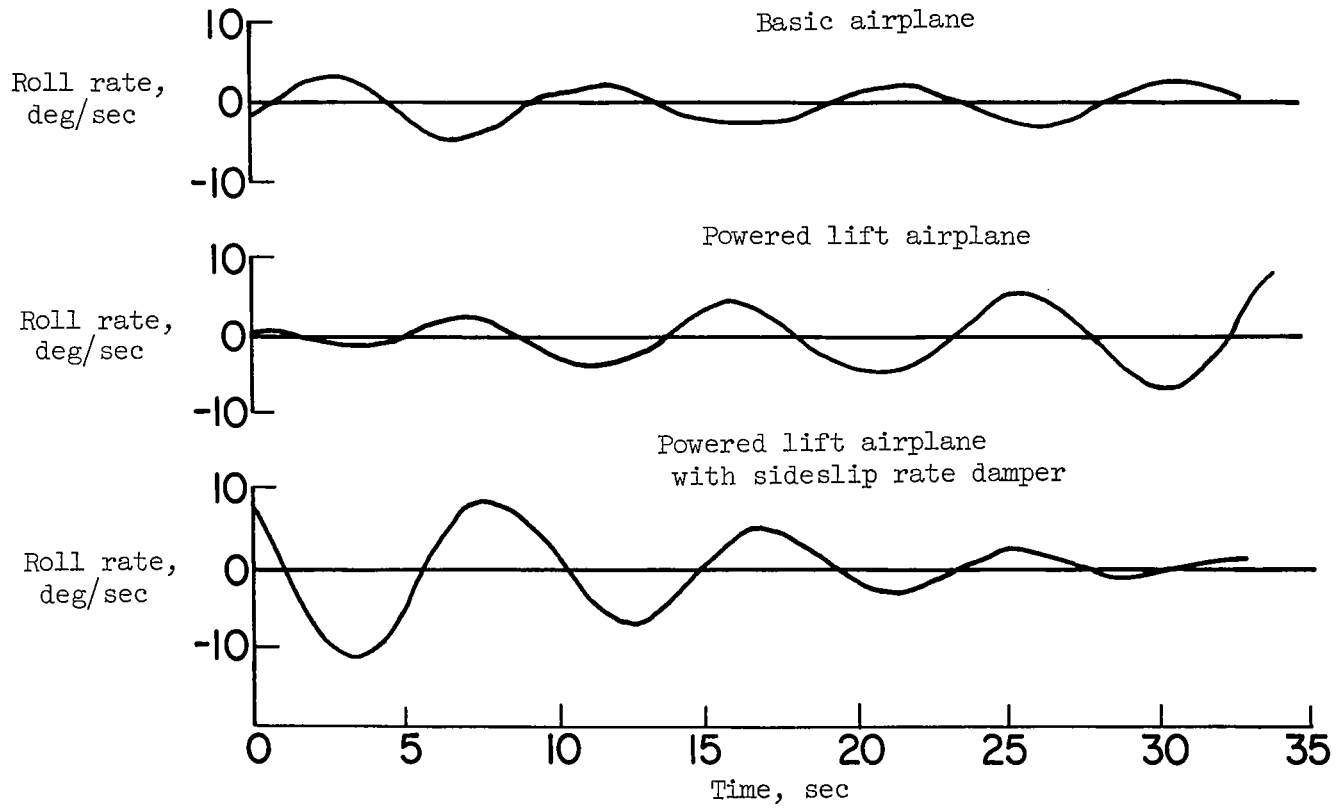


Figure 6.- Dutch roll characteristics.

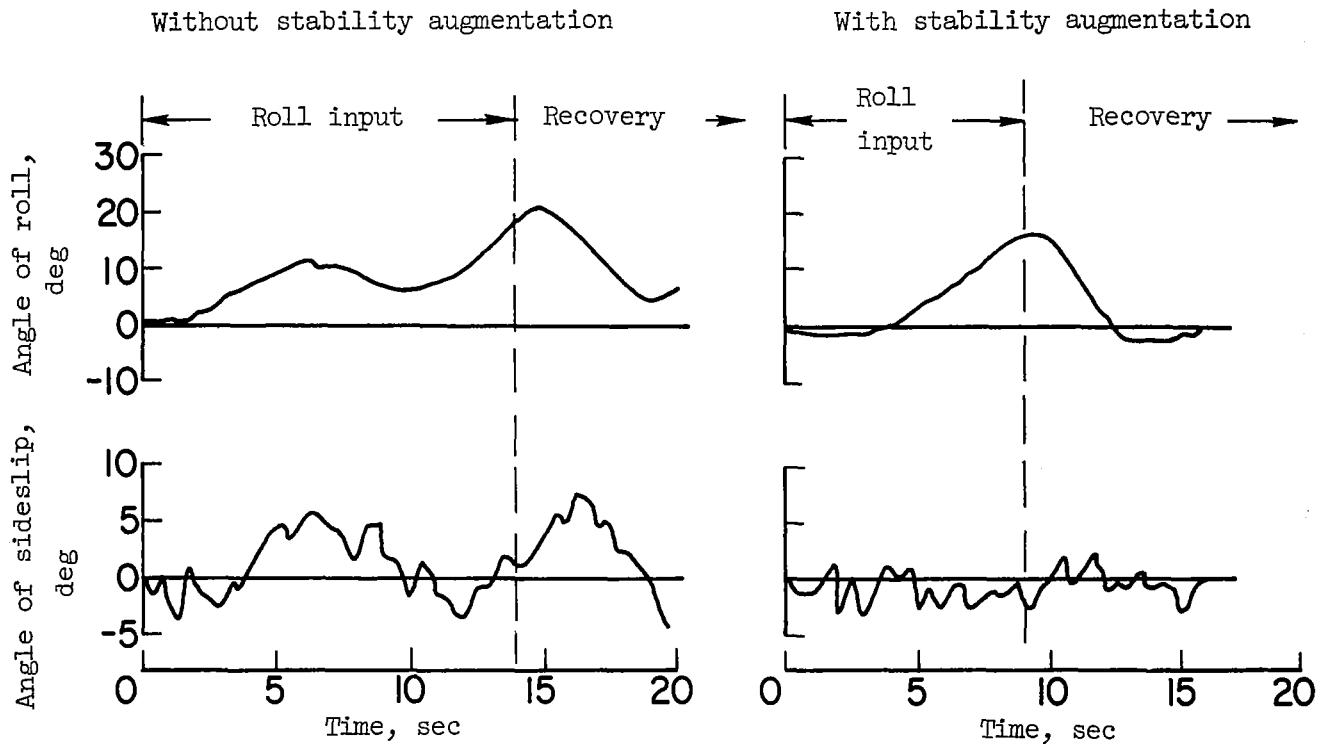


Figure 7.- Lateral-directional cross coupling of the powered-lift test configuration (configuration III) with and without stability augmentation (response to step roll inputs).

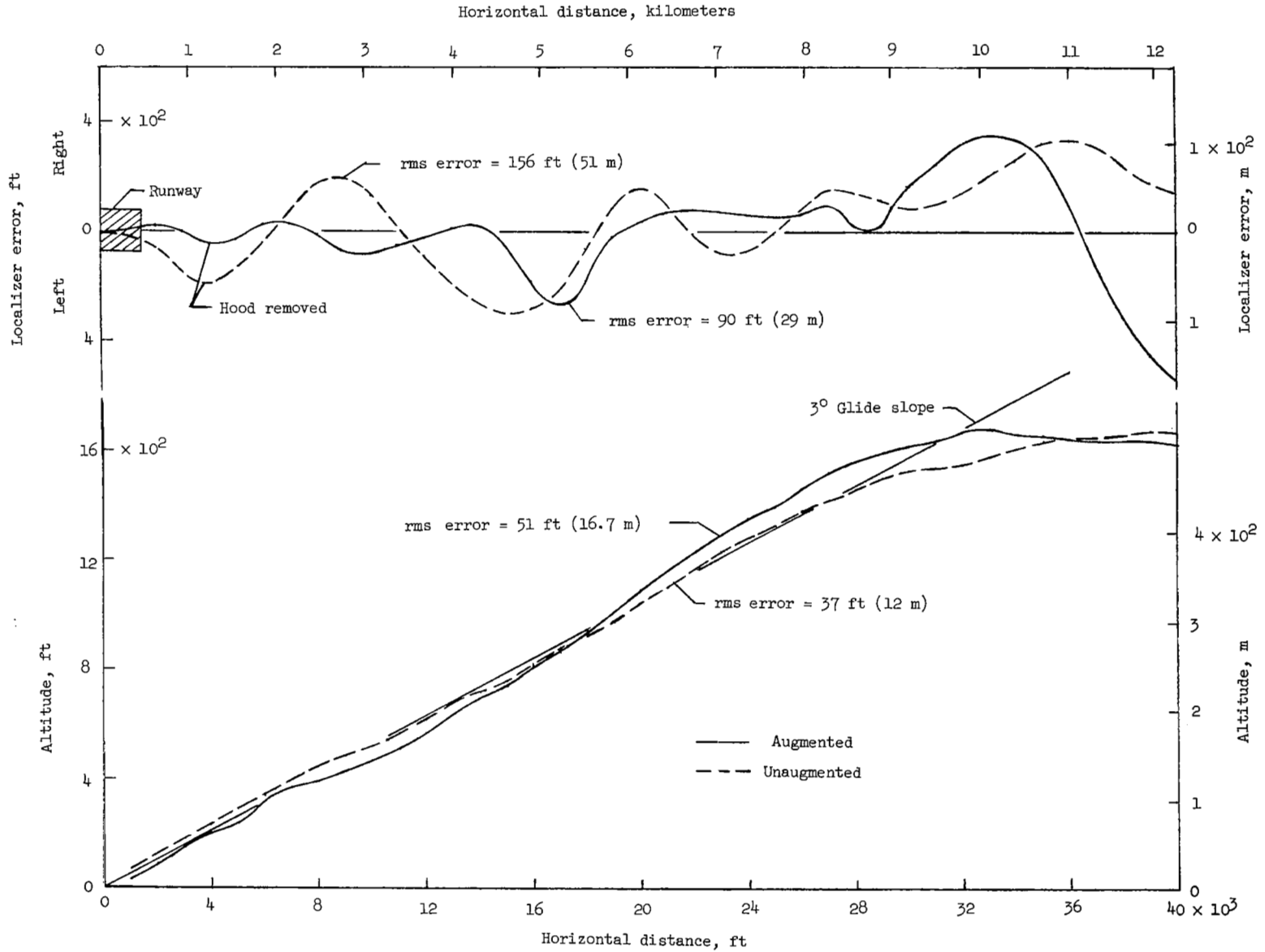


Figure 8.- Comparison of hooded approaches in configuration III at 88 knots with and without lateral stability augmentation. (The unaugmented approach was made with a 4-knot crosswind.)

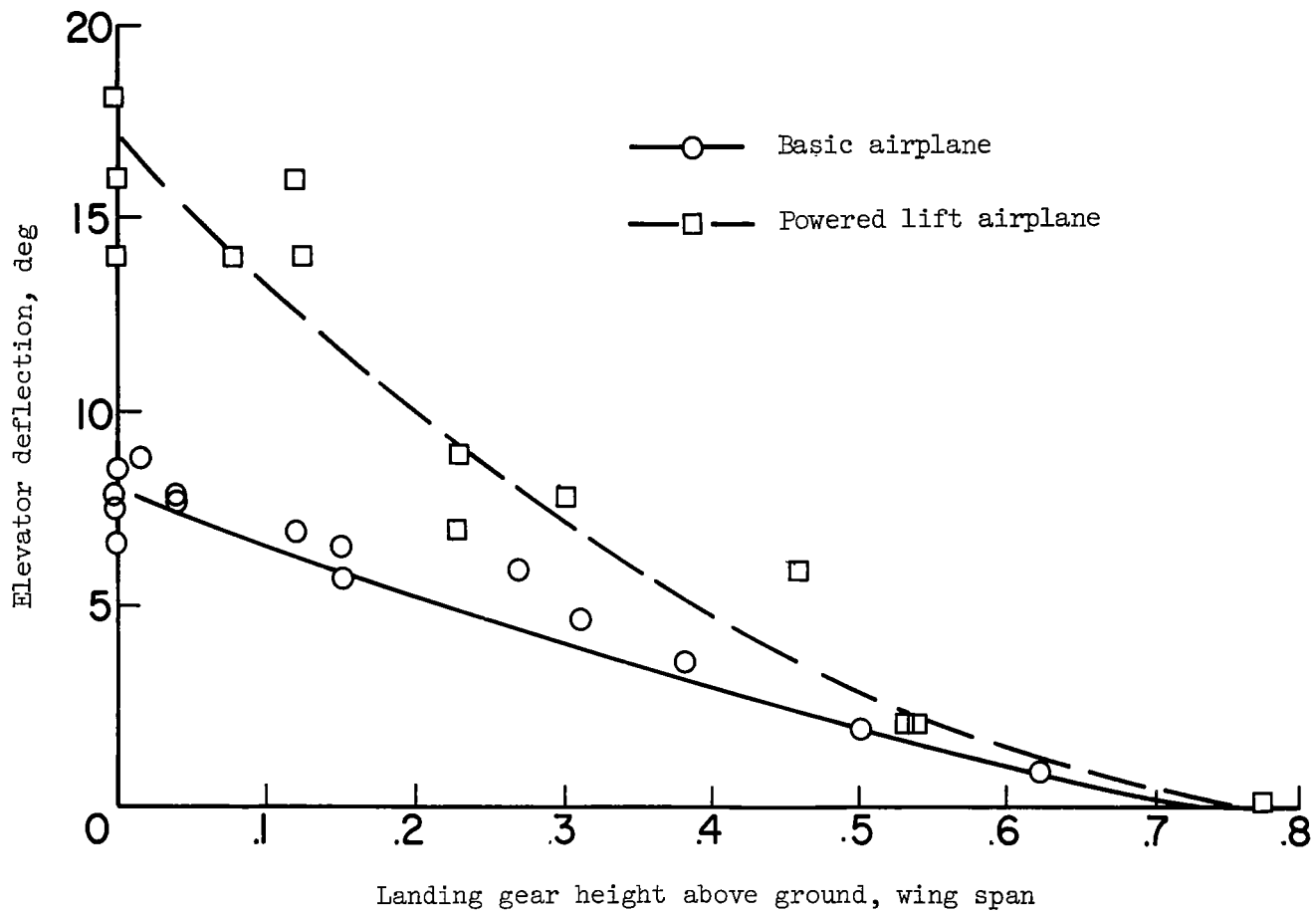


Figure 9.- Elevator deflection during flare with and without powered lift.

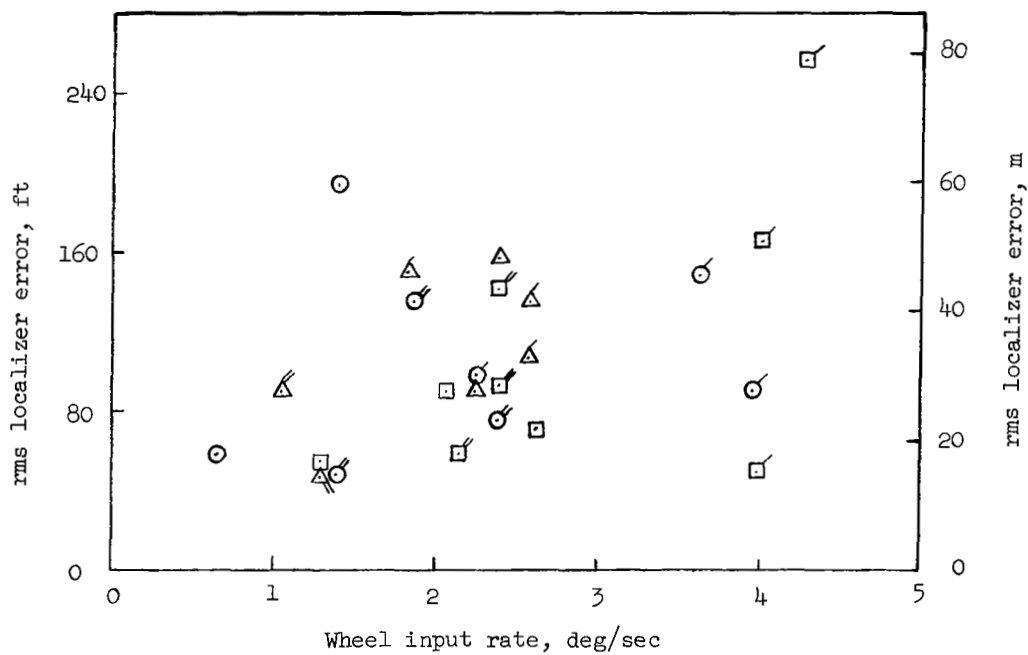
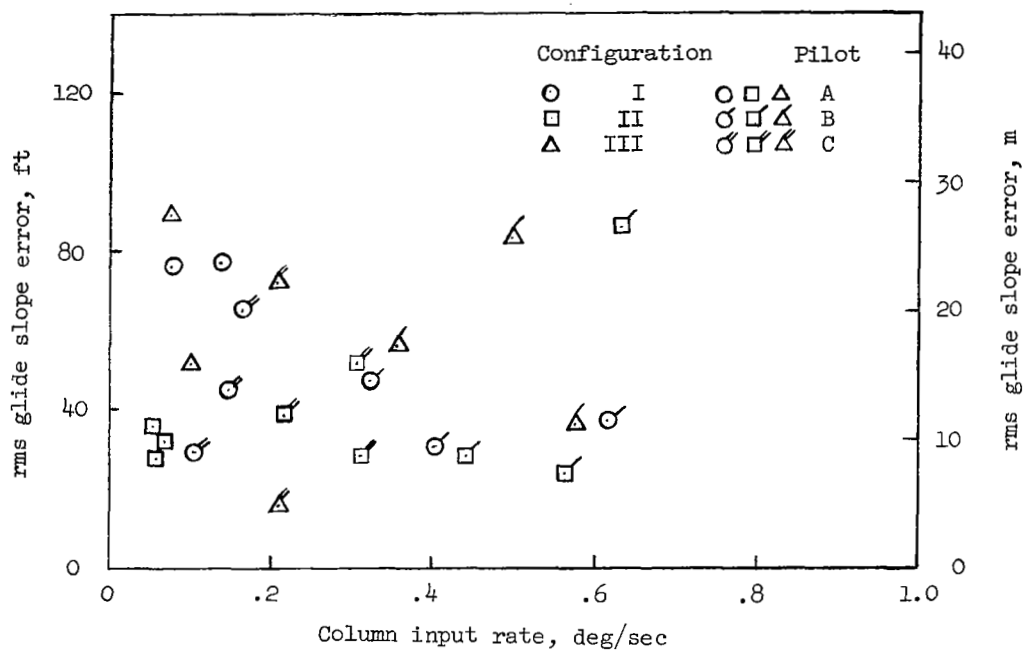


Figure 10.- Distribution of root-mean-square tracking errors and control input rates for three basic test configurations.

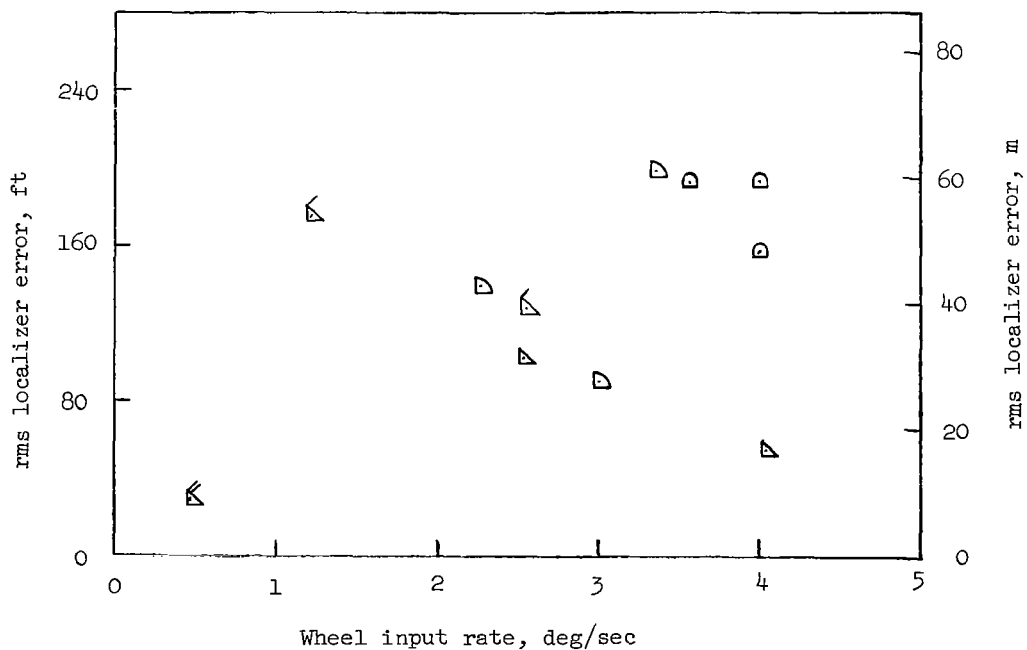
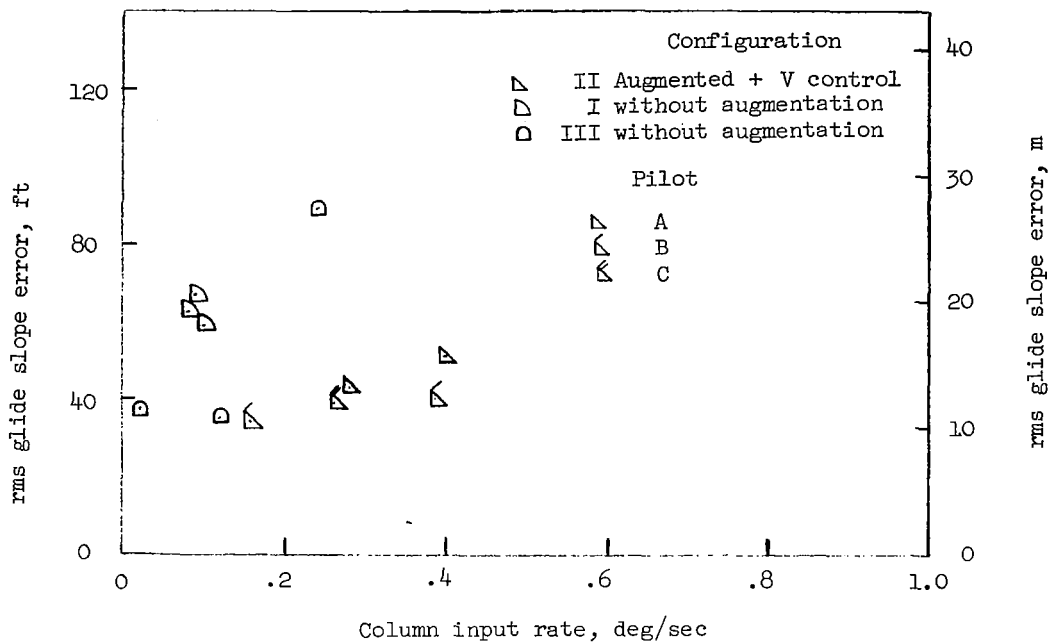


Figure 11.- Distribution of root-mean-square tracking errors and control input rates with automatic speed control added to the stability augmentation and also with no stability augmentation.

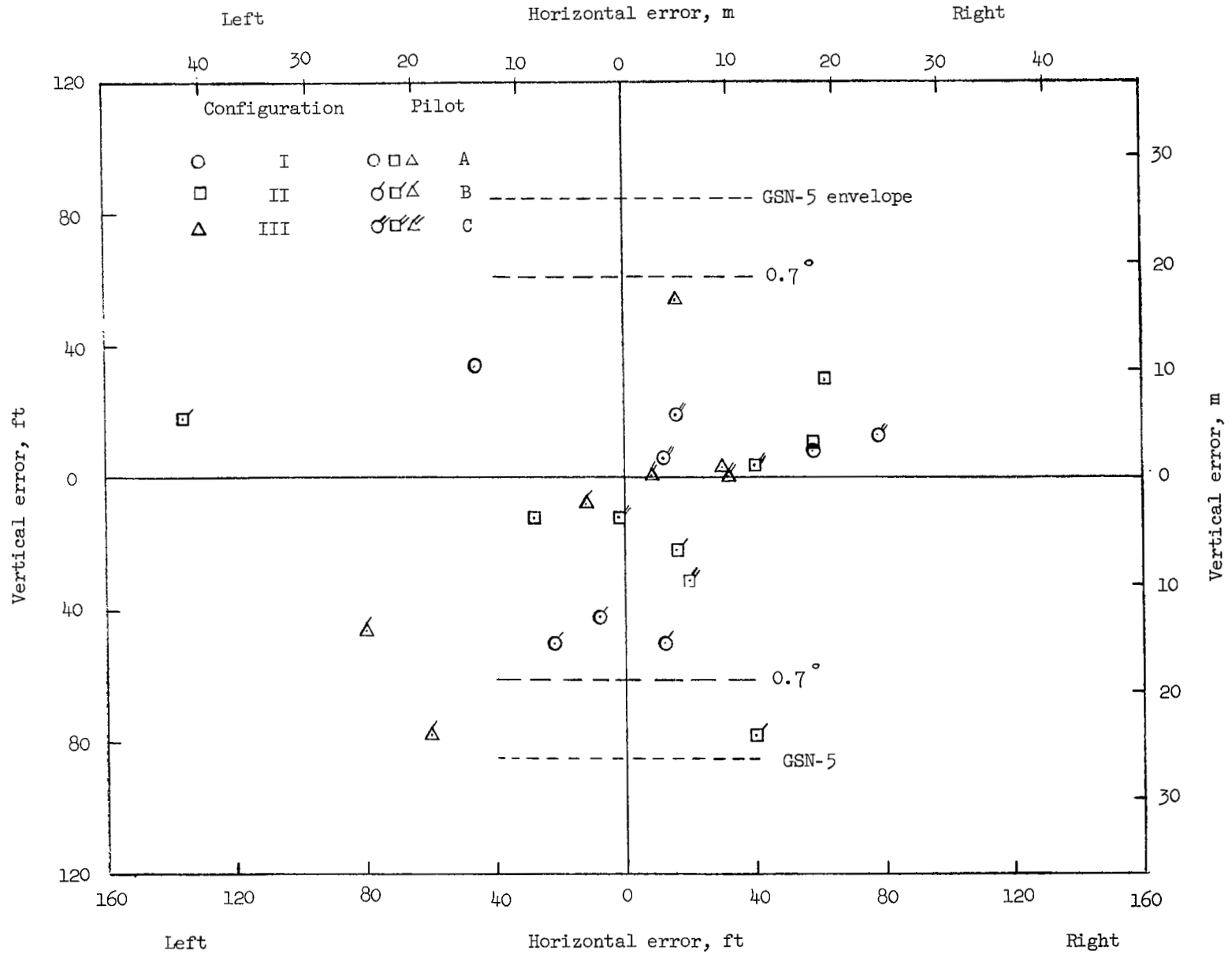


Figure 12.- Airplane position in the breakout window (5000-foot (1527-meter) range) for basic test configurations.

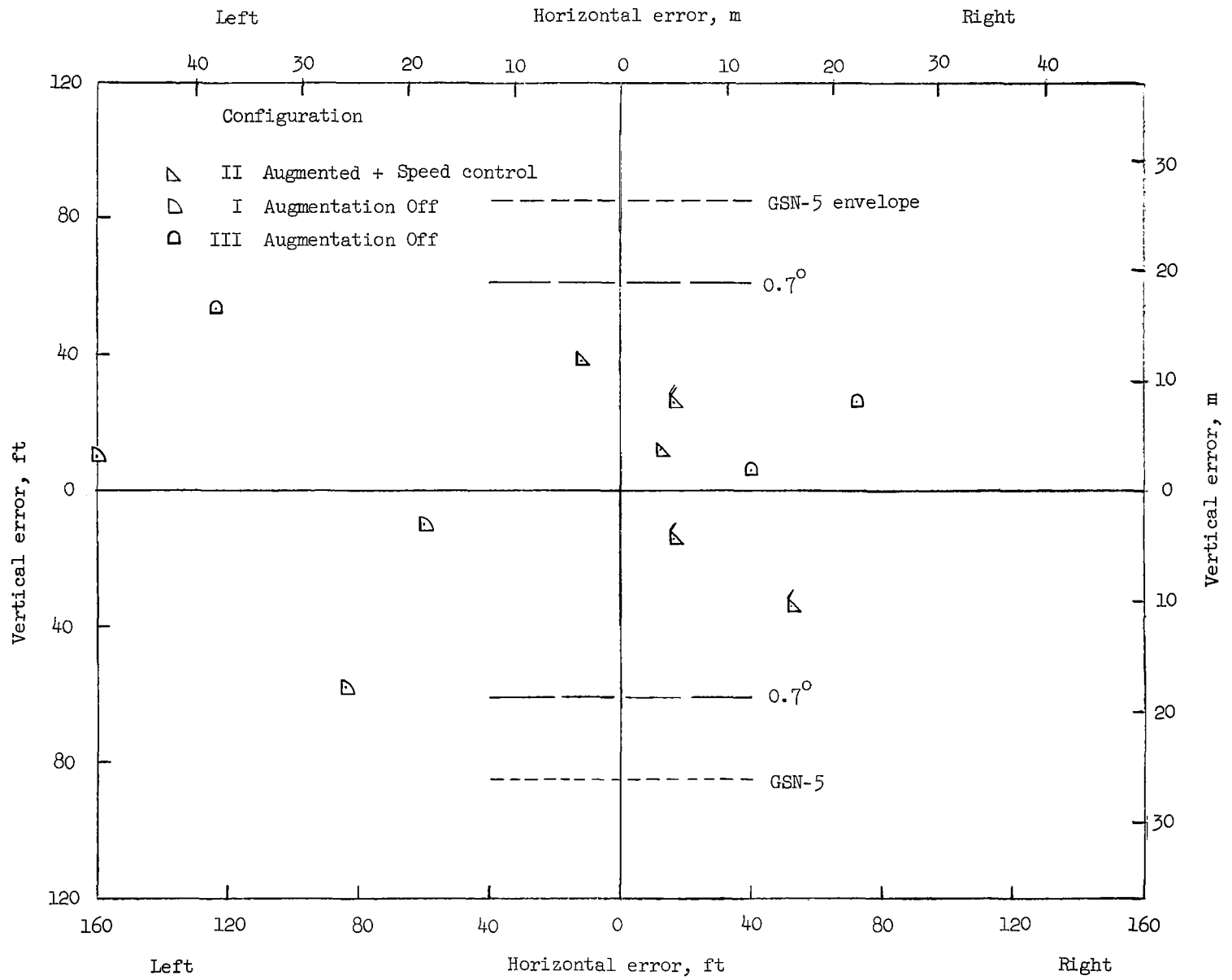


Figure 13.- Airplane position in the breakout window for supplementary test configurations.

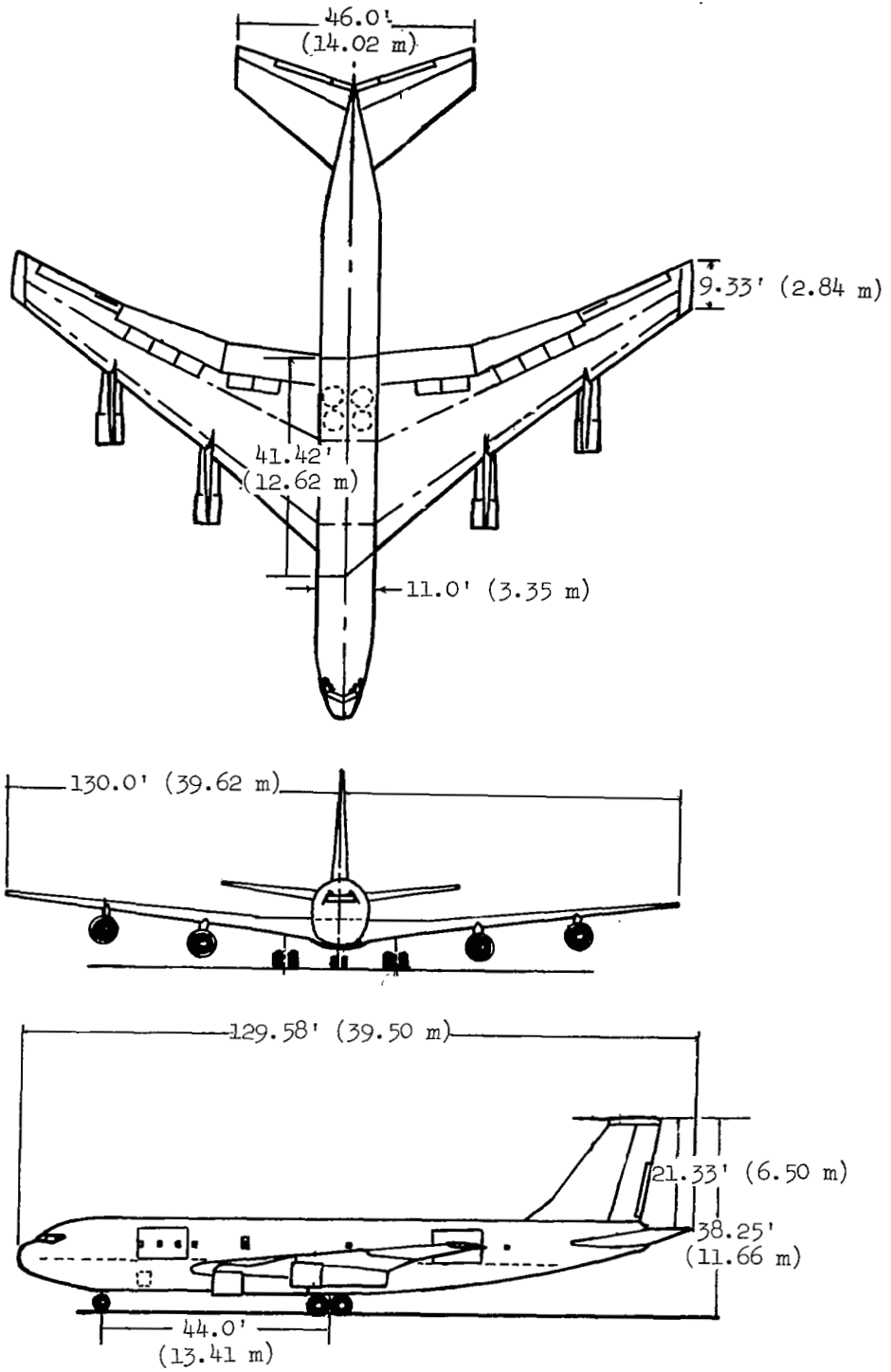


Figure 14.- Three-view drawing of test airplane.

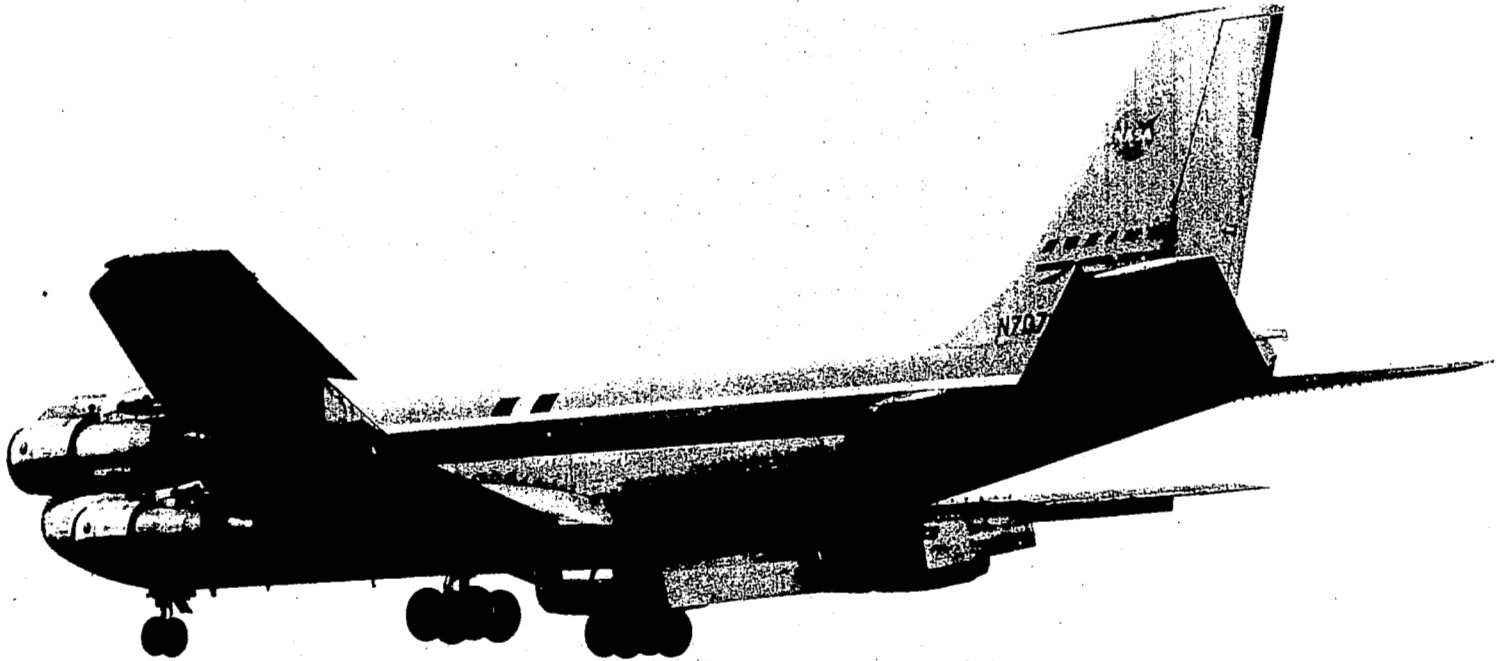


Figure 15.- Photograph of test airplane.

L-68-894

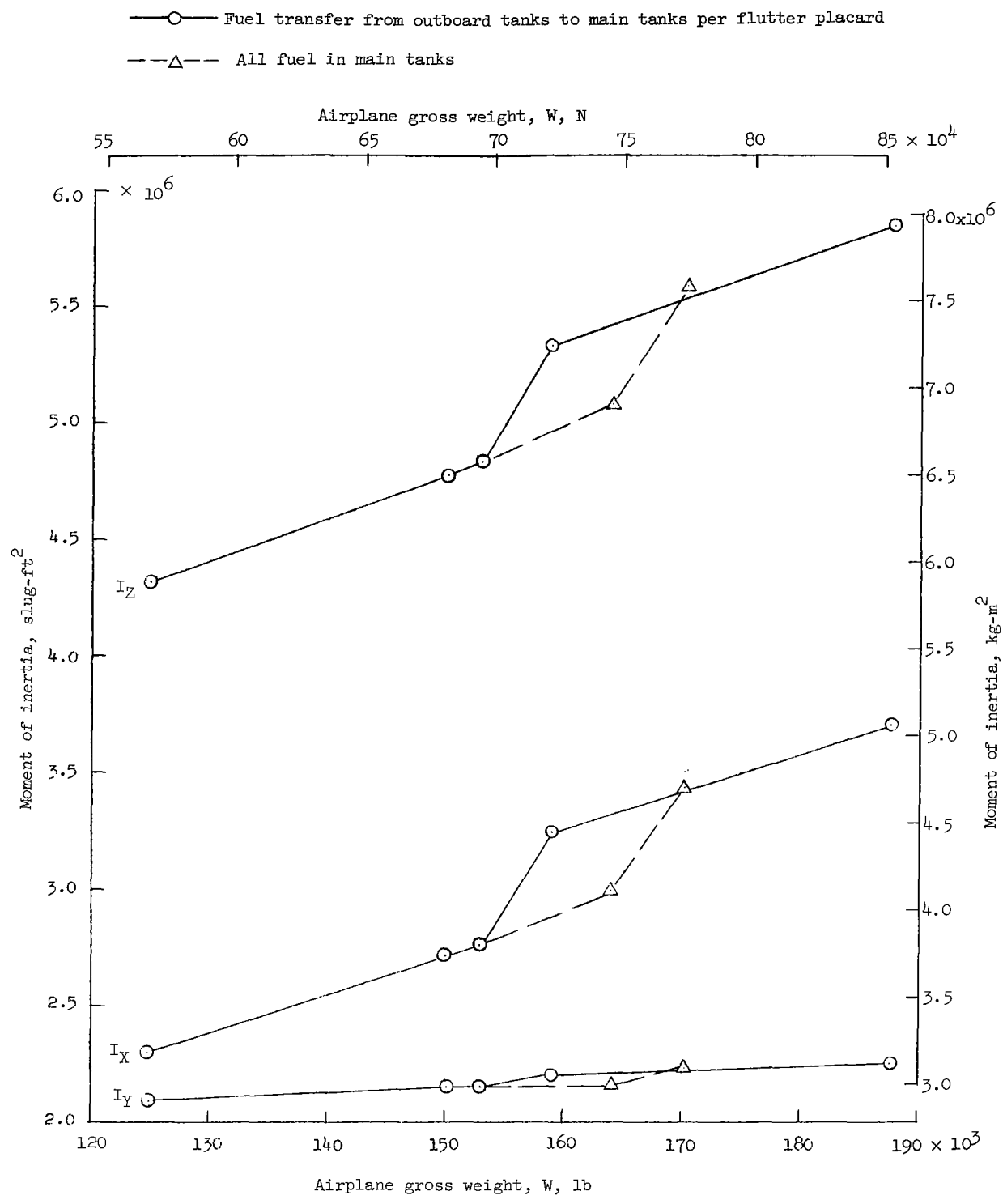


Figure 16.- Moment-of-inertia characteristics.

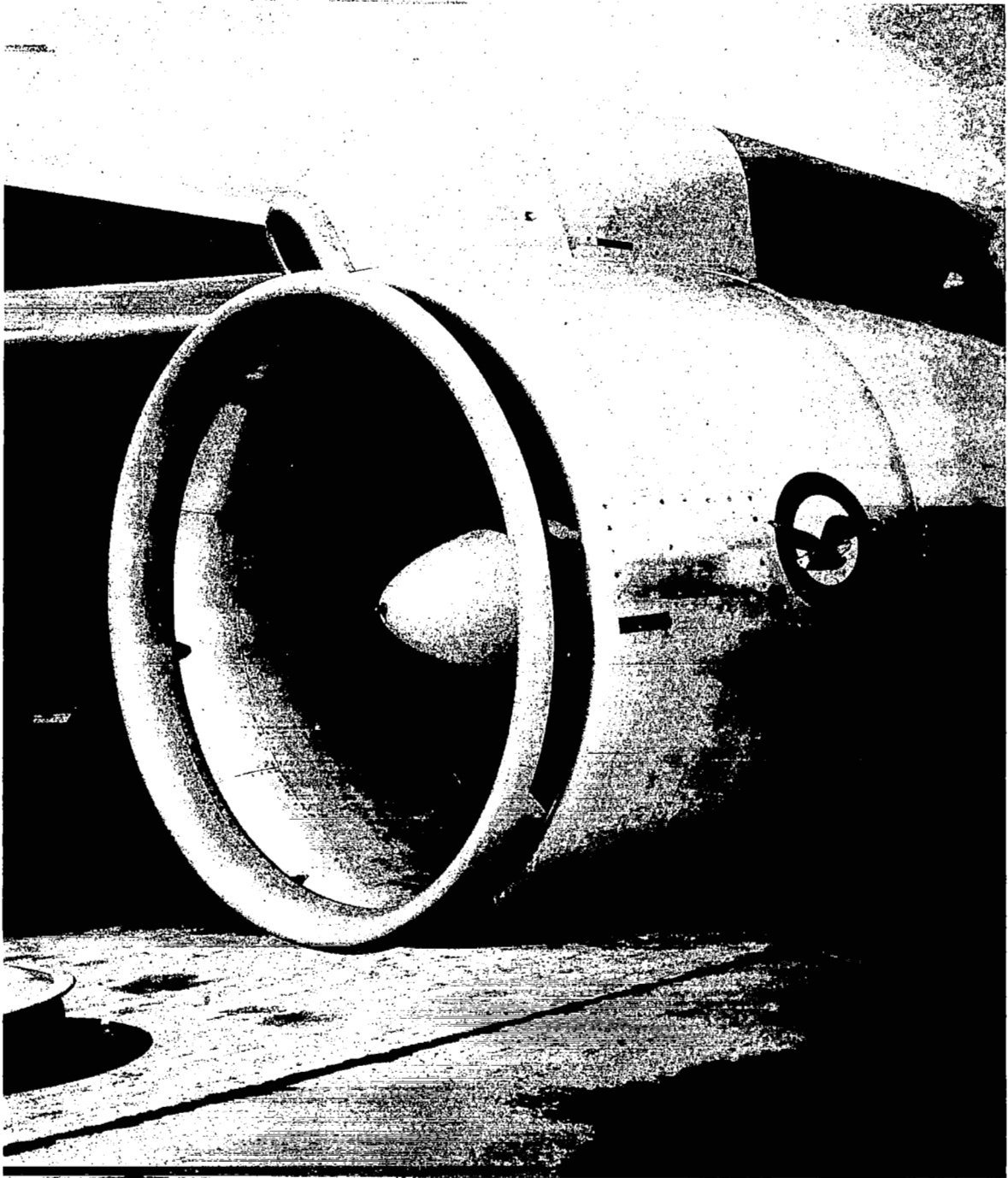


Figure 17.- Photograph of slotted intake.

L-64-6137

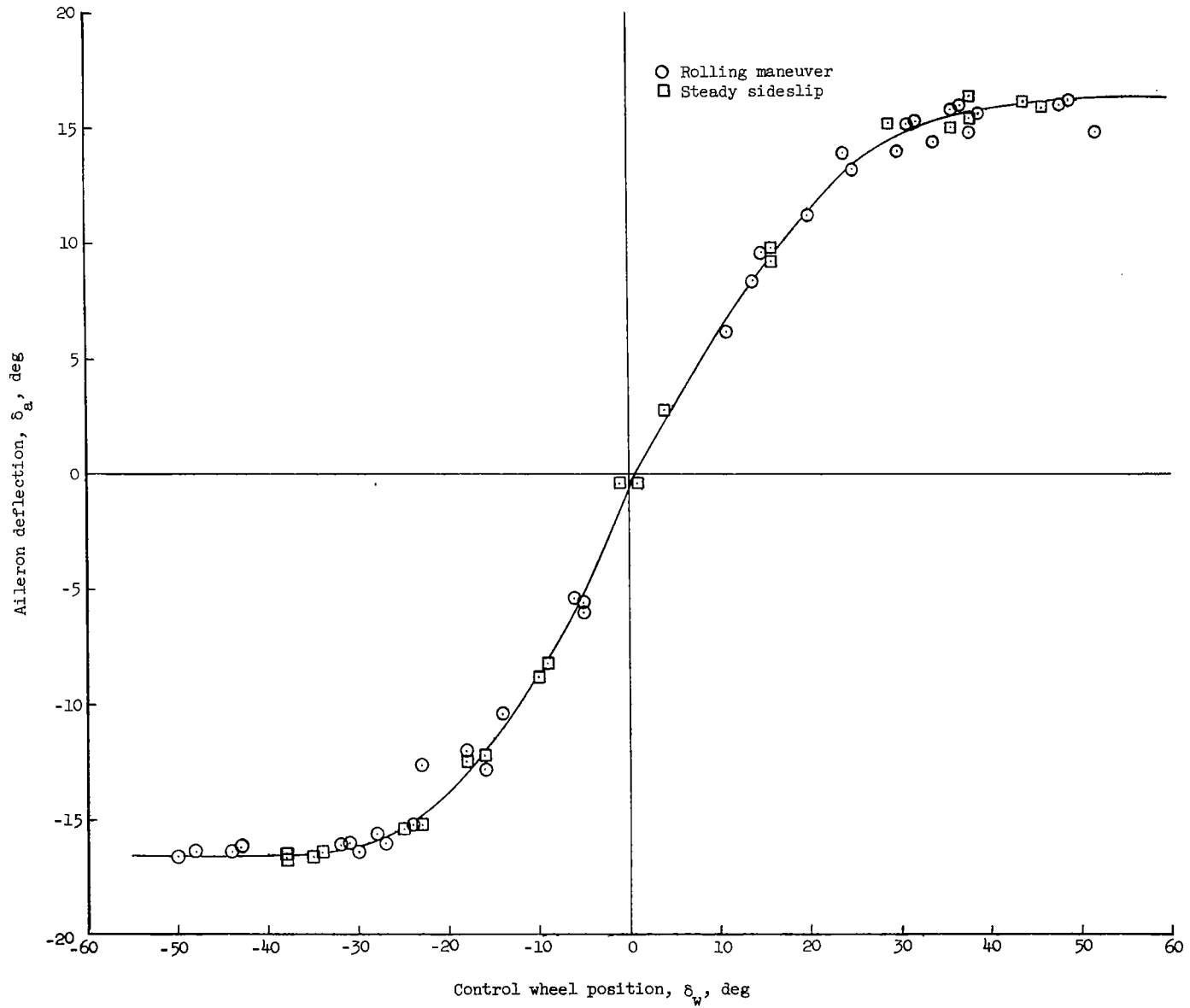


Figure 18.- Aileron deflection characteristics.

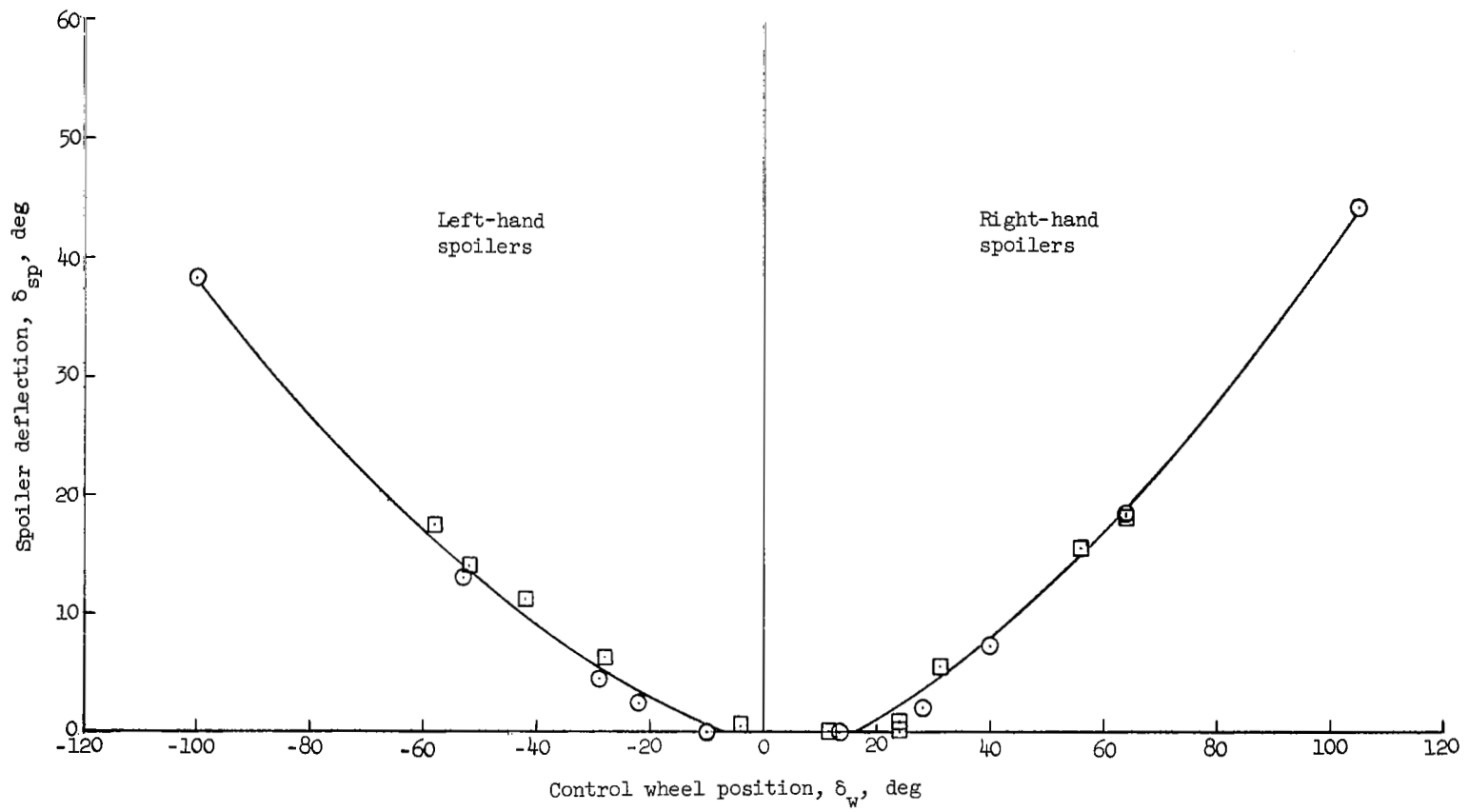


Figure 19.- Spoiler deflection characteristics.

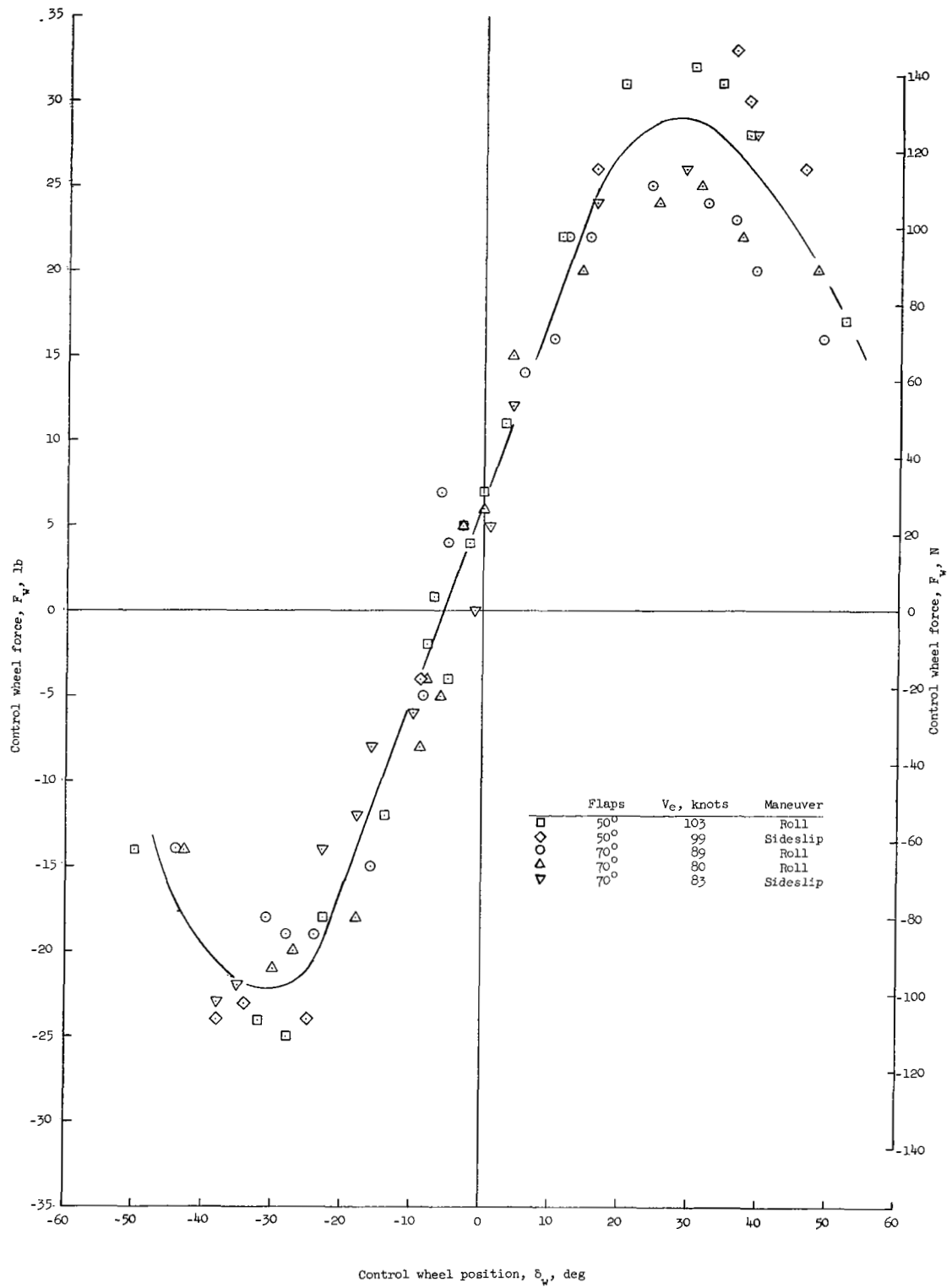


Figure 20.- Control-wheel-force characteristics.

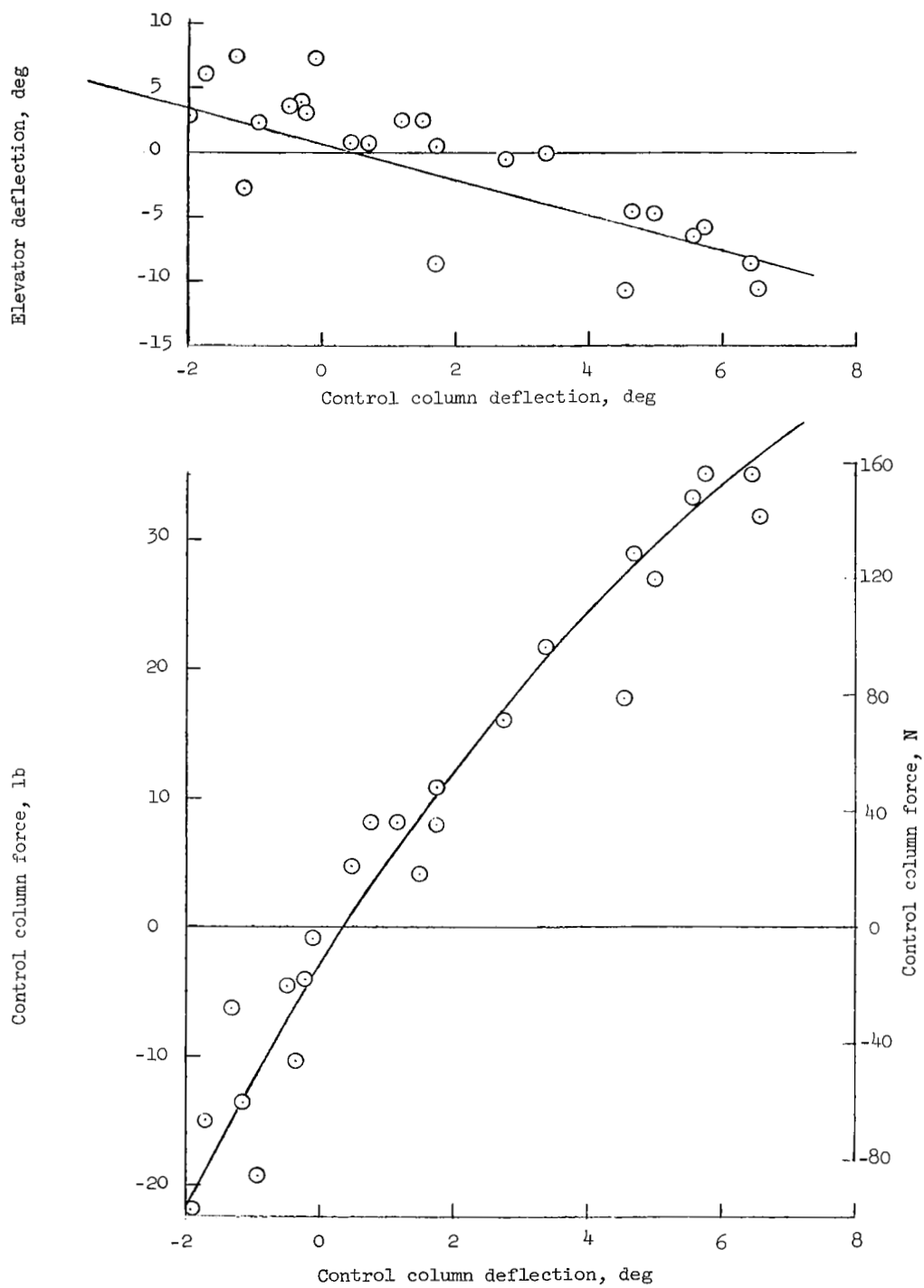


Figure 21.- Control column deflection and force characteristics at 100 knots.

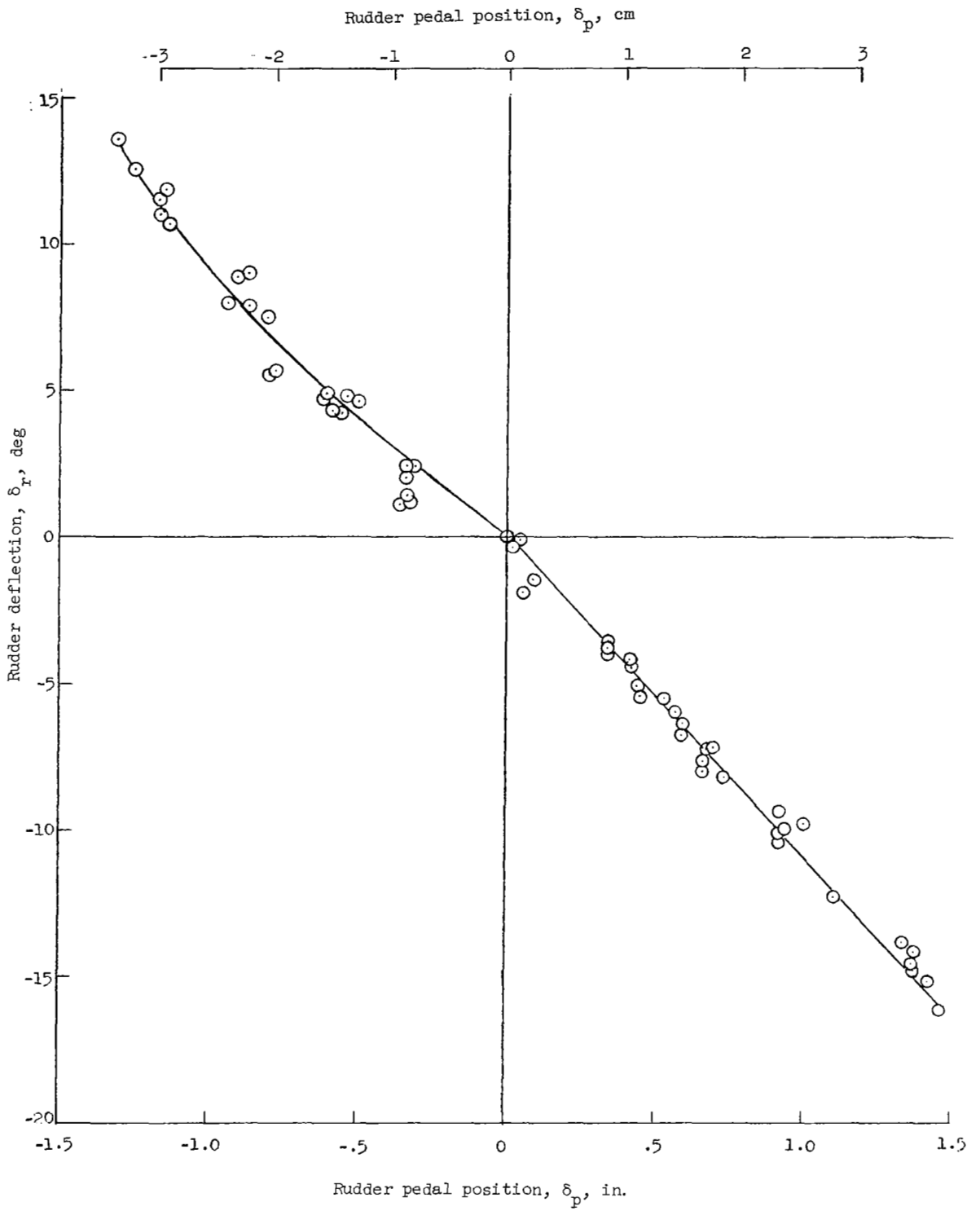


Figure 22.- Rudder deflection characteristics.

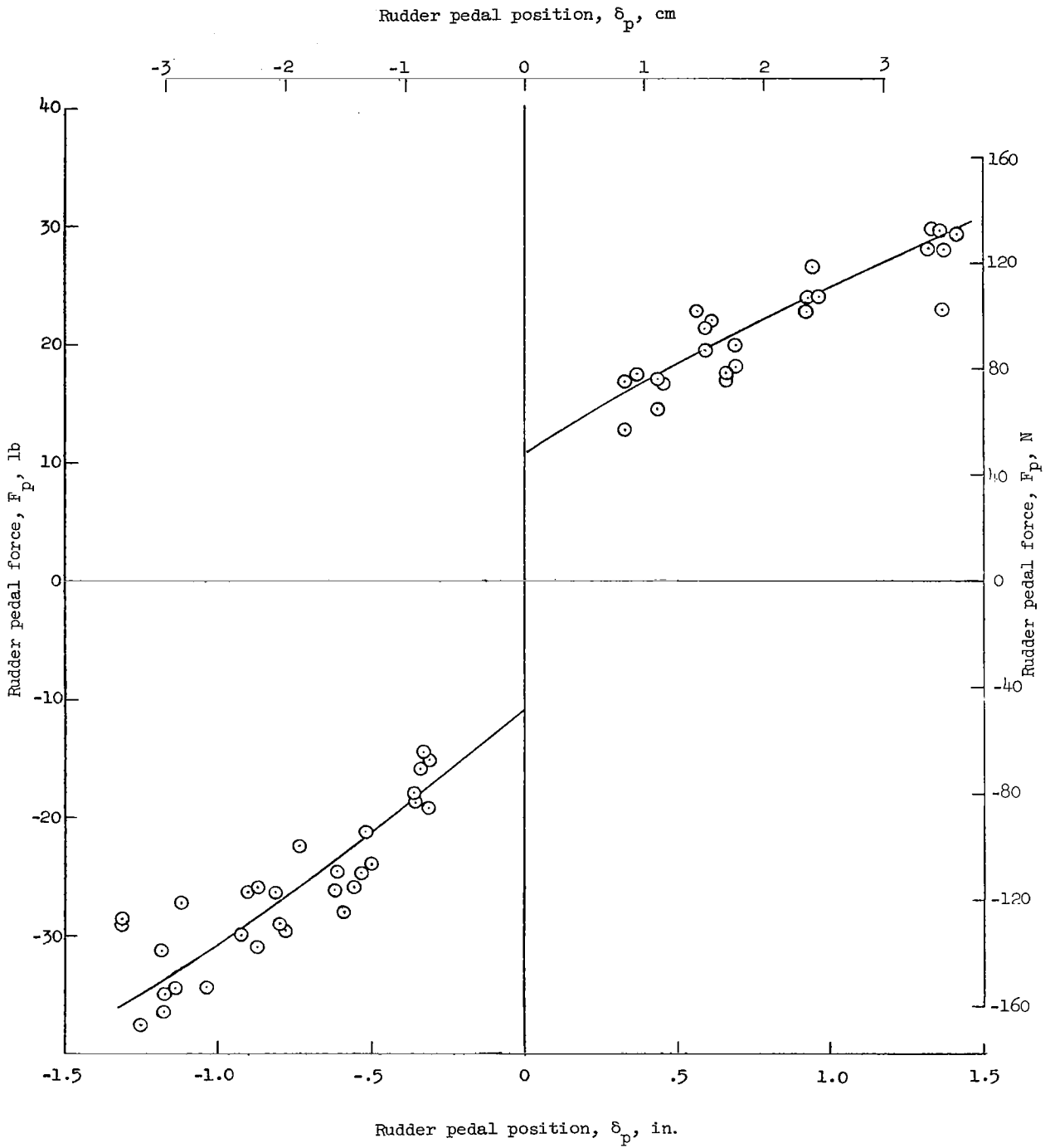


Figure 23.- Rudder pedal force characteristics at 100 knots.

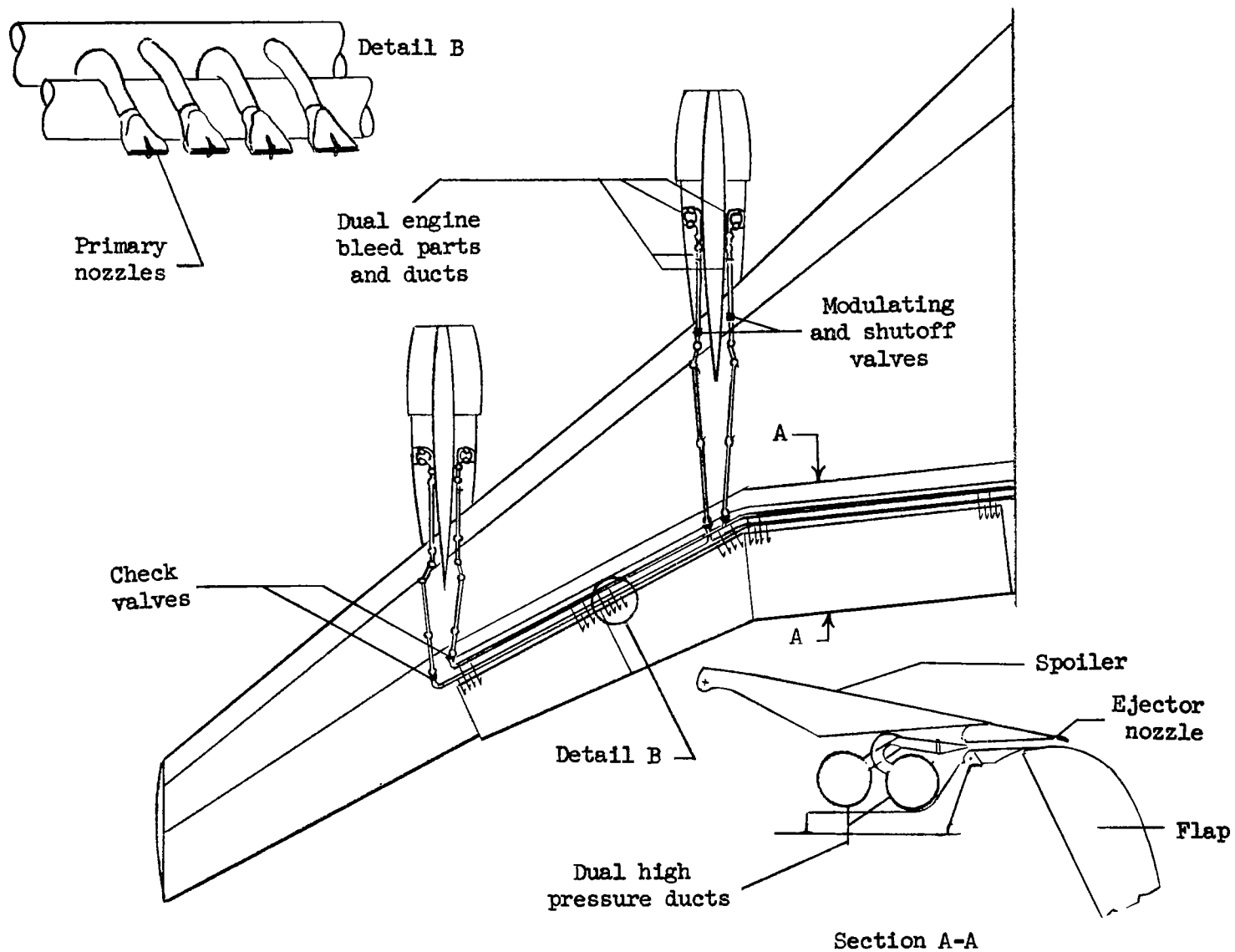


Figure 24.- Powered-lift system.

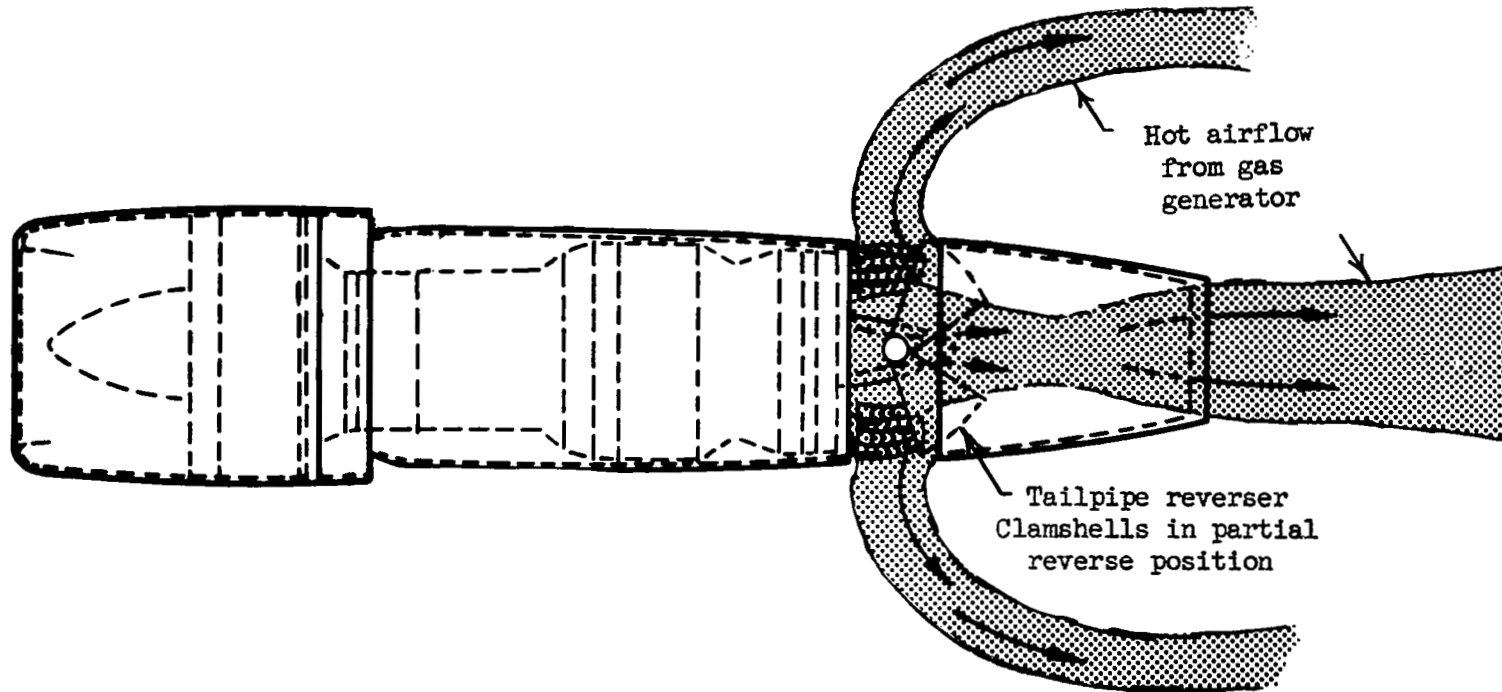


Figure 25.- Thrust-modulation system.

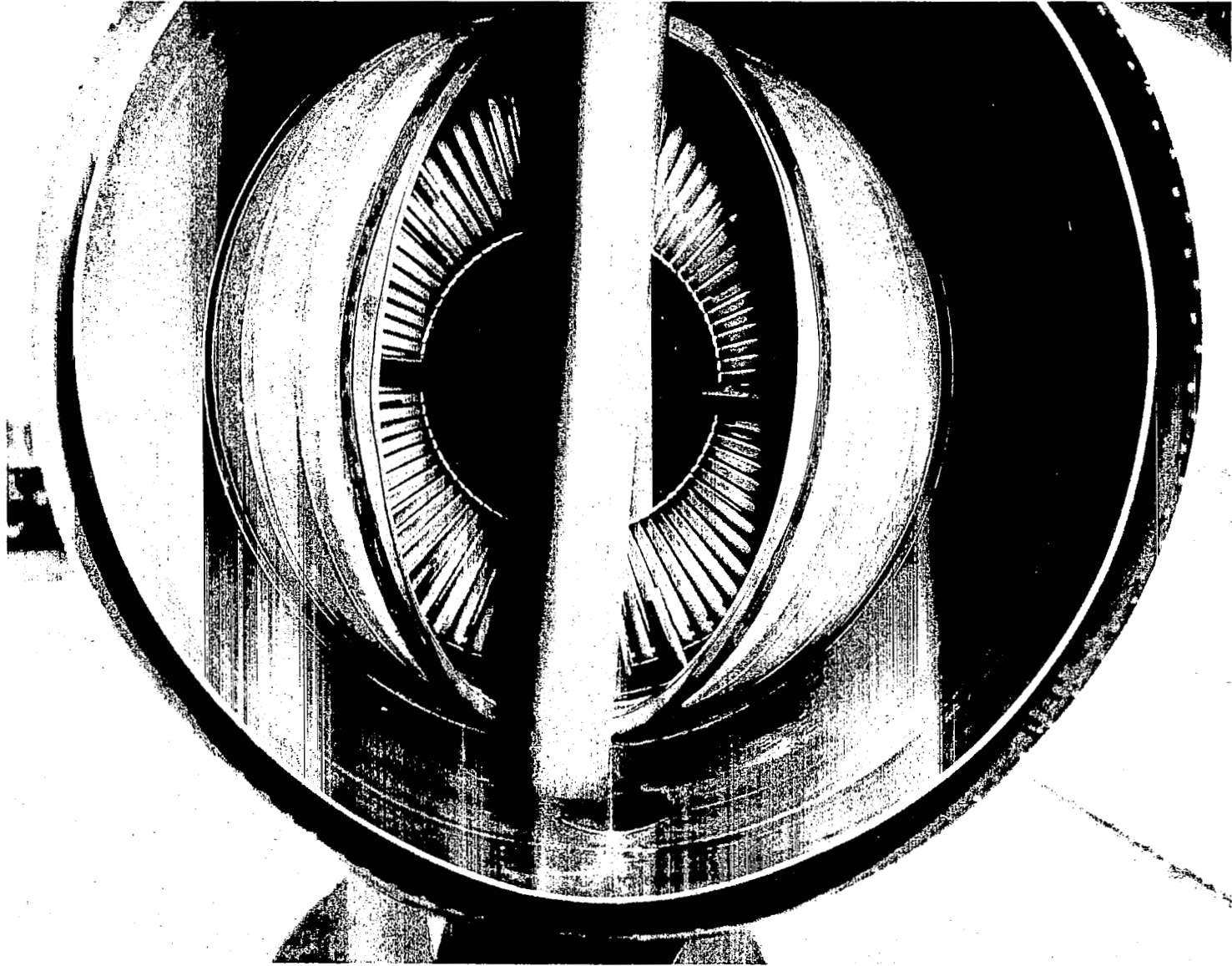


Figure 26.- Photograph of reverser clamshells.

L-64-6138

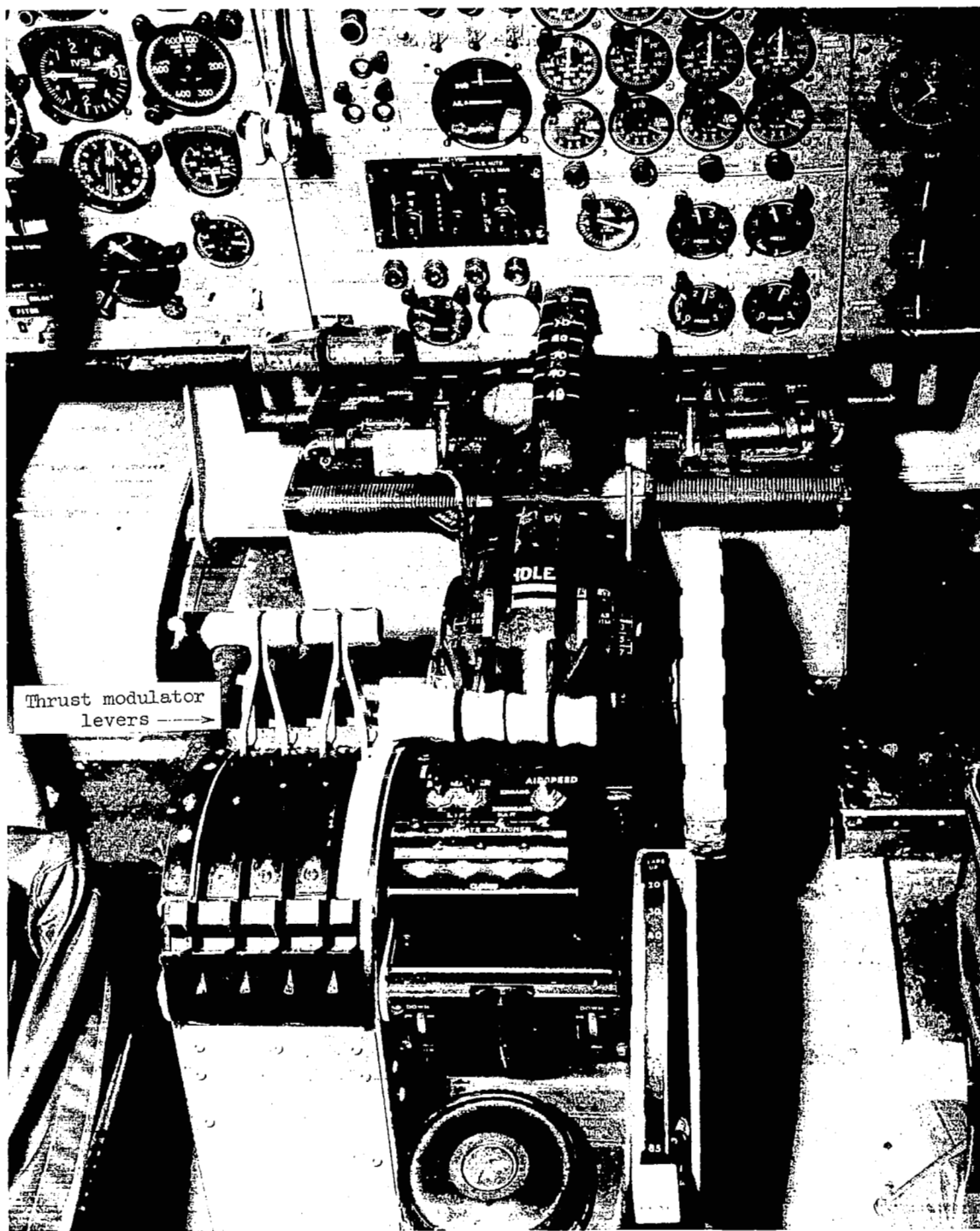


Figure 27.- Photograph showing thrust-modulation levers.

L-64-6129.1

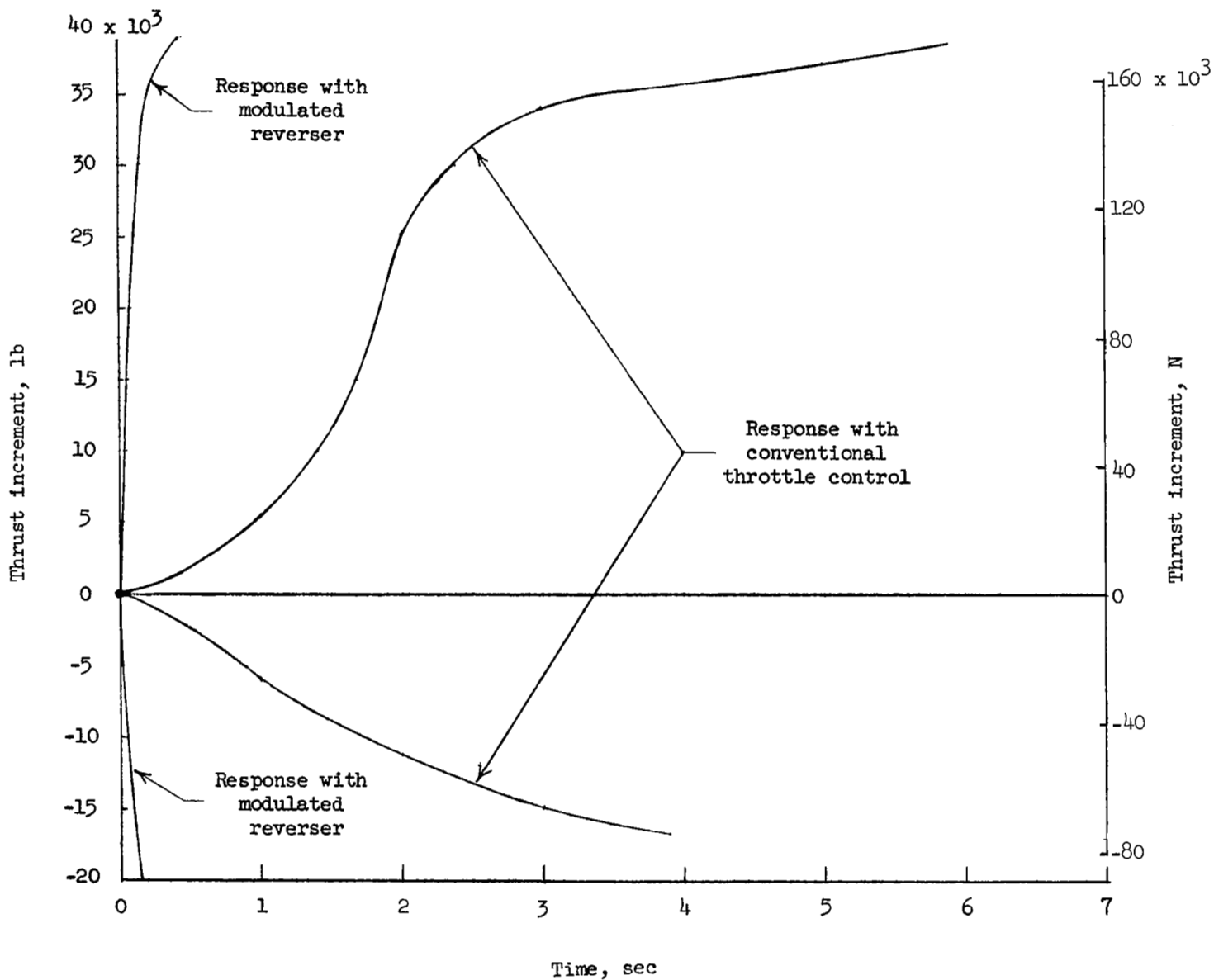


Figure 28.- Response characteristics of throttle control and thrust modulators (from approach power).

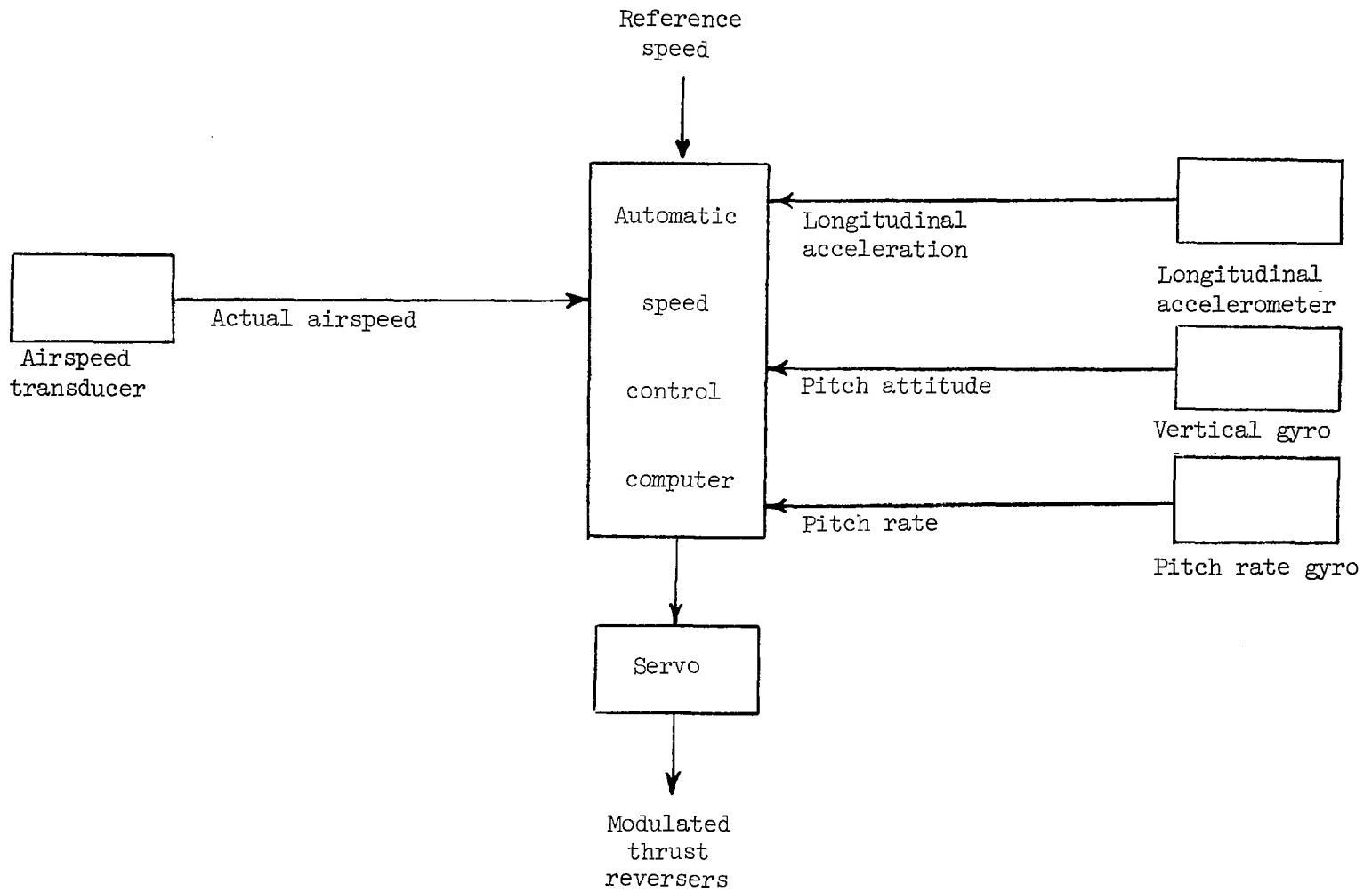
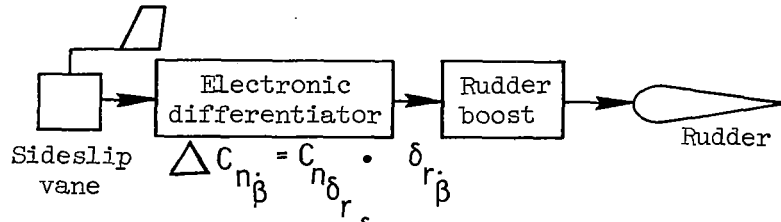


Figure 29.- Block diagram of automatic speed control system.

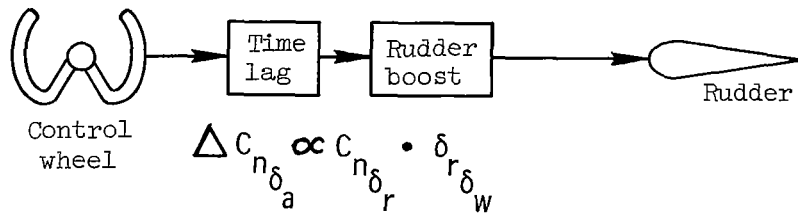
Sideslip rate damper



where  $\frac{\delta_{r\dot{\beta}}}{\beta_{\text{vane}}} = 2.72 \frac{\tau_1 s}{(\tau_1 s + 1)^2}$   
 $\beta_{\text{vane}} \approx 1.5\beta$   
 $\tau_1 = 0.25 \text{ sec}$

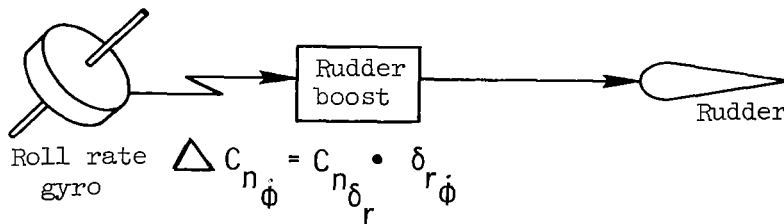
s = Laplace transform operator

Turn coordination programmer



where  $\frac{\delta_{r\delta_w}}{\delta_w} = 0.3 \frac{1}{\tau_2 s + 1}$   
 $\tau_2 = 1.0 \text{ sec}$   
 $\delta_w \approx 1.45 \delta_a$

Roll decoupler



where  $\frac{\delta_{r\dot{\phi}}}{\dot{\phi}} = 0.47 \frac{1}{\tau_3 s + 1}$   
 $\tau_3 = 1.1 \text{ sec}$

Figure 30.- Stability augmentation system.

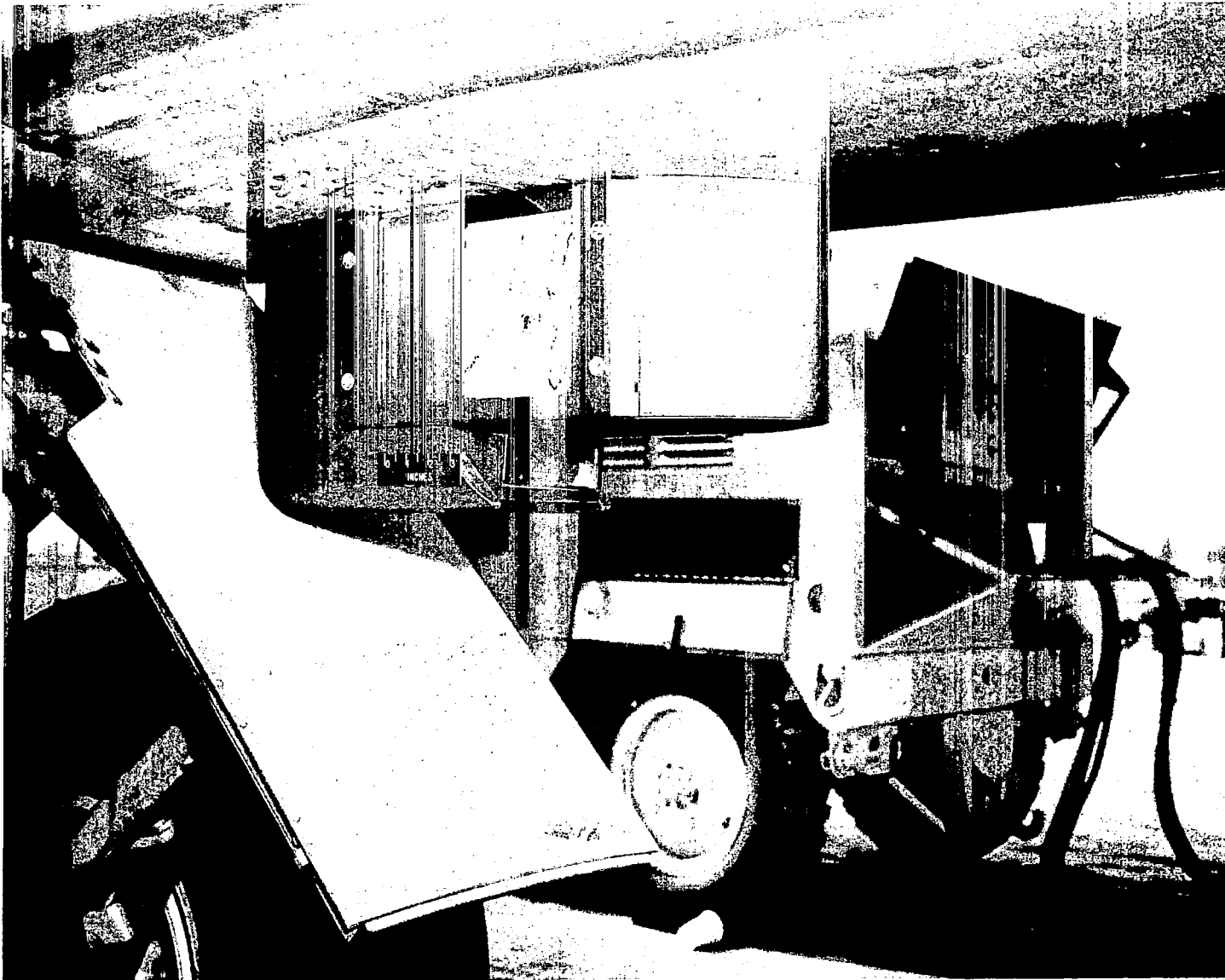


Figure 31.- Photograph of airborne theodolite.

L-64-6119

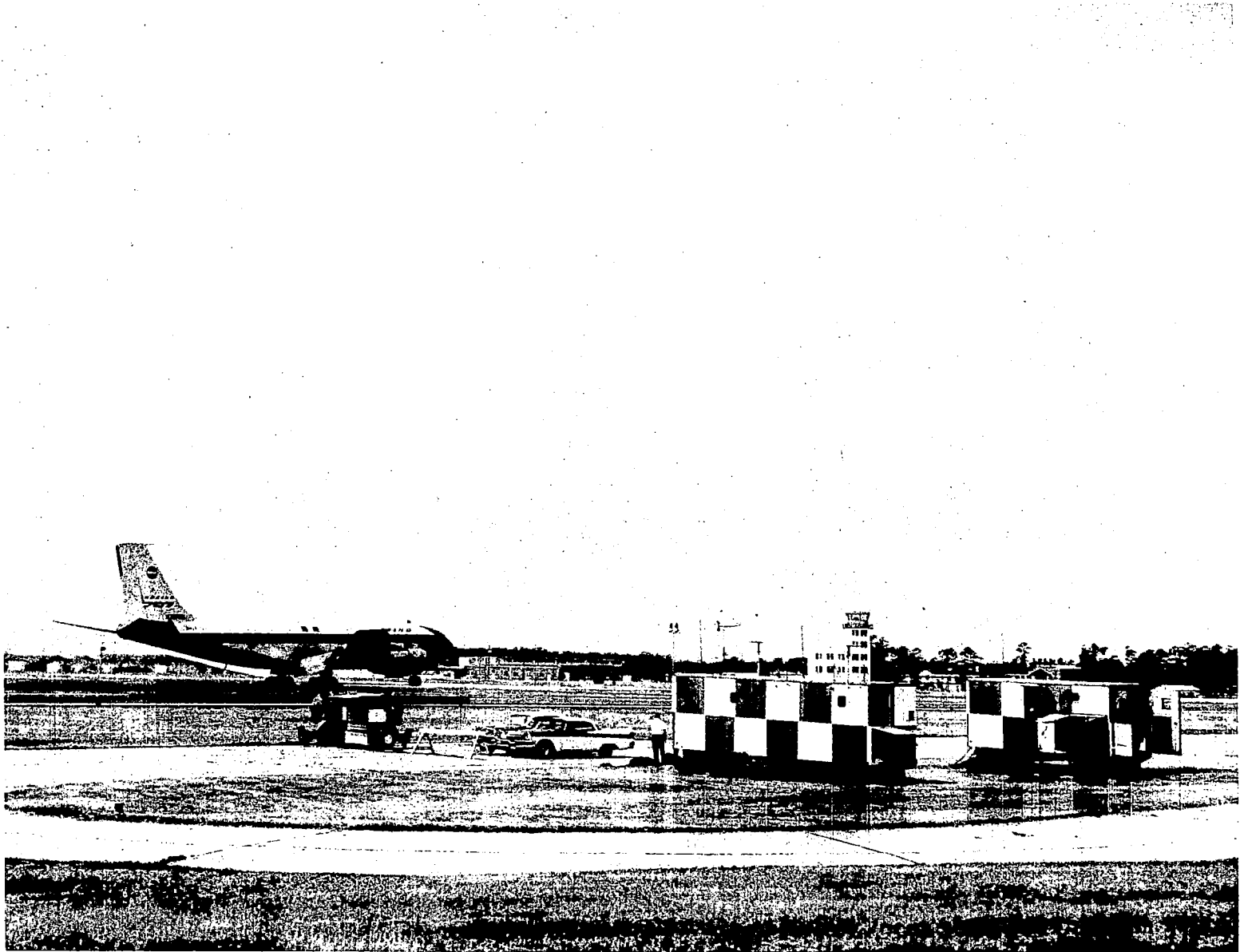


Figure 32.- Photograph of GSN-5 instrument landing system.

— Full-scale indicator deflection for GSN-5 radar  
 - - - Full-scale indicator deflection for standard ILS

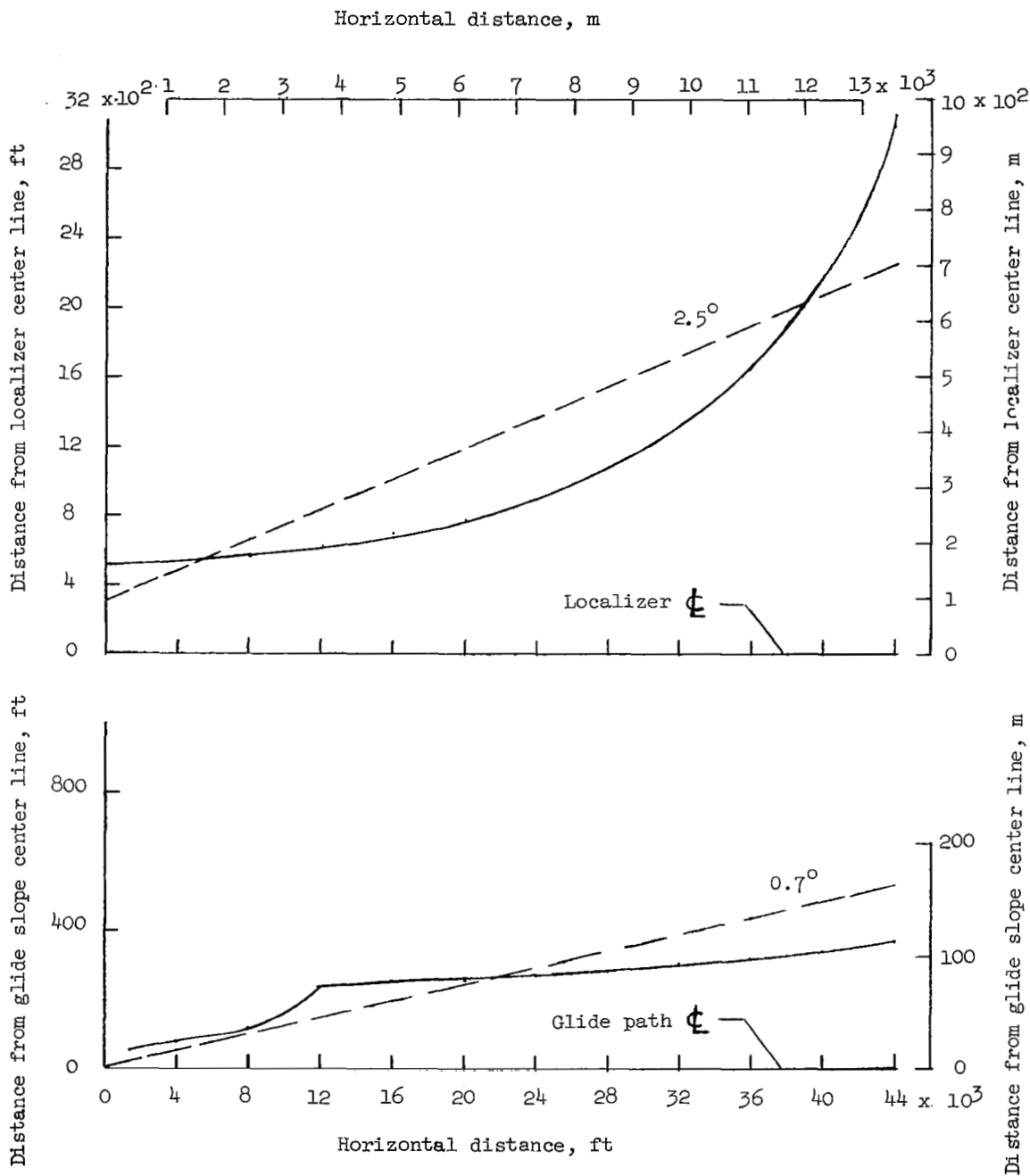


Figure 33.- GSN-5 glide slope and localizer profiles from 1500 feet (460 meters) touchdown spot.

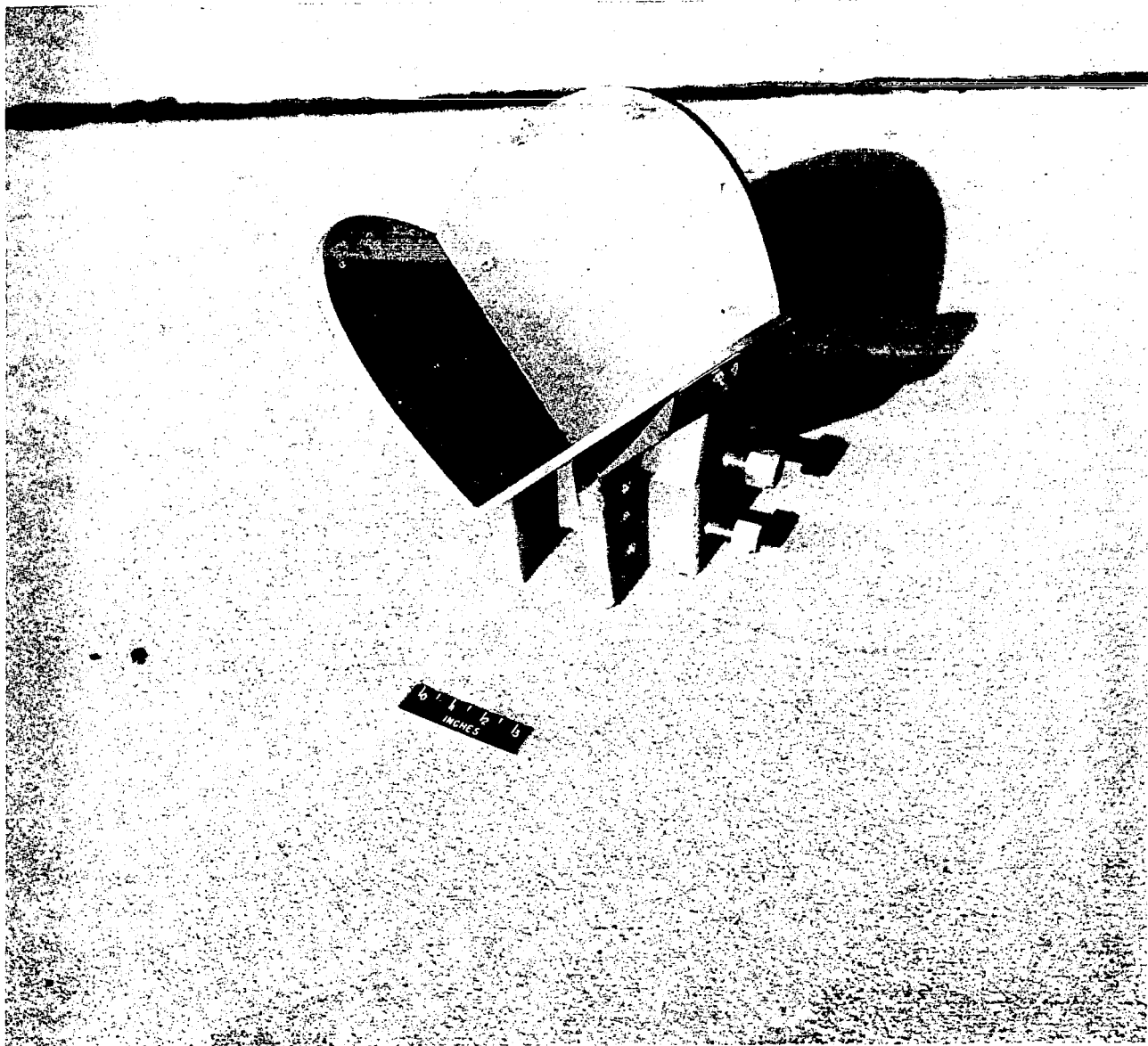


Figure 34.- Airborne corner reflector.

L-64-6126

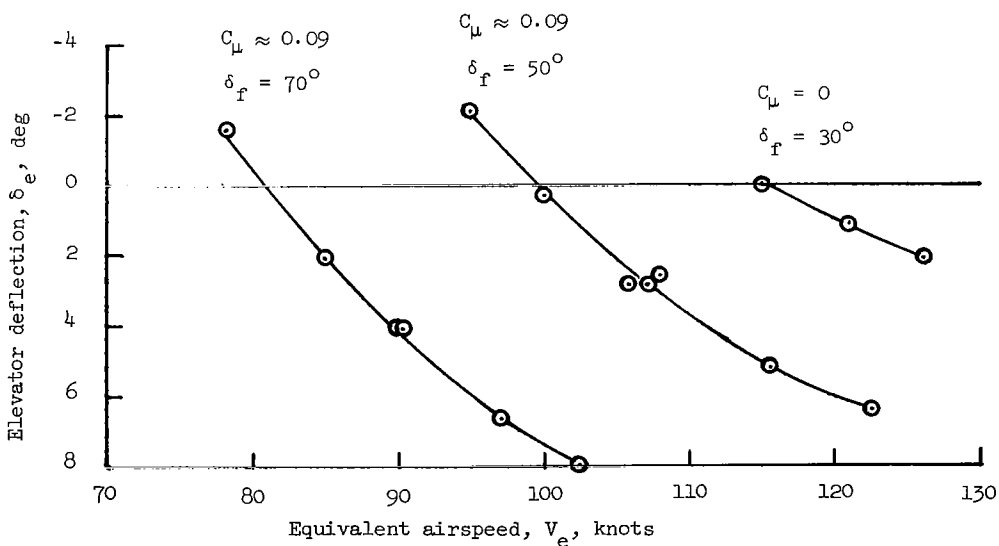
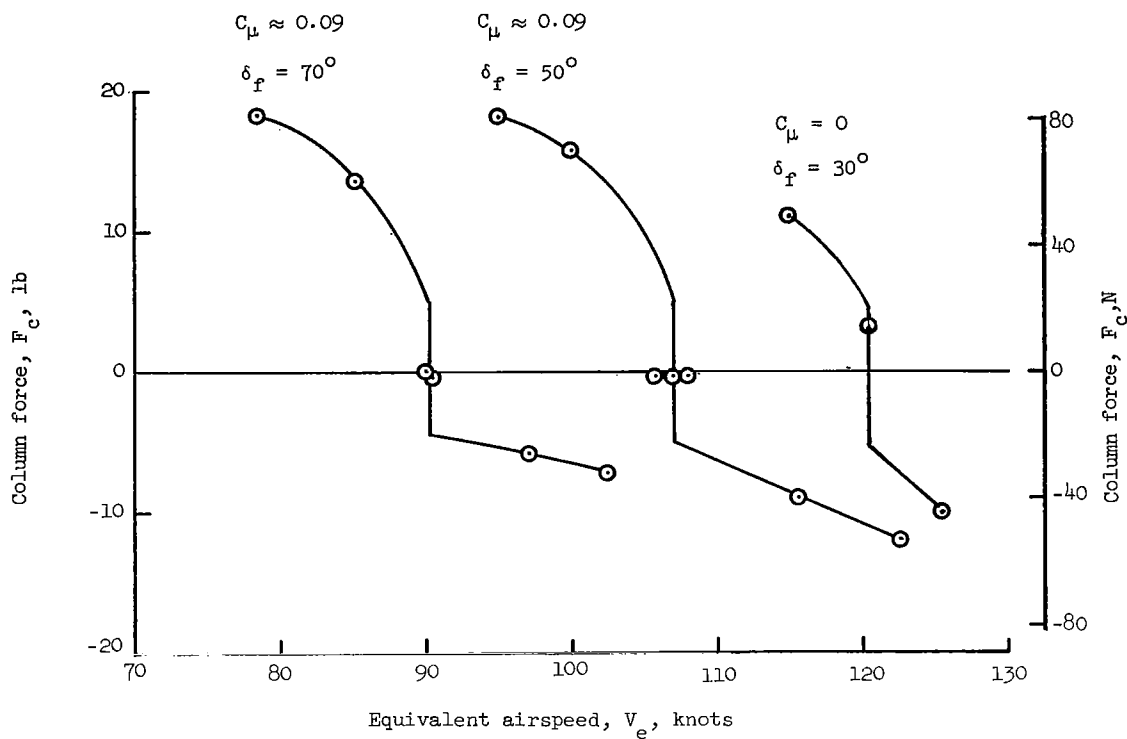


Figure 35.- Stick-free and stick-fixed static longitudinal stability characteristics of the airplane as a function of airspeed without and with powered lift.

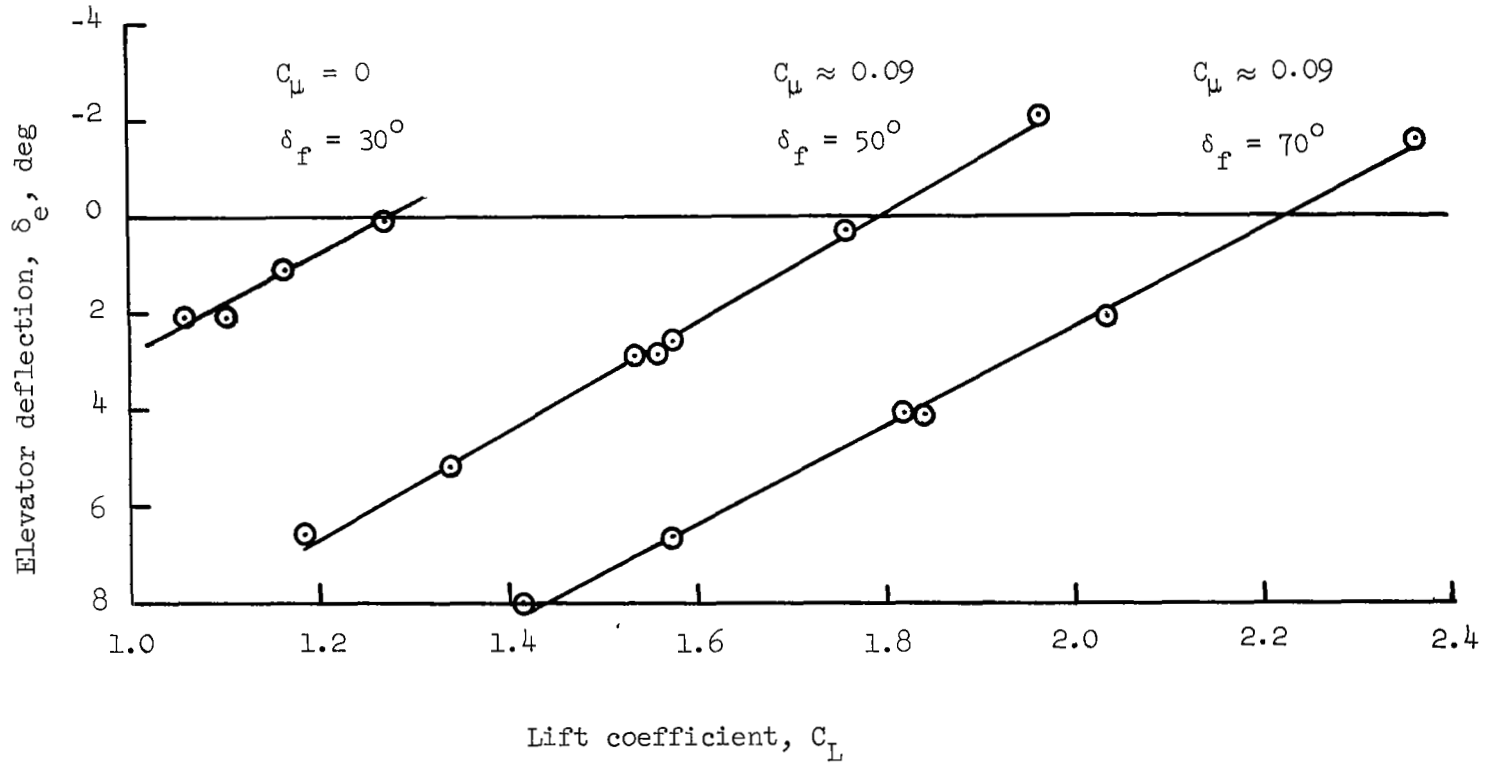


Figure 36.- Stick-fixed static longitudinal stability characteristics of the airplane as a function of lift coefficient without and with powered lift.

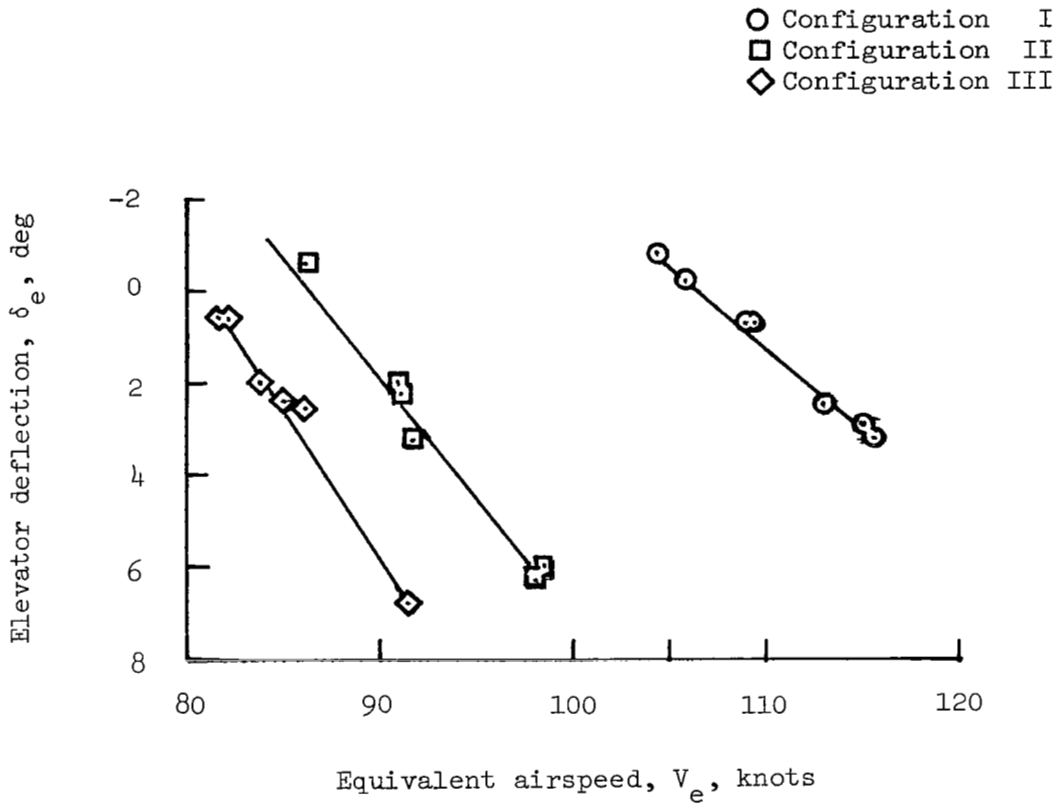


Figure 37.- Stick-fixed static longitudinal stability characteristics of the airplane for flight-test configurations I, II, and III.

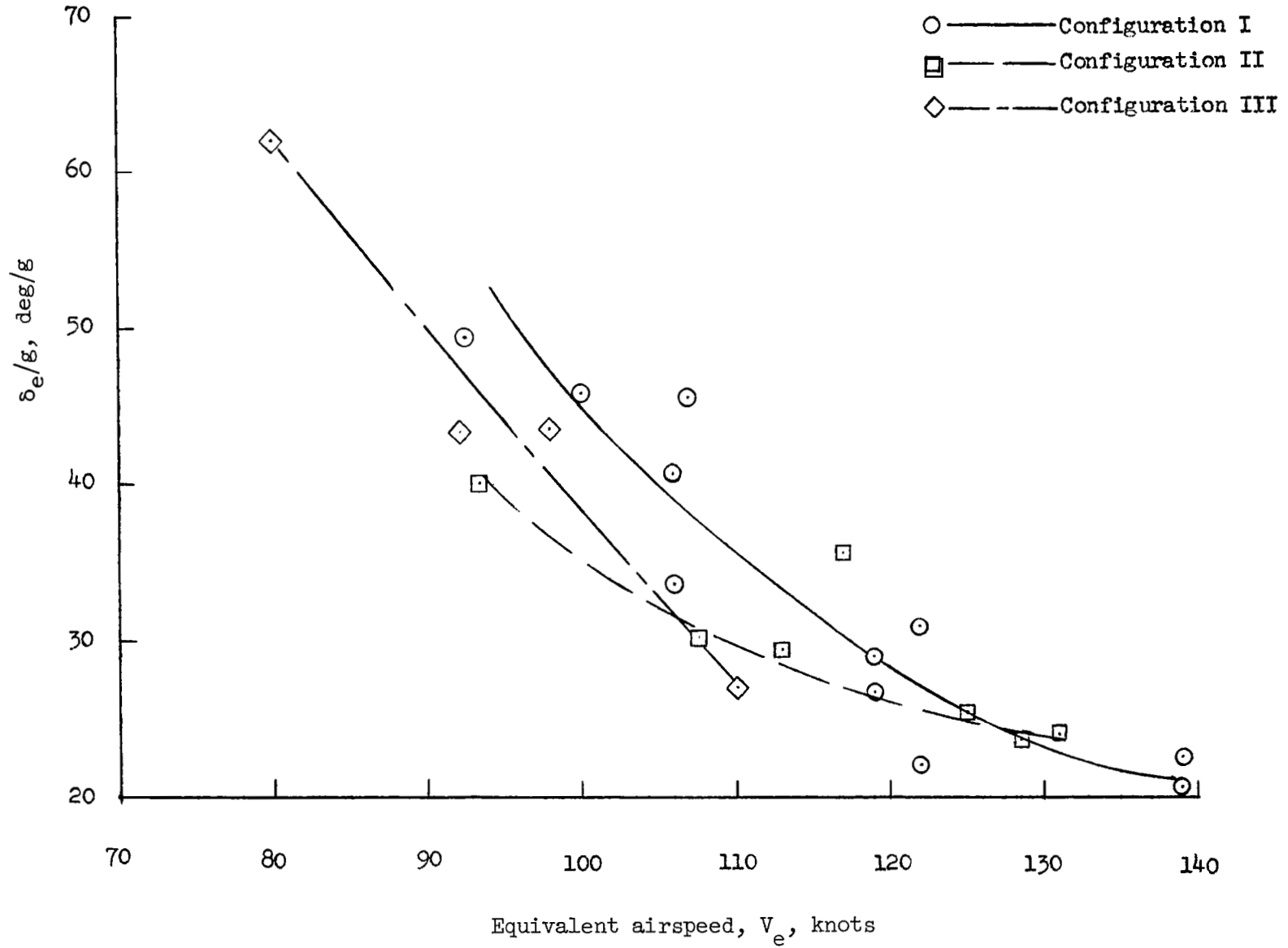


Figure 38.- Variation of elevator deflection per g with equivalent airspeed.

- ———  $\delta_F = 30^\circ, C_\mu = 0$
- ———  $\delta_F = 50^\circ, C_\mu \approx 0.04$
- ◇ — - - -  $\delta_F = 60^\circ, C_\mu \approx 0.09$

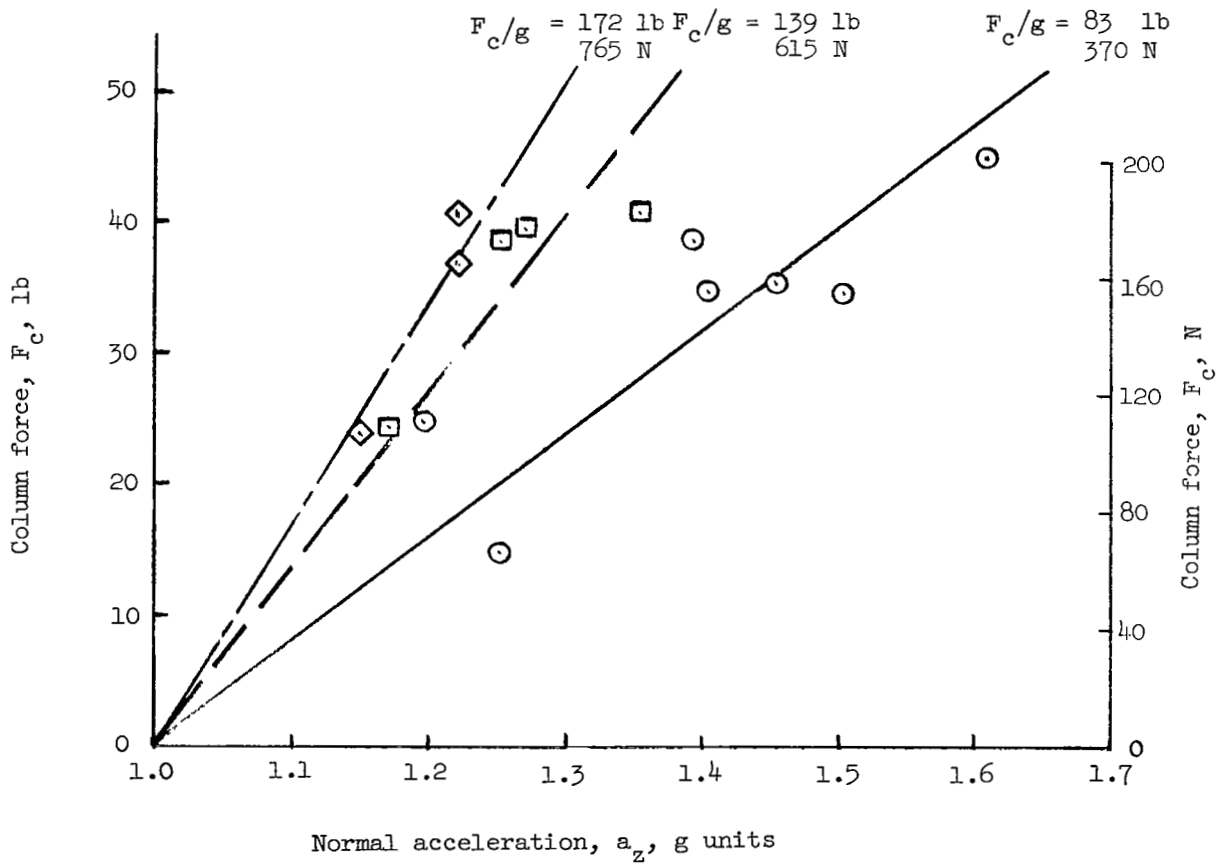
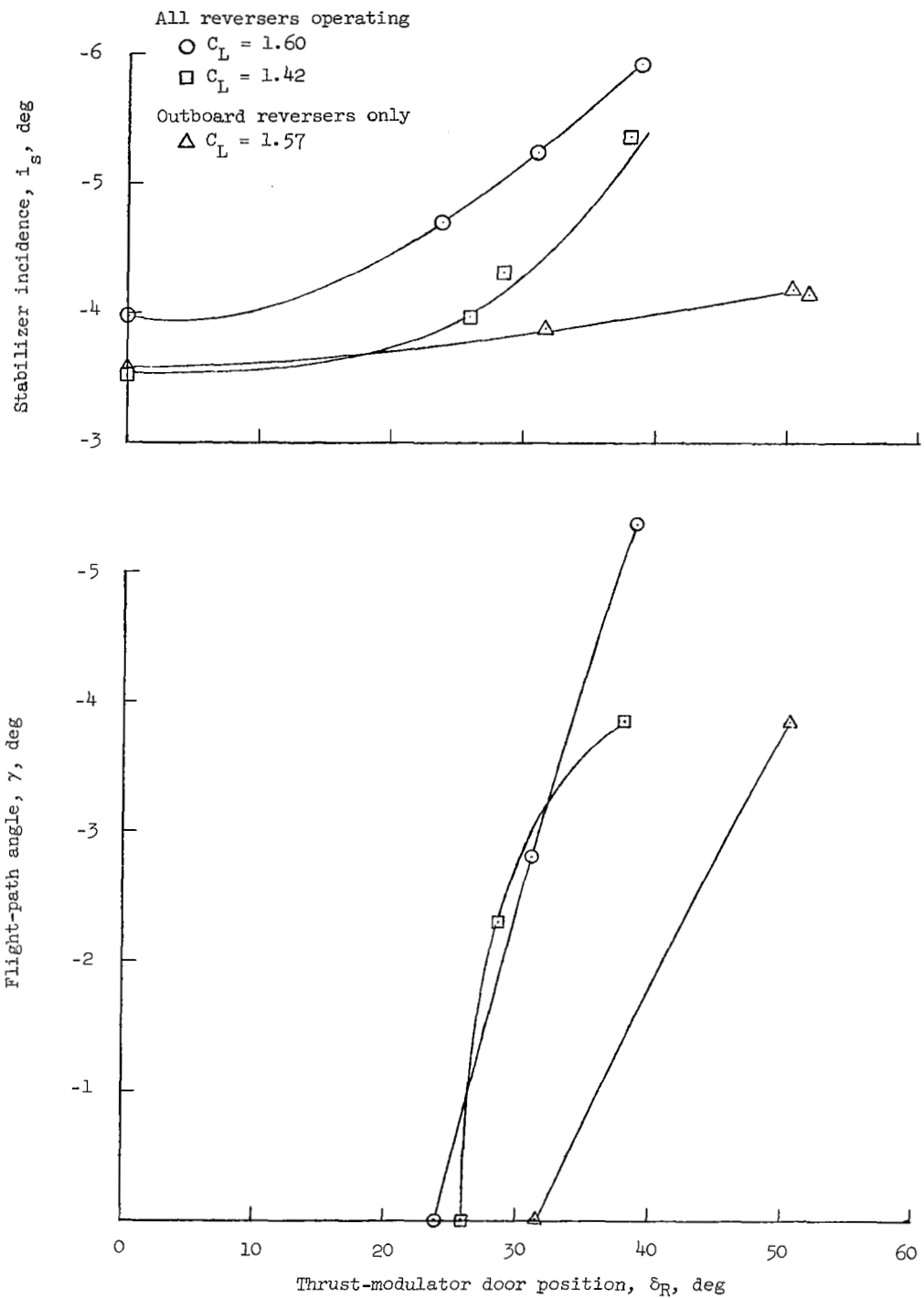
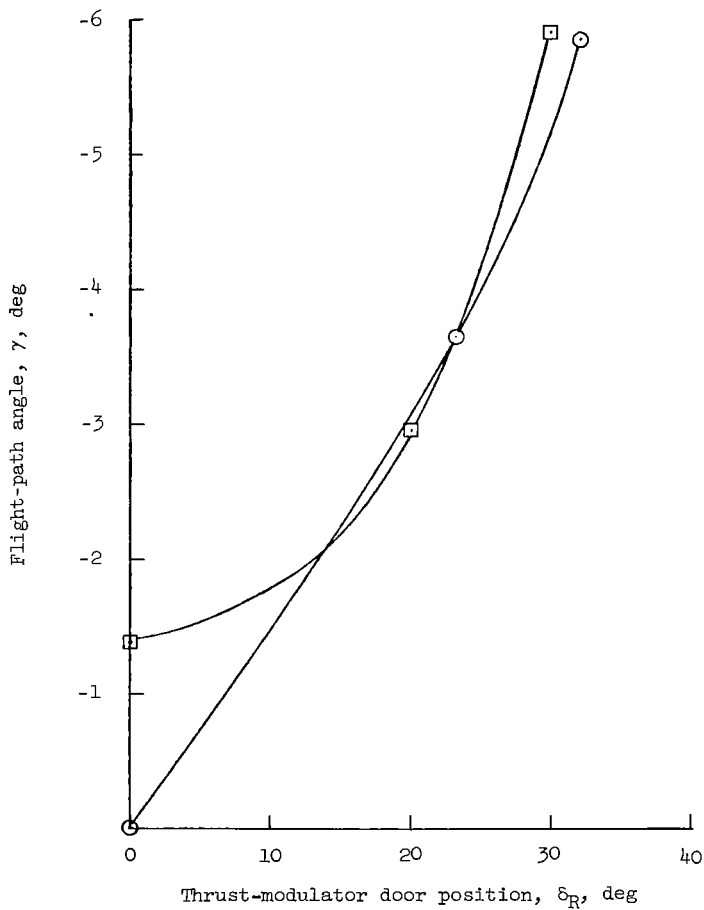
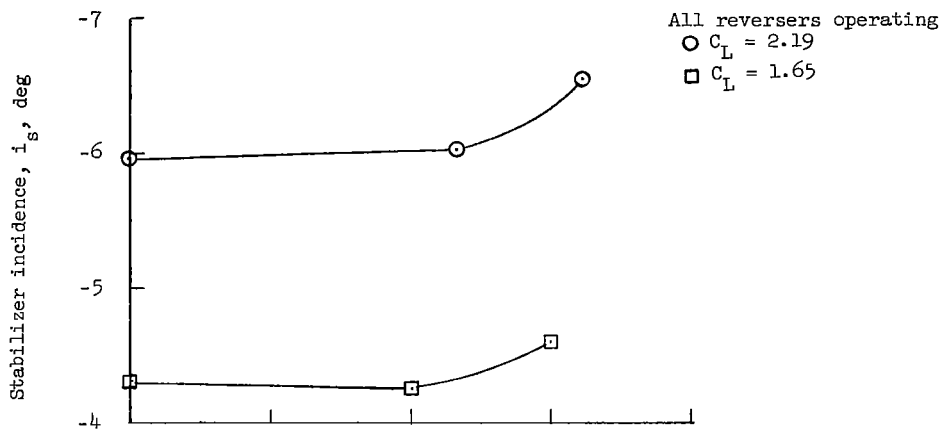


Figure 39.- Variation of control force with normal acceleration.



(a)  $\delta_f = 50^\circ$ .

Figure 40.- Effects of thrust modulation on flight-path angle and stabilizer incidence for trim with maximum continuous power.



(b)  $\delta_f = 70^\circ$ .

Figure 40.- Concluded.

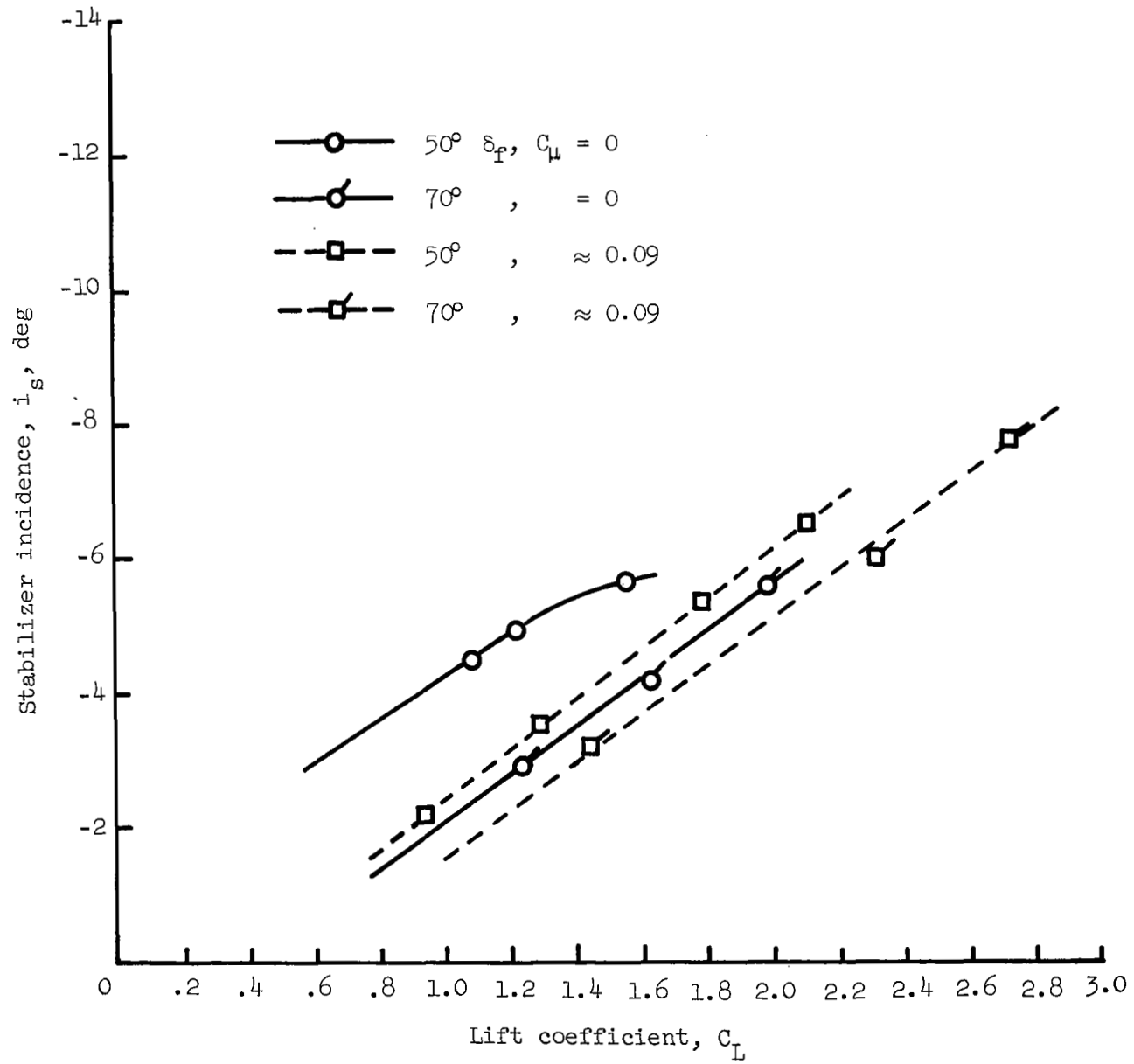


Figure 41.- Stabilizer incidence required for trim for various flap and powered-lift configurations.

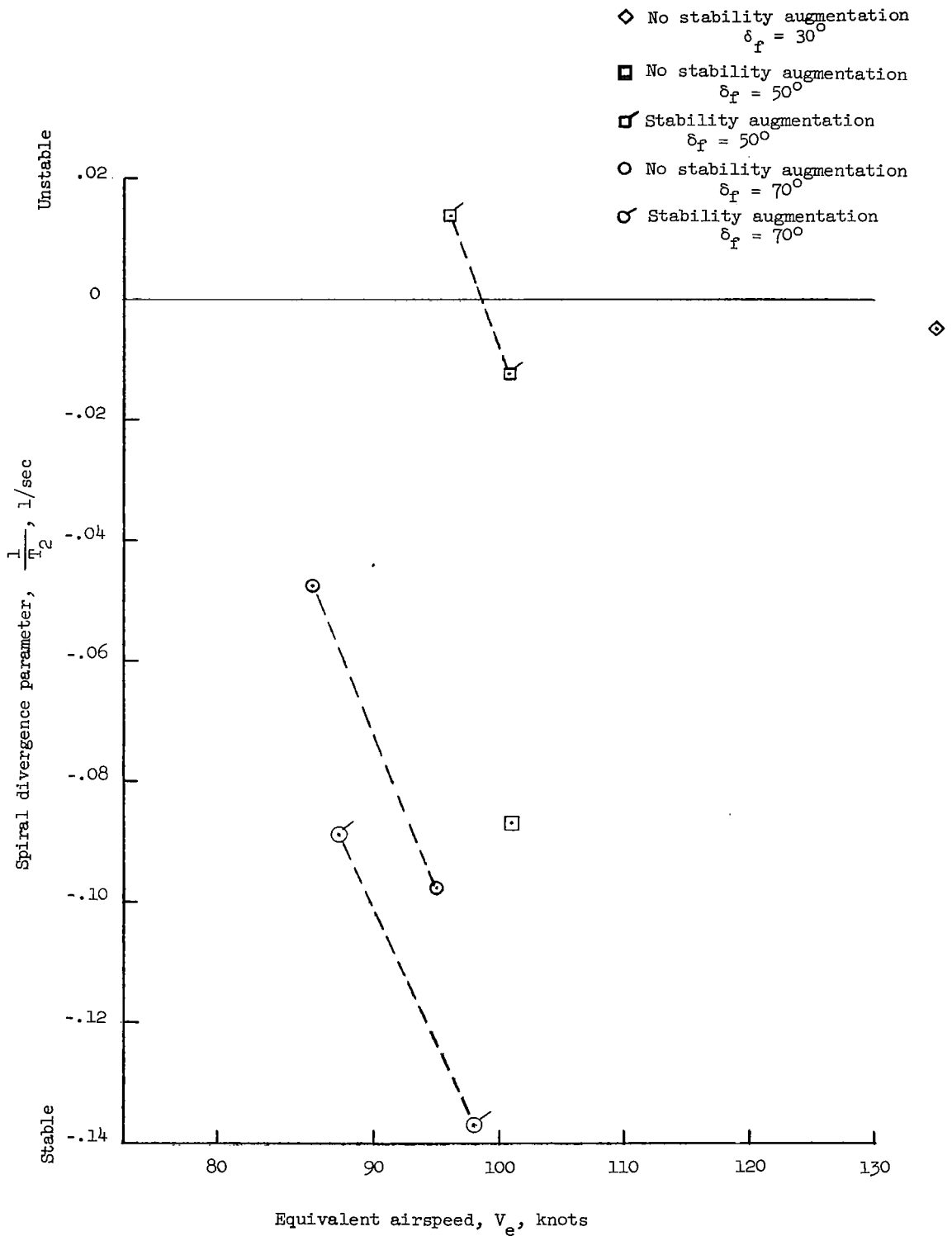


Figure 42.- Spiral stability characteristics of the airplane with and without stability augmentation. (Stability augmentation in this case included only the  $\beta$  damper.)

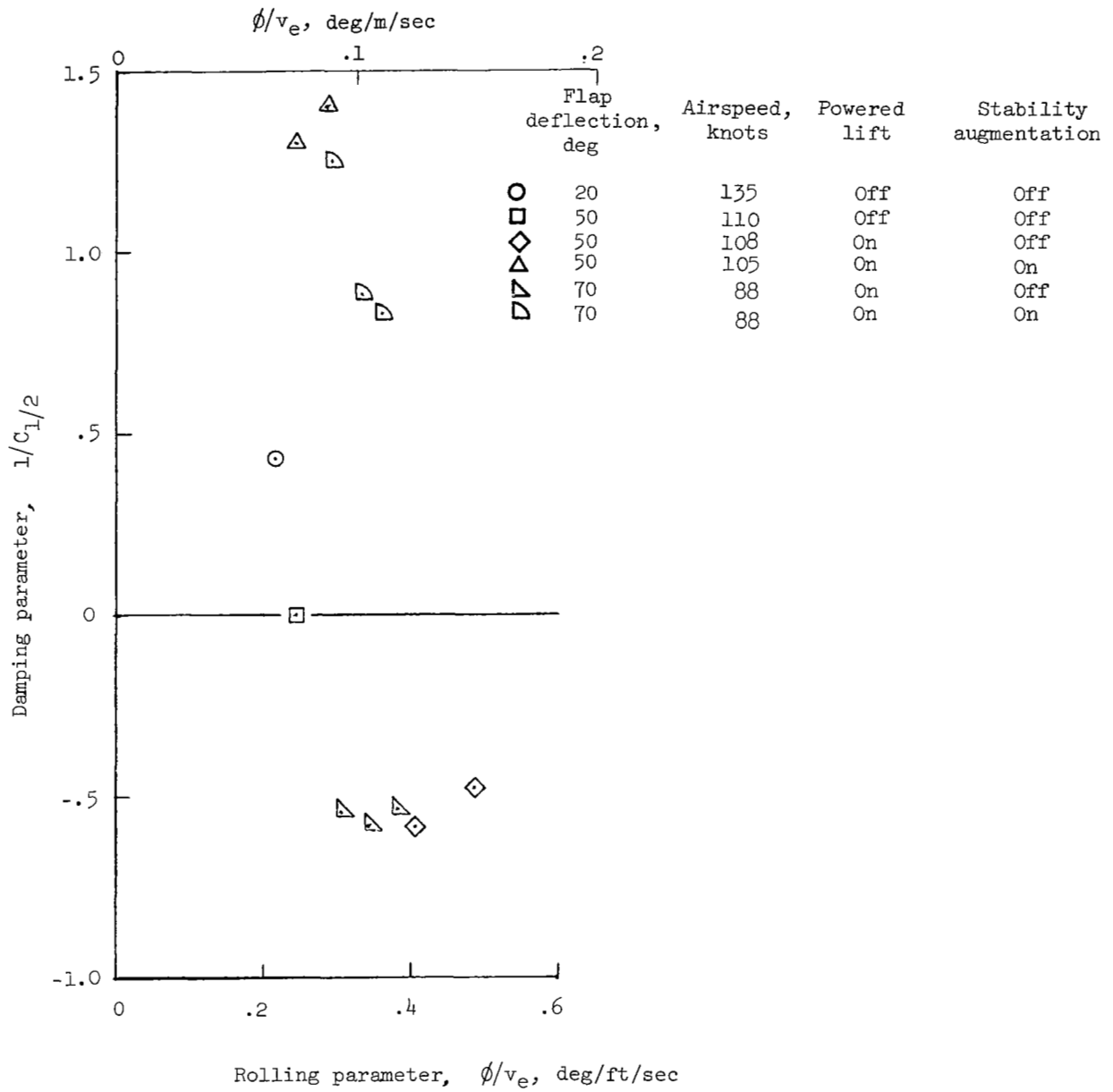
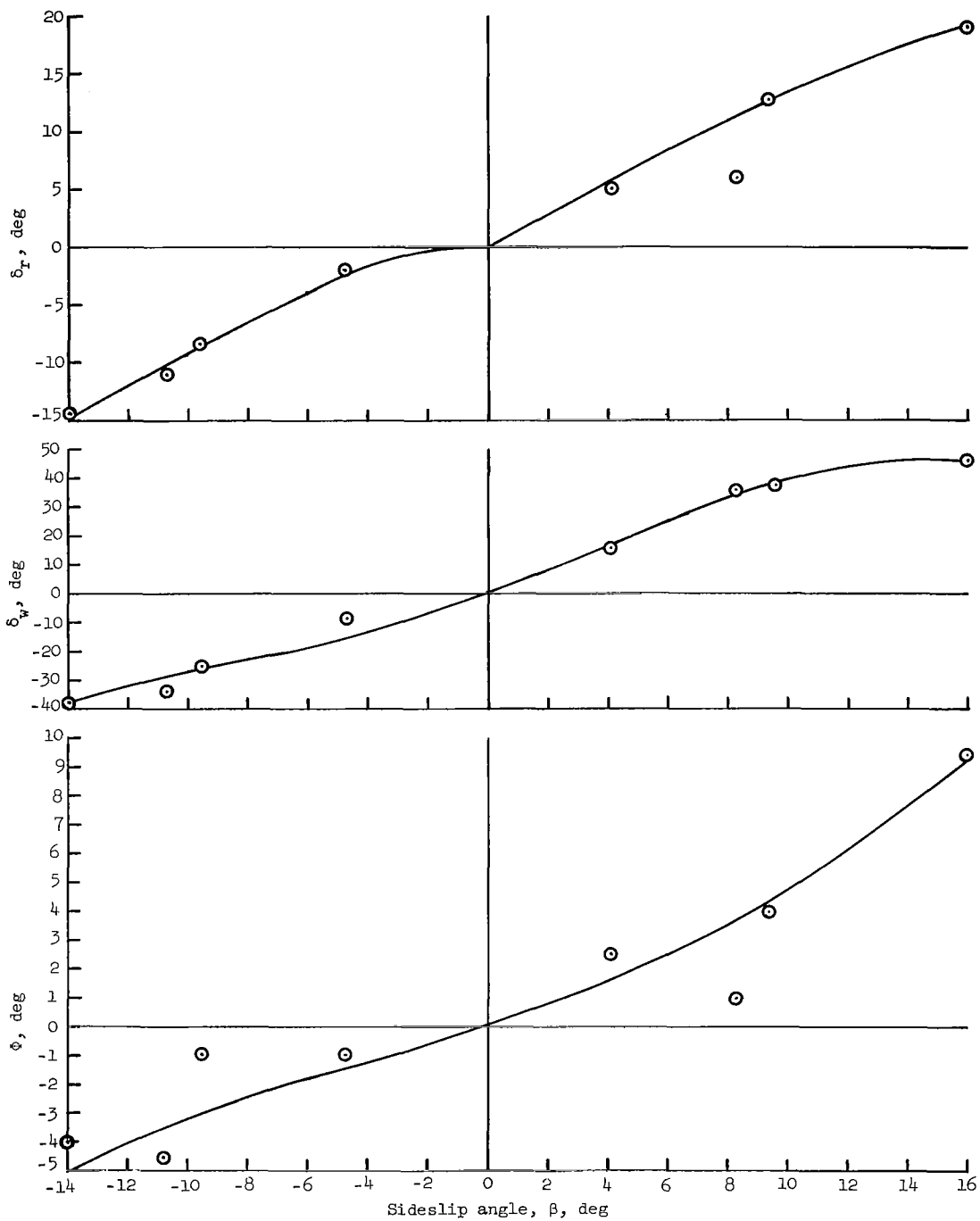
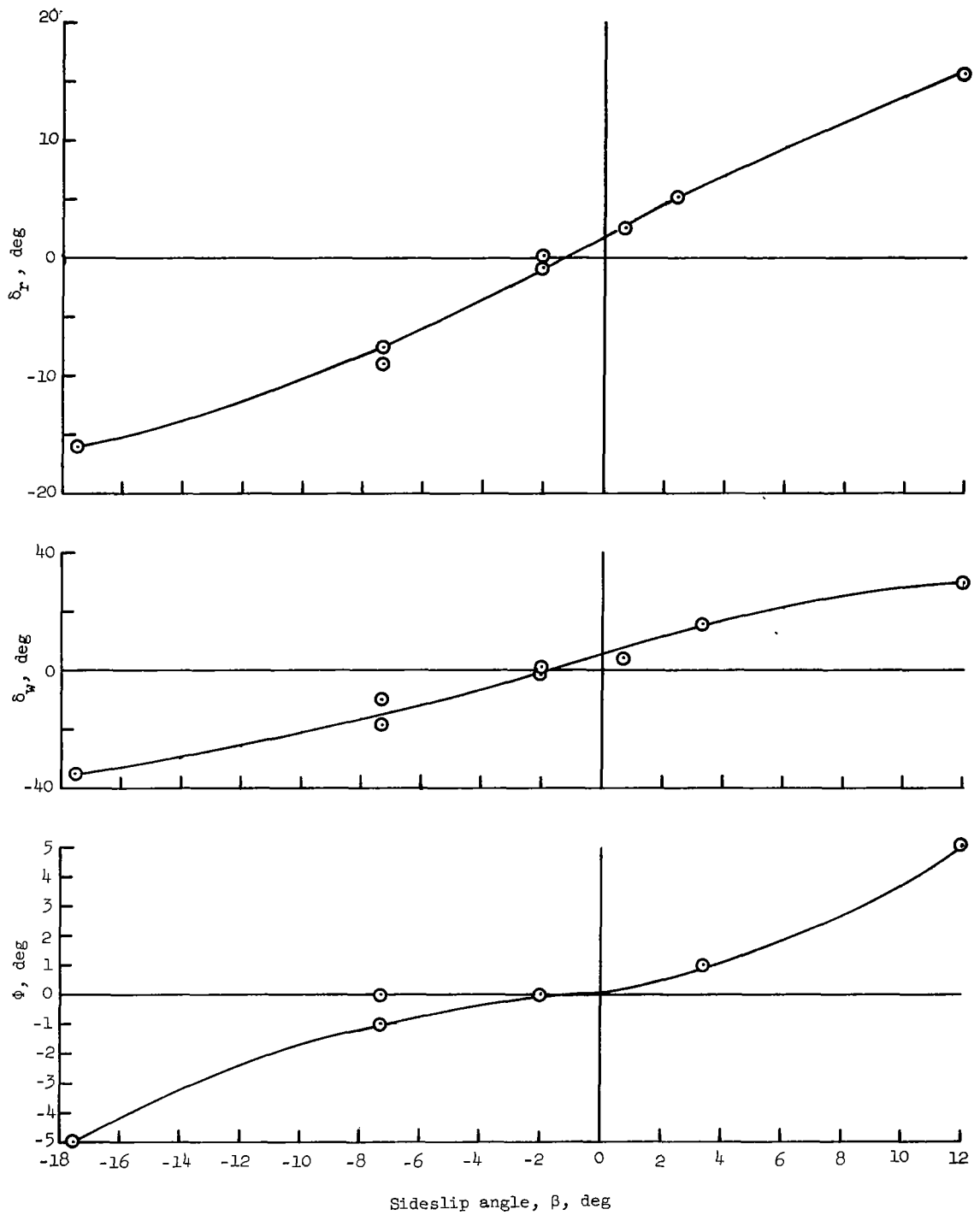


Figure 43.- Dutch roll characteristics of airplane with and without stability augmentation. (Augmentation in this case included only the  $\beta$  damper.)



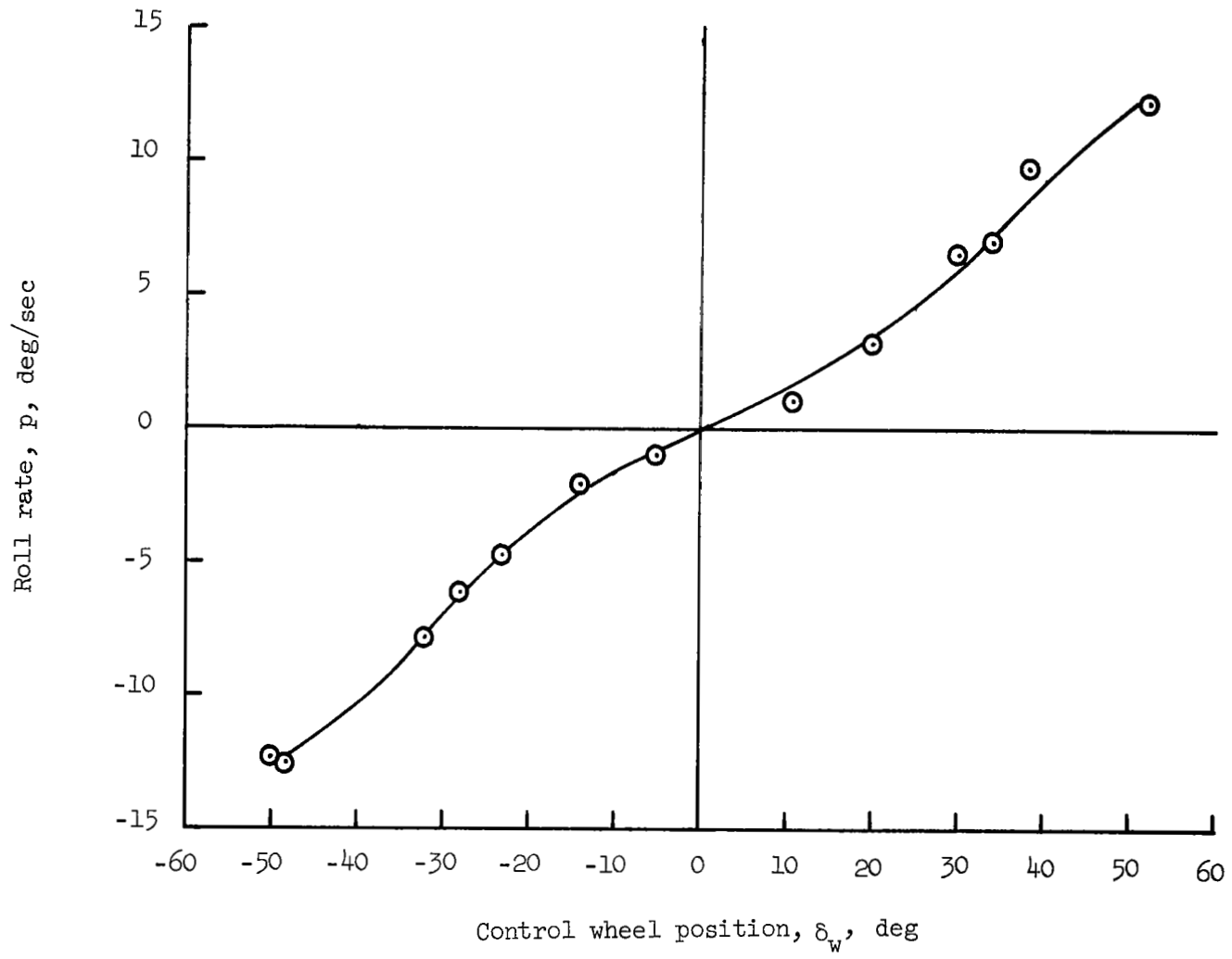
(a)  $\delta_f = 50^\circ$ ; airspeed, 100 knots.

Figure 44.- Lateral-directional static stability characteristics of the airplane with maximum boundary-layer control (sideslip rate damper operating).



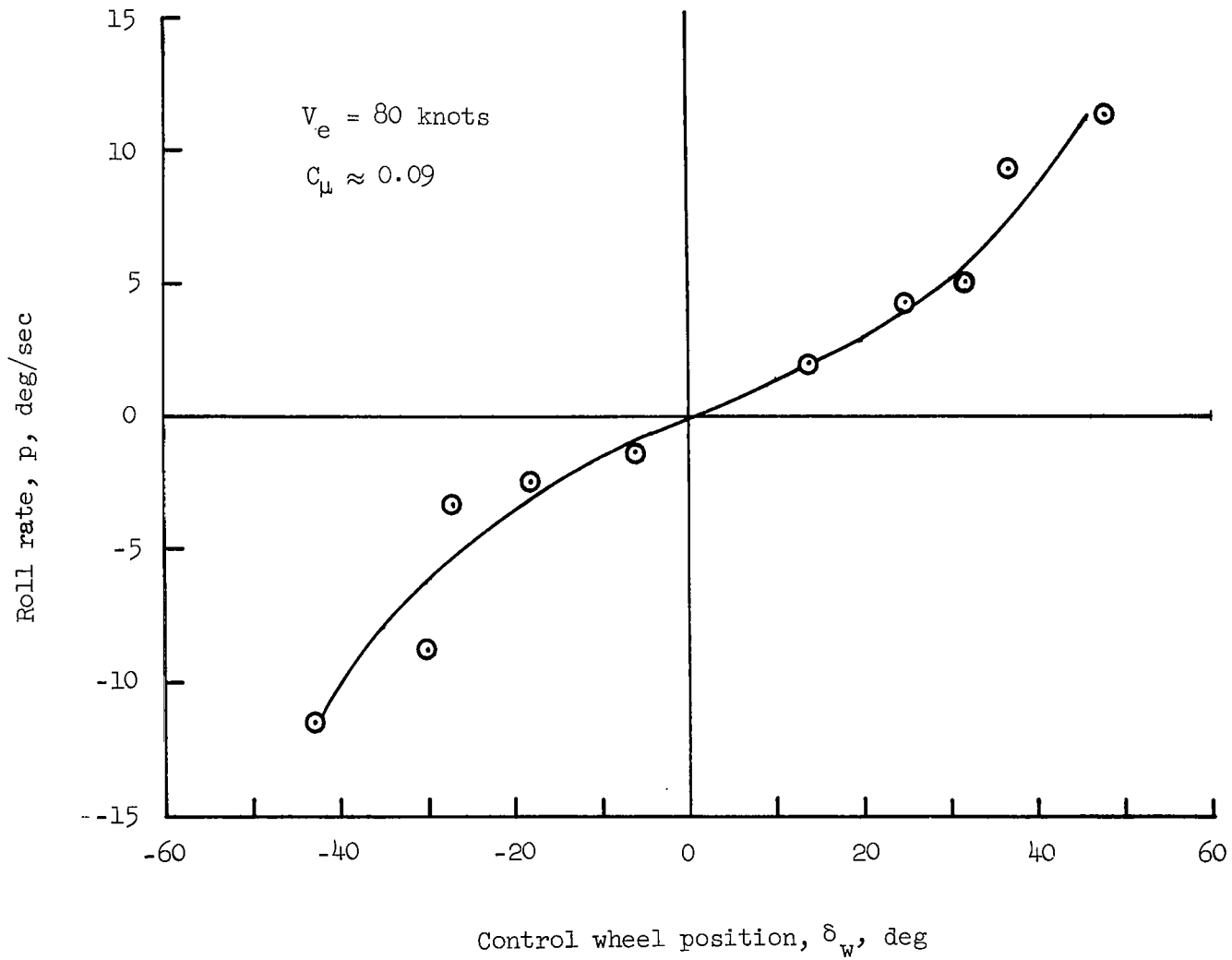
(b)  $\delta_r = 70^\circ$ ; airspeed, 85 knots.

Figure 44.- Concluded.



(a)  $\delta_f = 50^\circ$ ; airspeed, 105 knots.

Figure 45.- Lateral control characteristics with maximum boundary-layer control and with  $\dot{\beta}$  damper on.



(b)  $\delta_f = 70^\circ$ .

Figure 45.- Concluded.